Automated Diagnosis of Cardiovascular Disease on Cardiovascular Magnetic Resonance Imaging Using Deep Learning Models: A Review

Mahboobeh Jafari[1], Afshin Shoeibi[1,2,*], Marjane Khodatars[3], Navid Ghassemi[1], Parisa Moridian[1], Roohallah Alizadehsani[4], Abbas Khosravi[4], Sai Ho Ling[5], Juan M. Gorriz[2], Hamid Alinejad Rokny[6], U. Rajendra Acharya[7,8,9]

[1] Internship in BioMedical Machine Learning Lab, The Graduate School of Biomedical Engineering, UNSW Sydney, Sydney, NSW, 2052, Australia.

[2] Data Science and Computational Intelligence Institute, University of Granada, Spain.

[3] Department of Medical Engineering, Mashhad Branch, Islamic Azad University, Mashhad, Iran.

[4] Intelligent for Systems Research and Innovation (IISRI), Deakin University, Victoria 3217, Australia.

[5] Faculty of Engineering and IT, University of Technology Sydney (UTS), Australia.

[6] BioMedical Machine Learning Lab, The Graduate School of Biomedical Engineering, UNSW Sydney, Sydney, NSW, 2052, Australia.

[7] Ngee Ann Polytechnic, Singapore 599489, Singapore.

[8] Dept. of Biomedical Informatics and Medical Engineering, Asia University, Taichung, Taiwan.

[9] Dept. of Biomedical Engineering, School of Science and Technology, Singapore University of Social Sciences, Singapore.

* Corresponding author: Afshin Shoeibi (Afshin.shoeibi@gmail.com)

Abstract

In recent years, cardiovascular diseases (CVDs) have become one of the leading causes of mortality globally. CVDs appear with minor symptoms and progressively get worse. The majority of people experience symptoms such as exhaustion, shortness of breath, ankle swelling, fluid retention, and other symptoms when starting CVD. Coronary artery disease (CAD), arrhythmia, cardiomyopathy, congenital heart defect (CHD), mitral regurgitation, and angina are the most common CVDs. Clinical methods such as blood tests, electrocardiography (ECG) signals, and medical imaging are the most effective methods used for the detection of CVDs. Among the diagnostic methods, cardiac magnetic resonance imaging (CMR) is increasingly used to diagnose, monitor the disease, plan treatment and predict CVDs. Coupled with all the advantages of CMR data, CVDs diagnosis is challenging for physicians due to many slices of data, low contrast, etc. To address these issues, deep learning (DL) techniques have been employed to the diagnosis of CVDs using CMR data, and much research is currently being conducted in this field. This review provides an overview of the studies performed in CVDs detection using CMR images and DL techniques. The introduction section examined CVDs types, diagnostic methods, and the most important medical imaging techniques. In the following, investigations to detect CVDs using CMR images and the most significant DL methods are presented. Another section discussed the challenges in diagnosing CVDs from CMR data. Next, the discussion section discusses the results of this review, and future work in CVDs diagnosis from CMR images and DL techniques are outlined. The most important findings of this study are presented in the conclusion section.

KeyWords: Cardiovascular Disease, Diagnosis, CMR, Deep Learning, Classification, Segmentation

1. Introduction
CVDs are one of the most common causes of death and endanger the health of many people around the world annually [1-2]. According to the World Health Organization (WHO), CVDs are the leading cause of

human death worldwide [3-4]. According to this statistics, 17.9 million people died from CVDs in 2016, accounting for 31% of all global deaths [5-7]. In addition, coronary heart disease and stroke are responsible for four out of five deaths from CVDs, and one-third of these deaths occur in people under 70 years [8-10]. Some of the most important CVDs include coronary arteries disease (CAD) [11-12], rheumatoid arthritis [13-14], myocarditis [15-17], cardiovascular diabetes [18-19], etc. Figure (1) shows the patients with cardiovascular diabetes in the world.

The human heart is responsible for pumping blood and circulating it throughout the body [18], so any abnormality in it results in CVDs [19]. CAD is considered the most common type of CVD [20-22]. CAD is the plaque accumulation in the arteries that supply oxygen-rich blood to the heart [20-22]. Plaque causes narrowing or blockage, which restricts blood flow and thus reduces blood oxygen to parts of the heart [20-22]. Some of the most significant symptoms of CAD involve chest pain or discomfort and shortness of breath [20-22]. Cardiac arrhythmia is another of the most prevalent CVDs caused by atrial fibrillation and ventricular arrhythmias [23-24]. A cardiac arrhythmia occurs due to a non-uniform heartbeat. Weakness and pain in the chest area are the most important symptoms of arrhythmia [23-24]. Congenital heart disease (CHD) is another human CVDs. There is a defect in the structure of the heart or large arteries are present by birth [25-26]. Signs and symptoms of CHD include rapid breathing, a blue tingein the skin (cyanosis), poor weight gain, and tiredness [25-26]. Figure (2) shows the common CVDs together with their details. In recent years, major advances in cardiac research have been made to improve the diagnosis and treatment of CVDs as well as decline their case fatality.
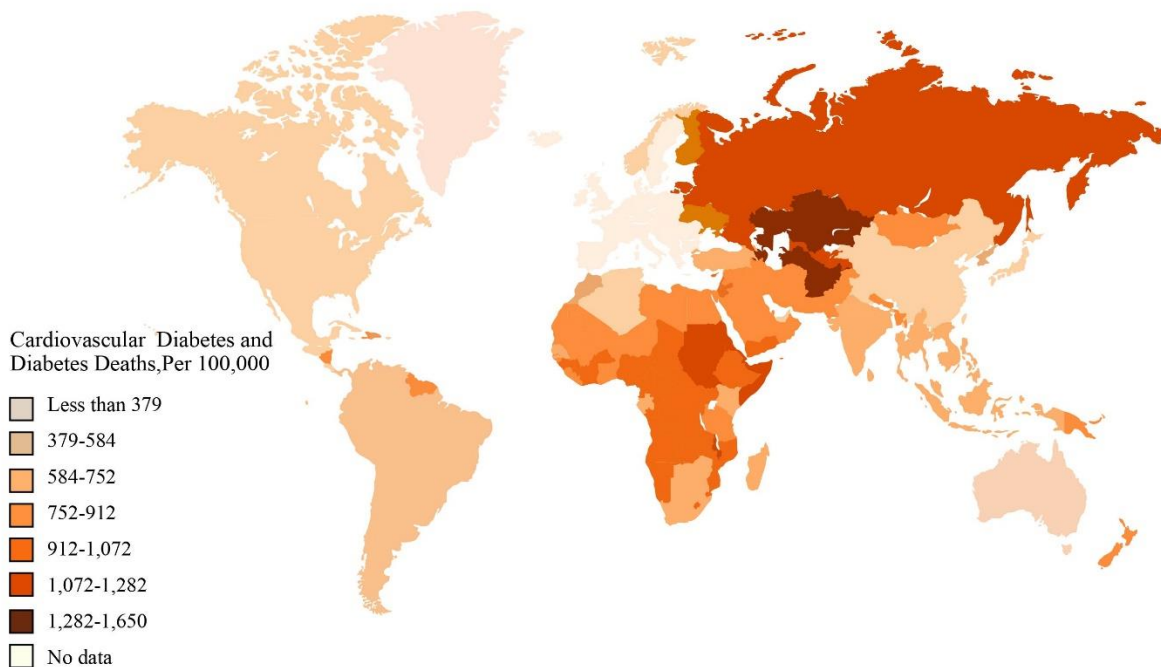

Fig. 1. Patients with cardiovascular diabetes in the world.

Cardiac ultrasound or echocardiography (Echo) works by utilizing sound waves which is a non-invasive modality to image heart tissue [27-28]. In this method, ultrasound waves are taken advantage of to produce echocardiography images of the heart [27-28]. Echo helps physicians detect various types of CVDs by assessing the heart's structure, analyzing how the blood flows in them, and evaluating the heart's pumping

cavities [27-28]. Advantages of echocardiography include readily accessible, portability, high temporal resolution, and no ionizing radiation [29].

CT is a non-invasive imaging technique that can be applied to detect a variety of CVDs, brain diseases, etc. [30-31]. In particular, cardiac CT provides the anatomical evaluation of the heart, especially CAD [32]. This imaging technique involves two techniques: non-contrast CT and contrast-enhanced coronary CT angiography (CTA) [30-31]. Non-contrast CT makes use of the density of tissues to generate the image so that various densities can be simply distinguished using different attenuation values [30-31] [33-34]. In addition, the amount of calcium in the coronary arteries can be calculated using non-contrast CT [30-31] [33-34]. In comparison, contrast-enhanced coronary CTA provides the ability to generate extraordinary images of the heart, arteries, and coronary arteries [30-31] [33-34]. Radiation exposure is one of the major weaknesses of cardiac CT imaging. Frequent exposure to radiation is associated with deleterious health effects, including an increased cancer risk [30-31] [33-34].
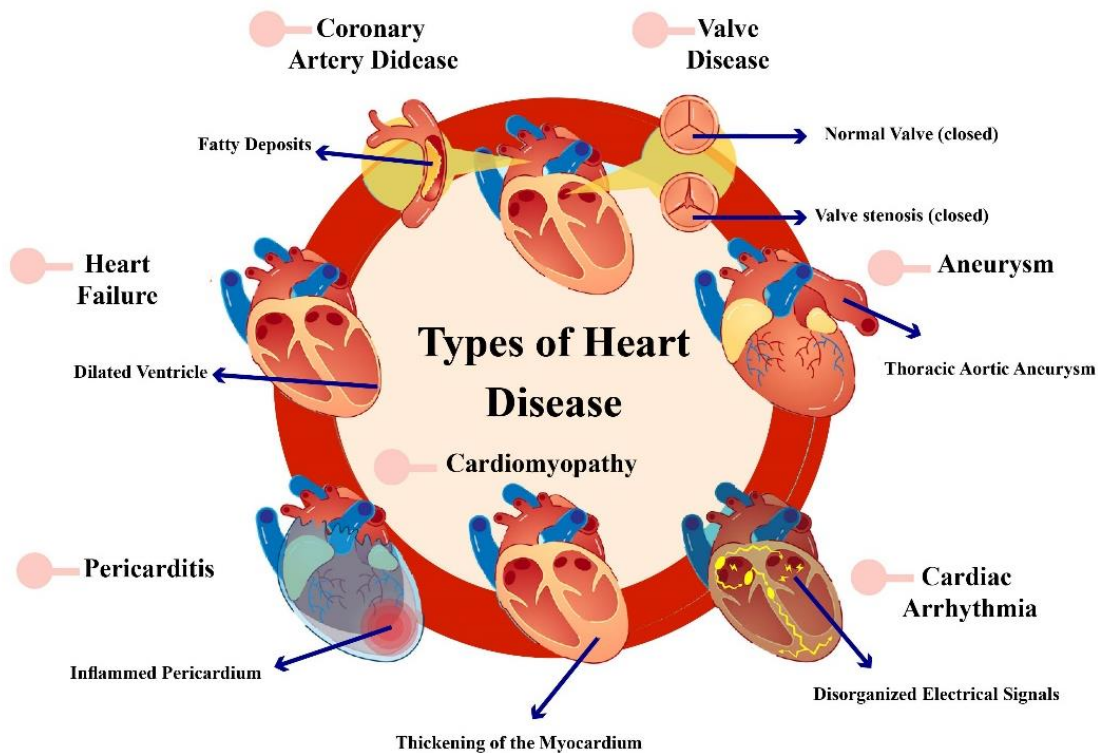

Fig. 2. Common types of CVDs with details.

CMR imaging offers an excellent quantitative assessment of cardiac chamber volume/function [374] and the extent of myocardial infarction/fibrosis [375]. It is a guideline-recommended modality for the diagnosis of diverse CVDs, including ischemic heart disease [37, 38], heritable or acquired cardiomyopathy [39], myocarditis [40], congenital heart disease [41], etc. For measurement of ventricular volume, function, and mass, accurate segmentation of the endocardial (and, in the case of myocardial mass, epicardial) contours on standard cine CMR images is a necessary prerequisite. Typically, the contours are drawn —either manually or software-assisted—on a stack of contiguous parallel slices of two-dimensional (2D) short-axis time-series cine CMR images of the ventricles at desired phases of the cardiac cycle, e.g., end-diastole and -systole, to derive the corresponding time-aligned three-dimensional (3D) ventricular volumes using Simpson's method of disc without the need for geometric assumption [376]. Indeed, cine CMR analysis is the gold standard for right ventricular (RV) volume/function measurement as the RV can be optimally

visualized on CMR without being limited by issues of acoustic window access, as with echocardiography [377]. Late gadolinium enhancement (LGE) [378] is an established CMR imaging technique in which images acquired ten to twenty minutes after gadolinium-based contrast administration are used to define in granular detail regions of myocardial infarct, fibrosis, infiltrate, etc. Indeed, segmentation can also be performed to outline and quantitate areas of abnormal tissue, e.g., myocardial infarct [379], microvascular obstruction [380], and non-infarct fibrosis [381], which may have prognostic significance.

In addition to quantitative measurements, CMR must be qualitatively interpreted by medical experts, which is time-consuming and subject to human bias. The presence of noise and imaging artifacts can further confound the interpretation, potentially resulting in misdiagnosis. However, CMRI data is the gold standard and most popular procedure for diagnosing cardiac diseases among physicians. To address CMRI challenges, researchers have proposed artificial intelligence (AI) techniques for the automatic diagnosis of CVDs using CMRI data [1-10]. In the presented papers, the main objective of the researchers is to achieve a tool for rapid detection of CVDs using CMRI images along with AI techniques. For this purpose, the researchers have conducted extensive research on ML-based approaches for diagnosing CVDs from CMRI data, including introducing various segmentation and classification approaches [42-44]. However, ML methods presented satisfactory results in early research on the diagnosis of CVDs. Nevertheless, due to high computational complexity, and inefficient performance with huge databases these methods were not able yield good performances. To tackle the challenges of ML methods, AI researchers introduced DL methods [45-47]. DL networks were able to overcome the limitations of ML methods [45-47]. The DL models were employed in various medical applications, including the diagnosis of CVDs [4], and reported satisfactory results. Researchers hope that in the near future, an accurate software platform for diagnosing CVDs using MRI data and DL techniques will be realized.

In this study, papers in diagnosis of CVDs using CMRI images and DL techniques were examined. The section 3 describes search strategy papers regarding preferred reporting items for systematic reviews and meta-analyses (PRISMA) guidelines [48]. In section 4, the conducted review papers in diagnosis of CVDs are studied. The computer aided diagnosis system (CADS) and their steps for diagnosis CVDs from CMRI images are provided in Section 5. This section discusses in datasets, preprocessing, and popular DL models for diagnosis of CVDs. Also, in this section, segmentation, classification, and fusion research based on DL methods are summarized in different Tables. Section 6 is allocated to the most important challenges in diagnosis of CVDs using CMRI data. The discussion of this paper, along with its details, is provided in section 7. Future work is also presented in section that suggest potential directions for future works. Finally, the conclusion and the findings of this study are discussed in the section 7.

2. Search strategy

This section searches papers based on PRISMA guidelines [48]. We have searched the papers published between 2016 and 2022 in the field of heart diseases using the general keywords "CVDs", "deep learning", "Segmentation", "classification", and "CMRI". Keyword searches are performed in repositories such as Science Direct, Frontiers, MDPI, IEEE Xplore, Nature, Springer, ArXiv, and Wiley citation databases.

The selection method of important articles for diagnosing CVDs with AI techniquesis presented in this section. The selection process of papers related to this field has been done in three levels. In Figure (3), the review process of papers based on PRISMA guidelines is provided. First, 400 articles were collected and then 100 articles were filtered out as they are not related to this area of research. Subsequently, another 28 articles were filtered due to the type of citation database or the method used. Finally, 200 articles were filtered out as they did not use DL techniques in their studies. Additionally, the exclusion and inclusion criteria used in this work are provided in Table (1).

Table 1. Exclusion and inclusion criteria used for the diagnosis of CVDs.

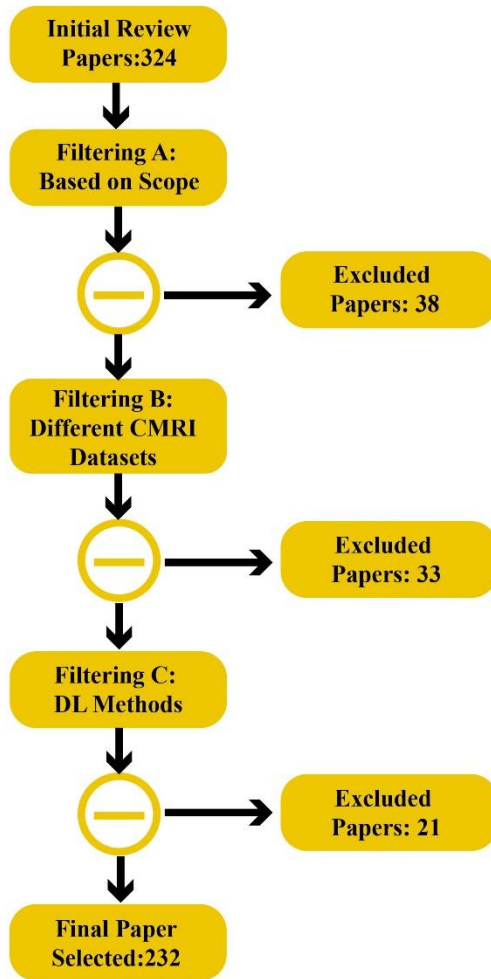| Inclusion	Exclusion
1. CMRI Images	1. Treatment of CVDs
3. Different types of CVDs.	2. Clinical methods for CVDs treatment
3. CVDs detection	3. Rehabilitation systems for CVDs detection (Without AI techniques)
4. DL models (CNNs, RNNs, AEs, CNN-RNN, CNN-AE, GAN, Transfer Learning, etc.)	

Fig. 3. Literature search procedure.

3. Review studies on AI-enabled image segmentation

Leiner et al. [11] reviewed advances in ML for image reconstruction, feature extraction, image analysis, and diagnostic evaluation of CMR images. They also highlighted important areas of research like image reconstruction, improving spatial and temporal resolution, perfusion analysis, and myocardial mapping. Segmentation of CMR images is an important area used for quantitative CMR assessment, including calculation of heart chamber volumes (and function) and delineation of abnormal myocardial tissues (e.g., myocardial infarct, fibrosis, etc.). Several review papers have been published on the use of AI for

segmenting cardiac and vascular structures as well as tissues like fat and scars on different imaging modalities such as CMR, computed tomography, echocardiography, etc. [2] [6] [9]. Litjens et al. [9] reviewed 80 papers on the diagnosis of CVD using CMR and other modalities. In this review paper, we discussed the most important DL models, including convolutional neural networks (CNNs). In addition, we reviewed few novel DL models, such as generative adversarial networks (GANs).

Studies on automated segmentation of the left ventricle (LV) on short-axis cine CMR images using ML [14] and DL [1] architectures have been reviewed in [14] and [1], respectively. In [10], 3D convolution architectures for handling volumetric LV CMR datasets were reviewed. Compared with 2D networks, 3D can capture the entirety of the spatial information while reducing the number of training data. Still, the high memory requirement limits the network depth and the filter's field of view. Wu et al. [8] also reviewed the papers on the segmentation of fibrosis and scars on late gadolinium enhancement (LGE) CMR images using DL models. In [4-5], AI methods for segmenting and quantitating regions of atrial fibrosis on LGE CMR images—which have diagnostic and prognostic implications in conditions like atrial fibrillation—were reviewed, and the challenges were discussed. The review papers published on image segmentation using AI methods are summarized in Table (2).

Table 2. Summary of review papers on image segmentation using AI.

Work	Year	Image input	Segmentation	Methods
[6]	2021	Multi-modal	Chamber and vessel borders, tissue	ML, DL
[2]	2020	Multi-modal	Chamber and vessel borders, fibrosis	DL
[9]	2019	Multi-modal	Chamber and vessel borders, fibrosis	DL
[14]	2018	Cine CMR	LV myocardial border	ML
[13]	2022	Cine CMR	LV myocardial border	ML, DL
[10]	2020	3D cine CMR	LV myocardial border	DL
[3]	2019	Cine CMR	LV and RV myocardial borders	ML, DL
[1]	2021	Cine CMR	RV myocardial border	ML, DL
[8]	2021	LGE-CMR	LV and LA fibrosis	DL
[4]	2020	LGE-CMR	LA fibrosis	DL
[5]	2022	LGE-CMR	LA fibrosis	ML, DL

4. Computer-Aided Diagnosis for Heart disease

Early detection of CVDs from CMR images extends patients' lifespan and quality of life. As mentioned in Section 3, many papers have been published for diagnosing CVDs using CMR images and AI methods. The main aim of research in CADS based on AI methods is to assist clinicians in interpreting CMR data for early detection of CVDs [1]. In general, researchers exploit ML and DL techniques in the implementation of CADS to diagnose CVDs [1-19]. DL models are state-of-the-art AI techniques that are evolving rapidly. For this purpose, the application of DL techniques in diagnosing CVDs has grown dramatically in recent years [8] [10]. The main objective of this study is to enhance the performance of CADS to assist doctors in the accurate diagnosis of CVDs. The CADS based on DL networks for the diagnosis of CVDs consists of CMR datasets, preprocessing, DL models, and evaluation parameters steps. Figure (4) illustrates the block diagram for CVDs detection using DL methods. To achieve better performance using CADS, CMR images are pre-processed to remove artifacts, increase contrast, etc. In the next step, DL models are fed with CMR images for diagnosis of CVDs. Ultimately, the evaluation criteria demonstrate the effectiveness of the proposed CADS for CVDs detection. As aforementioned, the diagnosis of CVDs is largely reliable on the physician's subjective interpretation. CADS based on DL can alleviate this subjectivity by improving the detection of CVDs and quantitative support for decision-making [14]. The following details of each CADS section for CVDs detection based on DL models are provided.
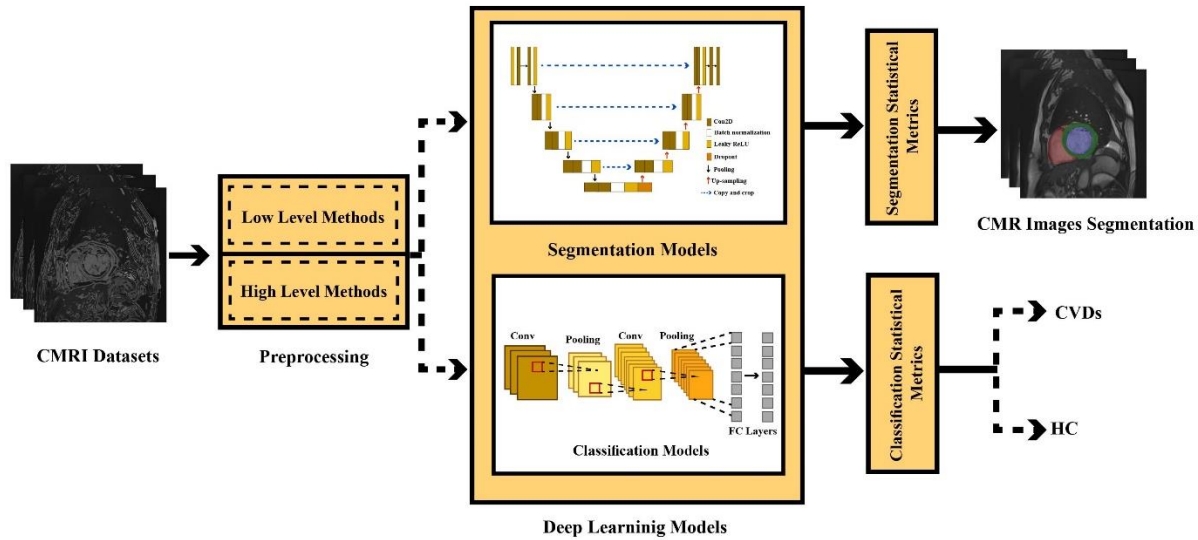
Fig. 4. Illustration of CVDs detection using DL methods.

4.1. Datasets

Datasets play an important role in the DL-based diagnosis of CVDs. To date, several datasets have been made available to researchers for CVD diagnosis, including ECG, echocardiography, and CMR. This section presents the most important available CMR datasets for CVDs detection. The remainder of this section describes the available datasets from CMR data. Also, a summary of CMR datasets available is summarized in Table (3).

4.1.1. Sunnybrook Cardiac Data (SCD)

The SCD dataset contains cine-CMR images of 45 individuals with four pathologies, namely, healthy, hypertrophy, heart failure with infarction and heart failure without infarction, and with medical interpretations [49]. In this dataset, images are acquired while the patient holds his breath for 10-15 seconds with a time resolution of 20 cardiac phases in the cardiac cycle [49]. The data is in DICOM format and includes Metadata parameters about the patient and the image. A set of contours is delineated manually for each patient record at end-diastolic (ED) and end-systolic (ES) slices [49]. These contours were drawn by Perry Radau of the Sunnybrook Health Science Center [49]. The data is provided for analysis by physicians without any pre-processing. In SCD, data is randomly split into three groups: 15 for training, 15 for testing, and 15 for an online challenge [49]. The training dataset contains CMR images and their ground truth for segmentation application. Furthermore, the test dataset does not involve ground truth for segmentation [49]. In 2009, a subset of the SCD dataset was first utilized in the myocardial segmentation challenge with CMR, held by a MICCAI workshop. The entire dataset is now available in the CAP [49].

4.1.2. The Automated Cardiac Diagnosis Challenge (ACDC) MICCAI 2017 Challenge

The ACDC is a public dataset containing short axis view CMR images of 100 patients recorded in NIfTI format [50]. Contour images for the end-systole and end-diastole are provided for each patient [50]. The expert references are manually-drawn on 3D volumes of LV, RV, and myocardial cavities in ED and ES slices [50]. Recordings were performed using two CMR scanners with Siemens Area (1.5T) and Siemens Trio Tim (3T) specifications for 6 years. Cine CMR images were captured during breath-holding with a retrospective or prospective gating and an SSFP sequence in the short axis view [50]. More information on this dataset is provided in [50].

4.1.3. The Kaggle Data Science Bowl Cardiac Challenge

Kaggle is made of 700 datasets for the training and validation phases and 440 datasets for the testing phase [51]. The Kaggle dataset does not provide standard gold LV contours. In addition, the goal and evaluation metric are based on the predicted LV volume at the end-diastole (ED) and end-systole (ES) [51]. More information on this dataset is provided in [51].

4.1.4. Left Ventricle Segmentation Challenge (LVSC)

The LVSC dataset was made publicly available to researchers in MICCAI 2011 [52]. The LVSC dataset contains 200 CMR images of CAD and myocardial infarction patients from several institutions [52]. The primary sequences are cine short-axis steady-state free precession (SSFP) images. Long-axis SSFP cine images are available only for a subset of subjects [52]. The scanners and imaging parameters vary and offer a heterogeneous combination of spatial resolutions of 0.7 to 2.1 mm / pixel and matrix sizes of 156*192 to 512*512. LVSC datasets fall into two groups [52]. The first group includes 100 annotated samples for training and testing. The second group consists of 100 samples without annotation for validation. The gold standard annotations include binary masks delineated by an expert indicating LV myocardium from basal to apical slices for all cardiac phases [52].

4.1.5. Right Ventricle Segmentation Challenge (RVSC)

The RVSC dataset was presented as a section of the 2012 MICCAI workshop [53]. This dataset contains CMR images in DICOM format that have been recorded with the Symphony Tim (1.5T) device. The RVSC dataset consists of manual epicardium and endocardium segments in the ED and ES phases from 48 patients [53]. For this dataset, the data is split as follows: training of 16 patients, test 1 includes 16 cases, and test 2 has 16 patients. For this dataset, ED and ES phases and basal and apical slices have been predefined [53].

4.1.6. CMR Dataset from York University

This dataset contains CMR images in DICOM format with ground truth segmentation of LV endocardial and epicardial [54]. CMR data were recorded from 33 subjects, where each subject's sequence consisted of 20 frames and 8-15 slices along the long axis to make a total of 7980 images [54]. In this dataset, segmentation has been done on images in which both the endocardium and the endocardium of the left ventricle are visible [54]. Thus, there are 5011 segmented CMR images and 10022 contoursin the dataset [54]. Metadata is also available, including pixel spacing, spacing between slices along the long axis, and age and disease of each subject [54].

4.1.7. Left Ventricle Full Quantification Challenge MICCAI 2018 (LVQuan18)

To accurately quantify LV, the STACOM 2018 workshop released the LVQuan18 dataset [55]. The training dataset includes processed SAX MR sequences of 145 subjects [55]. There are 20 frames for each subject. In addition, all ground truth values are provided for each frame [55]. The test dataset contains SAX MR processed sequences of 30 subjects [55]. For each subject, only SAX image sequences of 20 frames without ground truth values are provided [55].

4.1.8. Left Ventricle Full Quantification Challenge MICCAI 2019 (LVQuan19)

The LVQuan19 dataset is the new version of LVQuan18 released at the STACOM 2019 workshop [56]. The training dataset comprises 56 subjects from the processed SAX MR sequences [56]. For each subject, 20 frames are provided and all ground truth values. In the test dataset, the processed SAX MR sequences of 30 subjects are available [56]. At this stage, only the SAX image sequences of 20 frames are provided for each subject, while their ground truth values are not [56].

4.1.9. STACOM

This dataset comprises CMR images of 100 patients with CAD and myocardial infarction [57]. The subjects of this dataset are randomly split into two parts: training and testing [57]. Sixty-six subjects were selected for training, while 34 subjects were used for testing, which resulted in 12,720 training images and 6972 test images [57]. This dataset has a high diverse. Different types of CMR scanners have been employed to record images, and this dataset's CMR image sizes range from 138 x 192 to 512 x 512 pixels [57]. Moreover, each CMR image has a ground truth for the blood cavity and myocardium [57].

4.1.10. STACOM 2017

This dataset was published in a challenge STACOM 2017 for whole heart segmentation. The dataset comprises two parts: training and testing [58]. In the training section, there are 20 CMR images and 20 CT images with ground truth [58]. In the test step, 40 images were provided for each modality without ground truth [58]. CT images are taken from routine cardiac CT angiography and cover the whole heart, extending from the upper abdomen to the aortic arch. The CMR images were acquired using 3D balanced steady-state free precession (b-SSFP) sequences with an acquisition resolution of 2mm in each direction [58].

4.1.11. LASC STACOM 2018

This dataset was part of the STACOM 2018 challenge for LA segmentation [59]. It contains 100 3D LGE-CMRs recorded from patients diagnosed with atrial fibrillation (AF) [59]. A large proportion of data was provided by the University of Utah, while the rest were collected from multiple other institutions [59]. Each 3D D LGE-CMR volume was recorded using a 3.0 Tesla Verio and 1.5 Tesla Avanto scanners. In this dataset, the ground truth binary mask for the LA cavity was annotated by experts for each data [59].

4.1.12. Multi-Modality Whole Heart Segmentation (MMWHS) challenge

This dataset contains 20 CMR data obtained using a Philips Healthcare (1.5T) scanner [60]. The whole heart imaging CMR sequence is balancedsteady-state free precession (b-SSFP) [60]. This database also comprises 20 CT data. CT data were acquired using a Philips Medical Systems scanner [60]. CT images were obtained in axial view, covering the whole heart from the upper abdomen to the aortic arch. More data is provided in the reference [60].

Table 3. Details of dataset used for cardiovascular disease.

Ref	Dataset	Number of cases	Modality
[49]	SCD	45	CMR
[50]	ACDC	100	CMR
[51]	Kaggle	700 train, 440 test	CMR
[52]	LVSC	200	CMR
[53]	RVSC	48	CMR
[54]	York University	33	CMR
[55]	LVQuan18	145 train, 30 test	CMR
[56]	LVQuan19	56 train, 30 test	CMR
[57]	STACOM	66 train, 34 test	CMR
[58]	STACOM 2017	20 CMR and 20 CT for train, 20 CMR and 20 CT for test	CMR and CT-Scan
[59]	LASC STACOM 2018	100 3D LGE-CMRs	CMR
[61]	UK Biobank	500,000	Image, non- image, biological samples, etc.
[60]	MMWHS	20 CMR, 20 CT	CMR and CT-Scan

4.2. Preprocessing techniques

Preprocessing is one of the most substantial steps in CADS for diagnosing heart disease using CMR images. CMR images provide physicians important information about the structure of the heart and assist them in diagnosing CVDs quickly. Though beneficial, CMR data are affected by different artifacts. In addition, CMR images sometimes have low contrast. Hence may lead to inaccurate diagnosis of CVDs from CMR images by specialist physicians. Several preprocessing algorithms have been proposed to address these problems to enhance the performance of DL-based CADS for CVDs detection. Generally, CMR images in DL-based CADS are pre-processed by low-level and high-level procedures.

4.2.1. Low-Level Preprocessing

Low-level techniques are exploited for primary preprocessing of CMR images. The low-level preprocessing plays a significant role in improving CADS performance in CVDs detection. Some of the most important low- level preprocessing techniques comprises of filtering [62], intensity normalization [63], resizing [64], histogram matching [65], cropping [66], segmentation [67], and ROI extraction [68]. Filtering is applied to remove various artifacts from CMR images. Some of the most important filtering algorithms include median and Gaussian filters used in cardiac research [69-70]. Intensity normalization is modifying the range of pixel intensity values and increasing the detection efficiency of CVDs using CMR images [63]. CMR images are normally recorded in high dimensions, so resizing approaches help reduce the CMR dimensions so that they can be fed to the input of DL models [64]. A histogram is another low-level preprocessing technique that aims to enhance the contrast of CMR images [65]. In low-level preprocessing, cropping and segmentation techniques extract important information from CMR images [66]. Then, ROI methods are taken advantage to extract suspected disease areas from CMR images called ROI extraction [68]. Ultimately, the data obtained from ROI extraction is applied to the DL model input. Low-level preprocessing methods are used in all CVDs detection research on CMR using DL techniques.

4.2.2. High-Level Preprocessing

DL models' performance immensely declines when confronted with limited input data. In order to tackle the lack of input data and avoid overfitting, researchers use data augmentation (DA) techniques to increase the training dataset size [71]. Some of the most important DA methods include horizontal flipping and affine transformations rotation and have been investigated in CVDs detection studies [72-73]. GAN models are a new class of DL methods used for DA approaches [74-76]. In [74-76], GAN models have increased input data size.

4.3. Deep Learning models

This section describes the most significant DL models used for CVDs detection using CMR images. First, 2D-CNNs [77] and 3D-CNNs [77] are presented with their details. In the following, pre-trained models are introduced, which are a particular mode of CNNs architecture [77]. GAN models [74-76] are an important class of DL models described in this section. U-Net [78-79] and FCN [80] models are two groups of CNNs used for image segmentation applications. A more detailed description of these methods is provided in this section. In another section, AEs and CNN-AEs models [81-82] are introduced to diagnose heart disease. Ultimately, the RNNs and CNN-RNNs models [83-84] are introduced.

4.3.1. Convolutional Neural Network (CNN)

In recent years, DL models have significantly grown in various fields, including medicine [85-90]. CNN architectures have fared exceptionally well in analyzing medical images. Convolutional, pooling, and FC layers are the essential components of a CNN model for the feature extraction and classification [77]. CNN

models use supervised learning at the learning stage and encompass different models for classifying and segmenting medical images [91-93]. The most significant advantage of CNN models compared to ML algorithms is feature engineering. The increasing advancement of CNN models has led to increased computational complexity; therefore, hardware resources are also rapidly developing [91-93]. Pre-trained models, 2D-CNNs, and 3D-CNNs are some of the most important CNN models used for classification in the CMR images diagnose CVDs. Further, FCN and U-Net architectures are some of the most popular CNN techniques for CMR image segmentation to diagnose CVDs. Details of CNN models are discussed in the following sections.

A) 2D-CNN

In medical approaches, there are often many spatial dependences between the images, making feature extraction difficult [92]. Convolutional layers in CNN models function as spatial filtering [77]. This helps extract useful features by considering spatial dependencies in medical images. Therefore, using convolutional layers lead to automated feature extraction from medical images. The pooling layers in the CNN models function similar to dimension reduction algorithms in ML [77]. Lastly, several fully connected (FC) blocks are used in the last CNN layersto classify input data [77]. , The high efficiency of 2D-CNN models, has led to their massive popularity in studies of identifying CVD from CMR data. Figure (5) illustrates the working of 2D-CNN architecture for CMR image classification to diagnose CVDs.
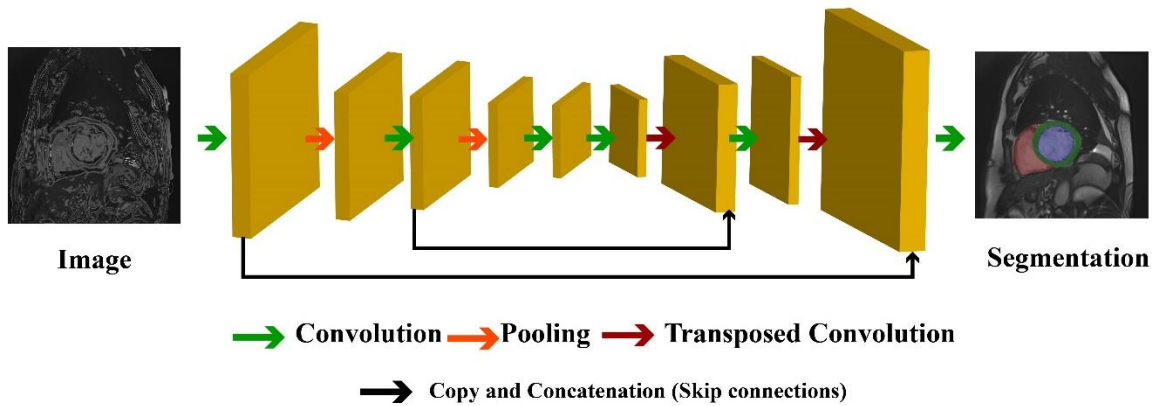

Fig. 5. A typical 2D-CNN for CVDs detection from CMR images.

B) 3D-CNN

Medical images such as brain CMR, CMR, CT, and ultrasound are recorded as 3D [94-95]. However, 3D images are highly complex, and it is often challenging for doctors to diagnose diseases based on these data. As a result, researchers have extended 2D-CNN models to 2D-CNNs to obtain more successful outcomes in disease diagnosis from 3D medial images [96-97]. In return, 3D-CNN models require a lot of input data for learning, and researchers often do not have access to datasets with many subjects [96]. Additionally, 3D-CNN models have high computational complexity; hence implementing them requires high-power hardware resources [97]. This always impose challenges in disease diagnosis using 3D-CNN models. Figure (6) illustrates the block diagram of a 3D-CNN architecture for classification of CMR classification for diagnosing CVDs.
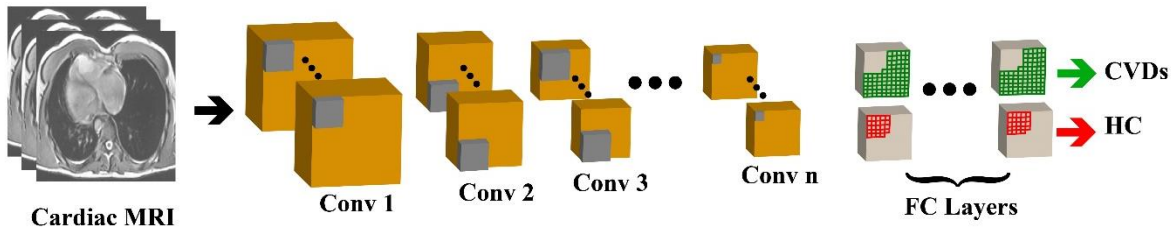
Fig. 6. A typical 3D-CNN for CVDs detection from CMR images

C) Pretrained Models

The most significant challenge of studies on disease diagnosis using DL techniques is the lack of access to datasets with many subjects [86]. AI researchers have managed to overcome this challenge in medical studies by proposing deep pre-trained models [98]. Pre-trained models are a group of CNN architectures initially trained on the ImageNet dataset [99-100]. In the following, the weights of the layers have been saved so that researchers can use these architectures to diagnose diseases with fewer subjects [99-100]. For instance, numerous papers have deployed pre-trained models to diagnose CVDs based on CMR images, and researchers have obtained satisfactory results [143]. VGG, AlexNet, etc., are some of the most crucial pre-trained architectures [99-100]. Further, some pre-trained architectures for deep compact size CNNs [101-102] and transformers [103-104] have recently been introduced. Figure (7) illustrates the typical pre-trained model used for CVDs detection from CMR images.
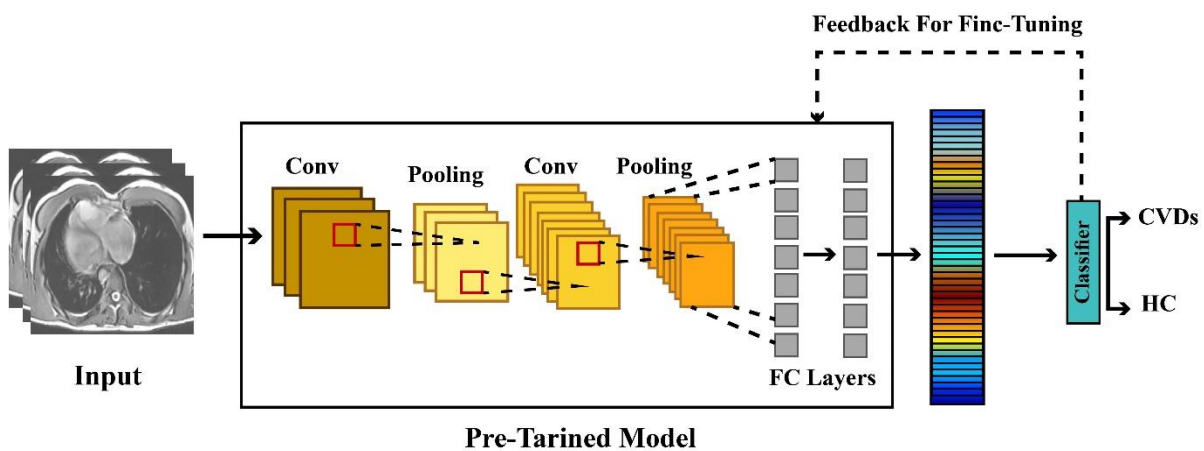
Fig. 7. A typical pre-trained model used for CVDs detection from CMR images.

4.3.2. GAN

Generative models have always received much attention due to their ability to model the underlying distribution of data [74-76]. Usually, they consider a simpler family of distributions and try to minimize the KL divergence with the underlying distribution. GANs use a different data generation mechanism, allowing them to create high-quality images. The idea is to create a 2-network minimax game, one network aiming to distinguish between real and fake images and the other trying to fool the first one [74-76]. After training, the generative part (second network) in GAN usually creates realistic data [74-76]. They have been widely used in medical diagnosis tasks, and cardiovascular disease diagnosis. Figure (8) shows the typical GAN model used for CVDs detection using CMR images.

Fig 8. A typical GAN model used for CVDs detection using CMR images.

4.3.3. FCN

Long et al. [105] introduced, FCN which is the most fundamental DL architecture used for image segmentation. It is a type of CNN family in which FC layers are not used [105]. Instead, an encoder-decoder structure is used in t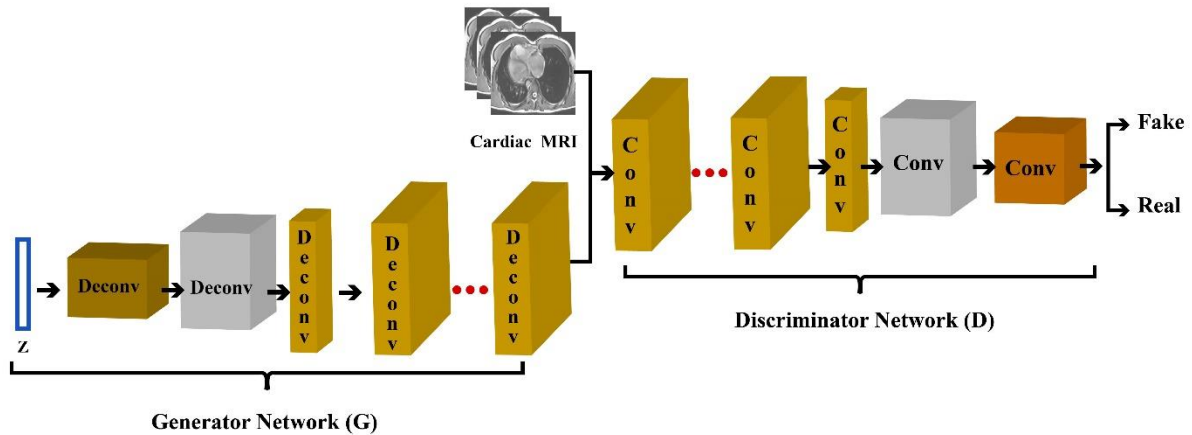he FCN architecture for image segmentation [105]. In FCN, the input image is first received with the desired size, then output with the same input dimensions is produced. By applying an image to the input of the FCN model, the encoder first changes the input into high-level feature representation. At the same time, the decoder interprets feature maps and restores spatial details to image space for pixel prediction through a series of convolutional operations and upsampling [105]. Authors in [105] provided more details for the FCN architecture. Figure (9) shows the typical FCN model used for CVDs detection using CMR images..
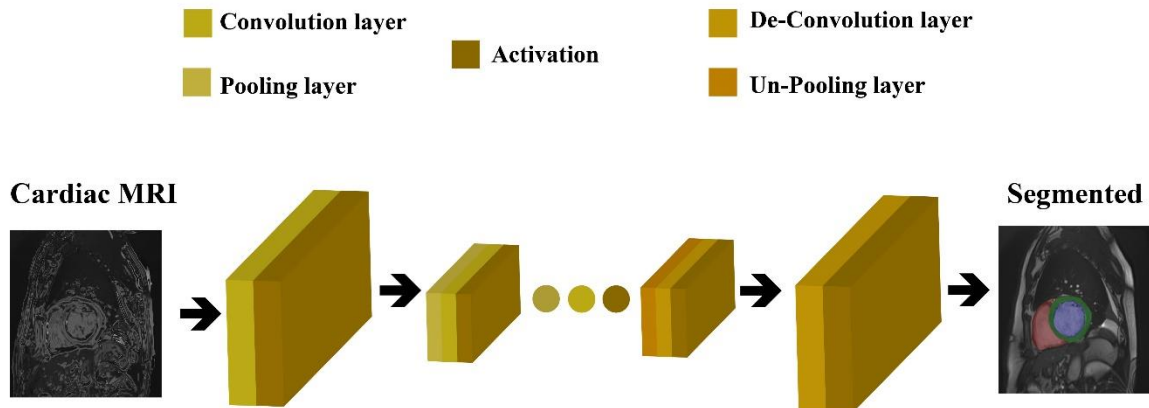
Fig. 9. A typical FCN model used for CVDs detection using CMR images.

4.3.4. U NET

Image segmentation is an important step in medical diagnosis, usually used for the localization of different diseases [78-79]. However, conventional CNNs fail to segment; as the image-sized mapping is required for the network's output. FCN and U-net are two famous networks suggested for segmentation [78-79] as they have an encoder-decoder structure that ideally learns required information in the encoder part and encodes

it into a latent space, and then decodes that to give a map of the segmented image as the output of the decoder [78-79]. Also, in U-Net, shortcuts between the encoder and decoder are introduced to increase information sharing and help the networks converge faster. These networks have also been used for cardiovascular diagnoses, such as [78-79]. Figure (10) shows the   typical U-Net model used for CVDs detection using CMR images.
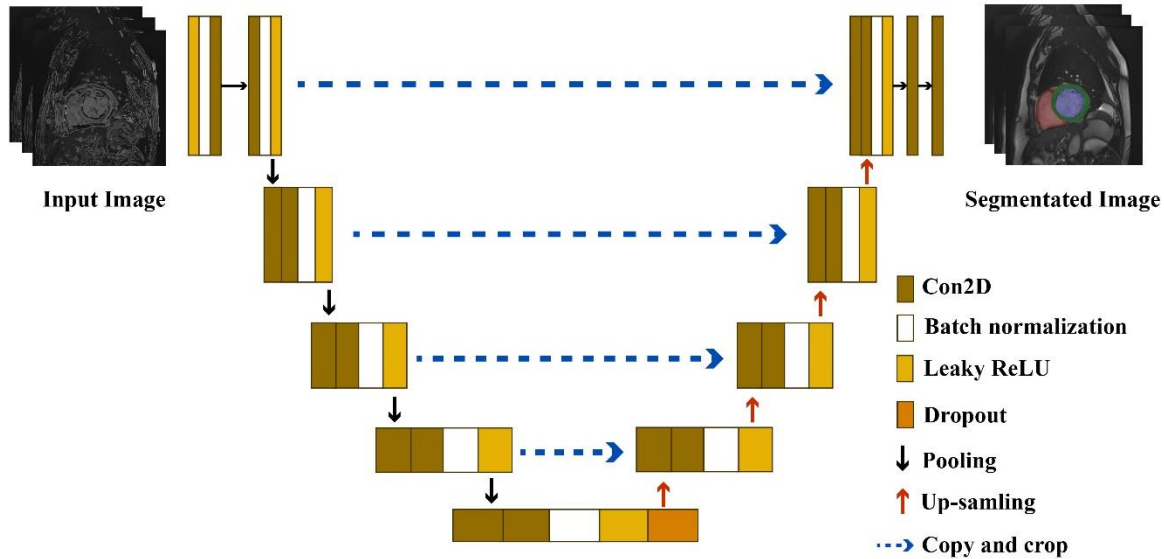
Fig. 10. A typical U-Net model used for CVDs detection using CMR images.

4.3.5. Autoencoder Models

Autoencoders (AE) are the oldest neural networks, but they are still used for many tasks and are even considered state-of-the-art in their domain [77]. The idea is simple; for many tasks, data space is too big, and dimensionality reduction can help dramatically solve the task [77]. Hence, two networks are put back to back, one for encoding the data into a smaller latent space and the other for taking the data back from latent space to the original space, aiming to minimize the re-construction loss [77]. Appropriately trained, AEs should learn to find a robust encoding that preserves the most critical information in data [77] [81-82]. AEs have many different types, such as denoising AEs, Sparse AEs, and Stacked AEs, all aimg to resolve one of the challenges AEs face [77] [81-82]. Amongst all types of AEs, Convolutional Autoencoders (CNN-AE) have been used widely in medical diagnosis [106-107]. The idea behind them is to exploit the convolutional abilities by changing the AE layers to convolution and encode spatial patterns into latent space. Figure (11) illustrates the block diagram of a CNN-AE architecture used to diagnose CVDs using CMR images.
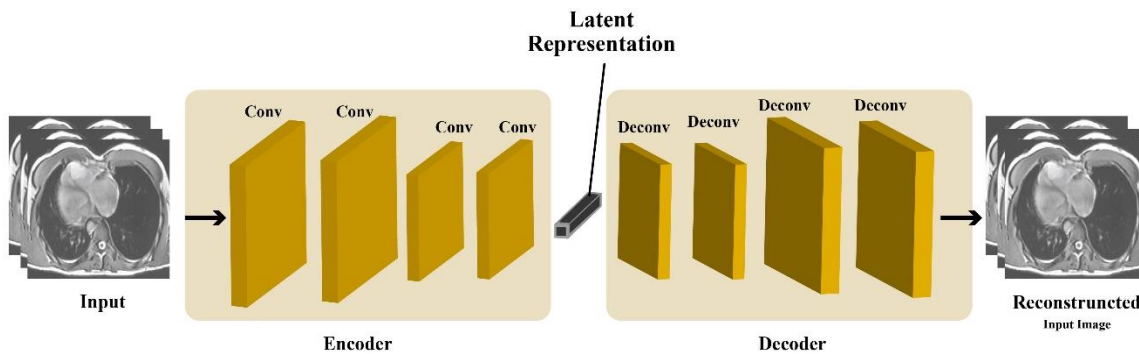
Fig. 11. A typical CNN-AE model for CVDs detection from CMR images
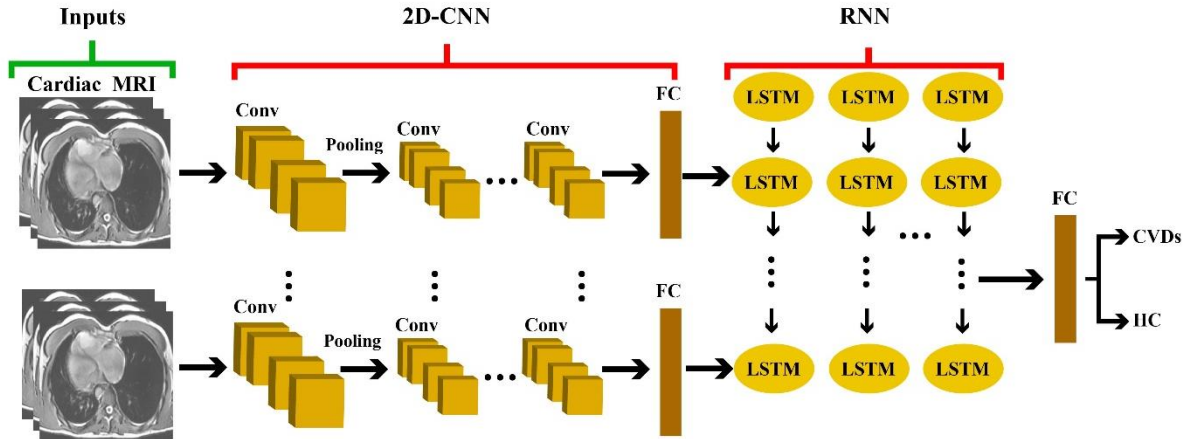
Fig. 12. A typical CNN-RNN model for CVDs detection from CMR images

4.3.6. RNN Models

When applying deep learning models to tasks such as natural language processing, some challenges, such as variable data length or lengthiness, are possible concerns [77]. Amongst these types of challenges, finding temporal patterns is arguably the most important and complicated one, given that these patterns can be of variable length, and previous DL methods have no mechanism to detect them [77]. RNNs, specifically long short-term memory (LSTM) and gated linear unit (GRU) models are built to resolve this issue [77] [83-84], and they are commonly used for signal processing [108], etc. Also, it is common to combine RNNs with other types of networks, such as convolutional ones, to take advantage of both. These models named as CNN-RNN are used to extract spatial and temporal and even Spatio-temporal information from sequential data [77] [83-84]. Figure (12) illustrates a block in the overall diagram of pre-trained CMR data classification architecture to diagnose CVDs.

4.4. Applications of DL for segmentation of CMR images

As aforementioned, to diagnose CVDs, DL-based segmentation and classification techniques are utilized. The summary of DL-based segmentation works done for CVDs diagnosis are summarized in Table (4). In Figure (13) shows various DL models employed in automated segmentation of diagnosis of CVDs in CMR images. According to Table (4) and Figure (13), CNN models are the most commonly used in CVDs detection using CMR images.
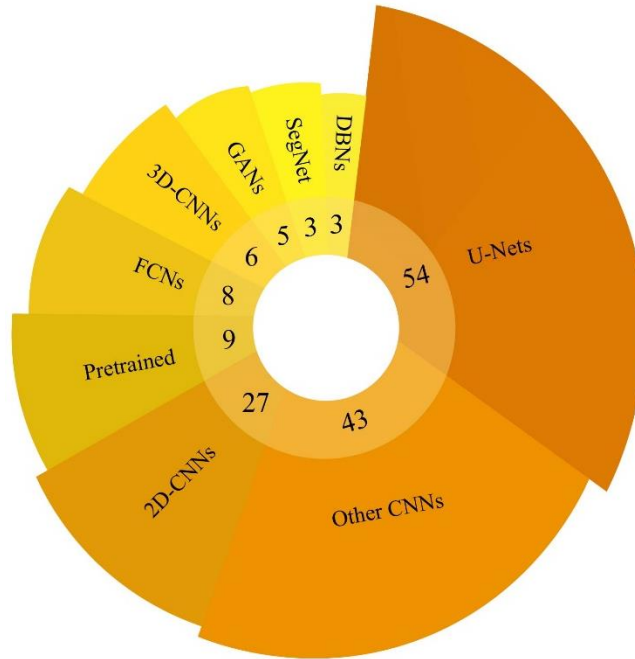
Fig. 13. Various DL models employed in automated segmentation for diagnosis of CVDs in CMR images.

Table 4. Summary of DL-based segmentation works done using CMR image. diagnosis of CVDs using DL methods

Ref	Application	Dataset	Number of cases	Preprocessing	DNN	Toolbox	Performance
[109]	LV	MICCAI 2009	45 Subjects	DA	2D-CNN	NA	DM=94.00%
					SAE		
[110]	RV and LV	MICCAI 2012	--	ROIs Extraction	2D-CNN	NA	DM=81.00% HD=7.79mm
		MICCAI 2009			SAE		
[111]	RV	MICCAI 2012	48 Subjects	ROIs Extraction	2D-CNN	Keras	DM for Endo=86.00% HD=6.9mm
							DM=84.00% HD=8.9mm
							EDV R=89.00, ME=7.1
							ESV: R=84.00, ME=9.6
							EF R=86.00, ME=7.5
[112]	LV, RV Endo, Epi, and LVM	Sunnybrook	45 Subjects	Different Methods	2D-CNN	Caffe	Sens=83.00% Spec=96.00%
		LVSC	200 Subjects				
		RVSC	48 Subjects				
[113]	Multi-slice LV	MICCAI 2009	45 CMR	DA	RFCN	NA	Dice=93.50% APD=1.56
[114]	LVM	York University	33 Subjects	DA	CNN	Caffe	DM=75.00%
[115]	Great Vessel	HVSMR 2016	20 CMR	DA	Deeply-supervised 3D FractalNet	Caffe	DM=93.00% HD=4.643mm
[116]	MYO and blood	MICCAI 2016	20 Scans	ROIs Extraction	2D-Dilated CNN	NA	Blood Pool: DM=93.00%
							MYO: DM=80.00%
[117]	RV	MICCAI 2012	48 Subjects	DA	2D-CNN	NA	DM= 82.50% HD=7.85mm
					SAE		
[118]	Myocardial	Sunnybrook	NA	DA, ROIs Extraction	Modified U-Net	Keras	DM=90.00%
[119]	LA and PPV	STACOM 2013	30 CMR	DA	CardiacNET	TensorFlow	Sens=90.00% Spec=99.00% DM=93.00%
[120]	LV	Sunnybrook	45 Subjects	Random Shuffled	2D-CNN	Caffe	DM=90.00% HD=5.43mm Sens=90.00%

Ref	Target	Dataset	Subjects	Preprocessing	Model	Framework	Results
							Spec=99.00%
[121]	LV, RV and MYO	MICCAI 2017	100 Subjects	--	2D and 3D-CNN	NA	DM=95.00%
[122]	RV and LV Endo and Epi	MHH	502 Subjects	DA	V-Net	TensorFlow	Different Results
		DSBCC	1140 Subjects				
		MICCAI 2009	45 Subjects				
		RVSC	48 Subjects				
[123]	LV	MICCAI 2009	45 Subjects	ROI, DA	DBN	NA	ADM=86.00%
[124]	LA	3D LGE-CMR	60 Subjects	DA	2D-CNN	TensorFlow	DM=94.20% Sens=91.80%
[125]	Shape-Refined Bi-Ventricular	Clinical	Different Subjects	DA	SSLLN	NA	DM: LVC=96.00%, LVW=87.30% RVC=92.90%, RVW=75.50%
[126]	Cardiac Bi-Ventricle	Clinical	145 Subjects	ROIs Extraction	Cardiac-DeepIED (ED+Conv-LSTM)	Keras	Acc LV=99.10% Acc MYO=97.60% Acc RV=98.20%
[127]	LV	MICCAI	45 Subjects	ROIs Extraction	SegNet	MATLAB	--
[128]	LV and RV	UK Biobank	3078 Subjects	ROIs Extraction	LV-Net	TensorFlow	DM LV-epi=92.30%
[129]	MYO and BV	MICCAI 2017	150 Subjects				Acc=96.00%
[130]	BV	MICCAI 2017	150 Subjects	ROIs Extraction	CCGAN	Keras	Different Results
[131]	LV	York University	33 Subjects	ROIs Extraction	2D-CNN	--	DM=87.24% Acc=98.39%
[132]	Scar	Clinical	30 Subjects	DA	2D-CNN	TensorFlow	Acc=96.83% Sens=88.07% DM=71.25%
[133]	LV and RV Endo	Clinical	90 Subjects	Contour delineation,	U-Net	Keras TensorFlow	DM=92.90 % JM=86.90%
[134]	LV	MICCAI 2013	83 Subjects	Resizing	CapsNet	TensorFlow	DM=94.17
[135]	LV	Clinical	900 Subjects	Manual Expert Delineations	SegNet	NA	DM Endo=90.00% APD Endo=1.95%
		MICCAI	45 Subjects				DM Epi=93.00% APD Epi=1.98%
[136]	LV	MICCAI 2009	Different Subjects	NA	DBN	NA	Endo AVP:2.08% Endo ADM:0.90%
[137]	LV, MYO, RV	Free-Breathing CMR Data	12 Subjects	DA, Karhunen-Loeve Transform Filter	U-Net and ResNet	Matlab 2019a	DM LV=91.90% DM MYO=80.60% DM RV=81.80%
		MICCAI 2017	150 Subjects				
[138]	LV, RV and MYO	MICCAI 2017	150 Subjects	Hough Transform, ROIs Extraction, Feature Selection, Feature Scaling, DA	DFCN-C	TensorFlow	DM=91.00% HD=5.43mm
		LV-2011	200 Subjects				
		2015 Kaggle	500 Subjects				
[139]	LV and RV	MICCAI 2017	150 Subjects	DA	GridNet-MD	Keras	DM=91.00%
[140]	Bi-Ventricle	MICCAI 2017	150 Subjects	DA	C-cGANs	Keras TensorFlow	DM LV=96.50% DM RV=94.90% DM MYO=89.30%
[141]	LV	Sunnybrook	45 Subjects	ROIs Extraction, DA	2D-U-Net	Keras	Different Results
		MICCAI 2017	100 Subjects				
[142]	LV and RV	Clinical	100 Subjects	DA	2D-U-Net	Keras TensorFlow	--
		MICCAI 2009	100 Subjects		3D-U-Net		
		Sunnybrook	45 Subjects		DenseNet		
		MICCAI 2012	16 Subjects				
[143]	LV and RV	MICCAI 2017	100 Subjects	DA	Proposed Method	PyTorch	DM RVC=90.30% DM LVM= 89.20% DM LVC=94.20%
		Clinical	100 Subjects				HD RVC=13.830mm HD LVM= 8.786mm HD LVC=6.641mm
[144]	LV	Clinical	100 Subjects	--	FC- U-net	PyTorch	DM Epi=96.00% DM Endo=94.00%
[145]	LV	York University	30 Subjects	--	U-Net and GoogleNet	Keras	DM=89.00%
[146]	LV	MICCAI 2011	Different Subjects	DA	2D-CNN	TensorFlow	DM=88.00%
		MICCAI 2009	100 Subjects				
[147]	LV	Sunnybrook	45 Subjects	--	FR-net	Caffe	DM=93.00%

							APD=1.41
[148]	LV	MICCAI 2017	150 Subjects	ROIs Extraction, DA	2D-CNN2	PyTorch	DM LV ED= 96.00% DM LV ES= 92.00% DM MYO ED=88.00% DM MYO ES=89.00%
[149]	Cardiac Walls	Clinical	20 Subjects	DA	PC-U Net	--	DM=88.50% HD=7.050mm
[150]	LV	Clinical	33 Subjects	CLAHE	DT-GAN	PyTorch	HD=2.23mm DM=93.00%
[151]	CMR	MICCAI 2017	100 Subjects	DA	DBAN	NA	DM=ED 96.00% DM ES=90.00% HD ED=6.7mm HD ES=8.1mm
[152]	Scar	Clinical	155 Subjects	DA	ACSNet	Keras TensorFlow	Acc LV=96.00%
		MICCAI 2017 Sunnybrook	245 Subjects				
[153]	MYO	MICCAI 2020	150 Subjects	--	3D U-Net	PyTorch	DM MYO=87.86%
[154]	LV, RV, and MYO	MICCAI 2017	150 Subjects	ROIs Extraction, YOLOv3	LFCN	TensorFlow	DM LV ED=96.00% DM LV ES=91.00% DM RV ED=93.00%, DM RV ES=85.00% DM MYO ED=87.00% DM MYO ES=89.00%
[155]	Cardiac Multi-task	MyoPS 2020	45 Subjects	DA	CMS-U-Net	PyTorch	DM MYO=58.10%
[156]	LV, RV, and MYO	Clinical	175 Subjects	DA	2D-CNN	NA	Acc=97.60%
[157]	LV blood pool and MYO	MICCAI 2020	150 Subjects	--	U-Net	NA	Acc=92.00% DM= 86.28%
[158]	LVM, LV, and RV	Different datasets	350 Patients	DA	U-Net	NA	DM= 85.48%
[159]		36 Unique Datasets	32 Subjects	DA	U-Net	Keras TensorFlow	DSC=88.00%
[160]	LV and RV	Clinical	Different Subjects	--	U-Net	NA	DM=95.00
[161]	LA, LV, RV Endo, and MYO, at ED and ES	STACOM	100 Subjects	GCAM	DR-U-Net	Keras TensorFlow	DM =92.80% HD=20.3mm ASD=1.38mm
[162]	LV,RV, and MYO	MICCAI 2017	100 Subjects	DA	U-Net	NA	DM=93.50%
		UK Biobank	100 Subjects				
[163]	RVM and LVM	MICCAI 2017	1902 Cardiac MR Images	DA	2D-CNN	Keras TensorFlow	DM=91.60%
[164]	LV Cavity, MYO, and RV Cavity	UK Biobank	100 Subjects	DA	2D-CNN	Python, Theano	DM LV=92.00% DM MYO=85.00% DM RV=89.00%
[165]	LV, RV, and MYO	MICCAI 2017	150 Subjects	DA	2D-CNN 3D-CNN	PyTorch	Different Results
[166]	LV	-	45 Subjects	DA	2D-CNN	Theano	CRPS =0.084 RMSE =65.6
		Kaggle	500 Patients				
[167]	AS	Clinical	20 Subjects	Different Methods	SSAE	--	AUC = 94.00%
[168]	LVM	Clinical	8 Subjects	--	ResNet-56	MXNet	DM= 86.00% HD=4.01mm
[169]	LV	LVSC	200 Subjects	DA	CPL Network MB Network	Python, TensorFlow	Sen=88.00% Spec=95.00%
		Kaggle	1140 Subjects				
[170]	LV Cavity	York University	33 Subjects	--	U-Net	Keras, Theano	DM=93.00%
		MICCAI 2009	45 Subjects				
[171]	VS	Automated Cardiac Diagnosis Challenge 2017	100 Subjects	DA	3D FCN	TensorFlow	DM=82.27% Prec=89.81%
[172]	LA, PV, and AFS	Clinical	???	Different Methods	SSAE	NA	Acc=91.00% Sen=95.00%
[173]	LV, RV And LV	MICCAI 2017	100 Exams	--	3D-CNN	NA	DM=90.00% HD=10.4mm

[174]	LV	Second Annual Data Science Bowl	7 Subjects	--	2D-CNN	MXNet	HD=3.70mm
[175]	LV, LVi, and RV	Clinical	--	DA	FastVentricle	Keras, TensorFlow	Different Results
[176]	LV	SCD MICCAI 2017 Kaggle	--	DA	U-Net	NA	--
[177]		Clinical	1,912 Subjects	DA	CVAE	TensorFlow	DM=87.92%
[178]	RV	Clinical	26 Subjects	--	3D CNN	--	DM=82.81%
[179]	RV	MICCAI 12	--	--	Multi-Task DNN	TensorFlow	DM=87.20%
[180]	LV	Clinical	30 Subjects	--	U-Net	PyTorch	DM=94.00%
[181]	MYO	Clinical	348 Subjects	--	RSE-Net Model	PyTorch	DM=82.01%
[182]	LA and PV	Clinical	???	--	Different Models	TensorFlow	Acc=99.70% DM=89.70%
[183]		UK Biobank	220 Subjects	DA	???	NA	Different Results
[184]	Scar	Clinical	Subjects	DA	Modified Version of ENet	NA	Acc=97.00% Sen=88.00% DSC=71.00%
[185]	LV	TWINS-UK	68 Subjects	--	T-FCNN	NA	DM=98.15%
[186]	LV, MYO, and RV	UK Biobank	5000 Images	DA	Syn-net LI-net	PyTorch	Different Results
[187]	Atrial	Clinical	3 Subjects	DA	Modified U-Net	NA	DM=94.88% HD=7.56mm
[188]	LV and MYO	Clinical MICCAI 2018 MICCAI 2019	75 Subjects 145 Subjects 56 Subjects	DA	2D-CNN	NA	--
[189]	LV	MICCAI 2009	45 Subjects	--	2D-CNN U-Net	NA	DM=95.10% HD=3.641mm
[190]	LV	SCD	45 Images	--	2D-CNN	NA	Acc=94.00% Sen=94.11% DM= 94.00%
[191]	BV	Clinical	145 Subjects	--	Bi-DBN	Theano	different Results
[192]	LV	STACOM MICCAI 2017	100 Subjects 100 Subjects	--	OF-net	NA	APD=0.90 DM =95.00%
[193]	LV	MICCAI 2019	56 Subjects	DA	CNN	Keras, TensorFlow	DM Epi=96.10% DM Endo=94.90% DM MYO=86.70%
[194]	LV, LV, RV	MICCAI 2017 MICCAI 2017	150 Subjects	--	2D-CNN	NA	DM=90.00%
[195]	LV	MICCAI 2017	150 Subjects	--	SegAN + U-Net B	NA	DM=95.87%
[196]	LV,RV, and MYO	Clinical	45 Subjects	DA	SRSCN	TensorFlow	DM MYO=81.20% DM LV=91.50% DM RV=88.20%
[197]	Multi-Sequence	MICCAI 2019	45 Subjects	DA	Dilated Residual U-Shape Network and CNN	Keras	DM LV=82.40% DM MYO=61.00% DM RV=71.00%
[198]	Segmentation	MICCAI 2017 BraTS 2017	150 Subjects 289 Subjects	DA	Weighted-RNN-GAN	Keras, TensorFlow	Different Results
[199]	LA	Clinical	100 Subjects	Resizing	CNN Inception V4 with AE	Keras, TensorFlow	DM=93.10% HD=4.2mm
[200]	LA and RV	Different Dataset	Different Subjects	ROIs Extraction	2D CNN, SAE	NA	Acc=98.66%
[201]	LV,RV, and MYO	MICCAI 2017	150 Subjects	ROIs Extraction	2D Residual CNN Bi-CLSTM	NA NA	Different Results
[202]	MYO	Clinical	195 Subjects	--	CNN	NA	DM=81.37%
[203]	LV, RV, and LVM	MICCAI 2017	100 Subjects	ROIs Extraction	L-CO-Net	NA	DM LV=96.80% DM RV=93.30% DM LVM=89.50%
[204]	Left and Right Chamber	Clinical	210 Subjects	--	U-Net	NA	Different Results
[205]	BV	MICCAI 2017	100 patients	DA	U-Net	PyTorch	DM RVC= 79.60% DM LVM=84.60% DM LVC=90.80%

[206]	LV	Sunnybrook	800 image slices	--	CNN with U-Net	NA	F1-S=95.90%
[207]	RA	Clinical	550 Images	DA	U-Net	NA	DM=94.88% JM=90.33% HD=7.5625mm
[208]	RA	Clinical	242 Subjects	--	U-Net	NA	HD=4.64mm
[209]	LV	InCor	59 Subjects	--	U-Net	NA	DM Endo=82.00% DM Epi=86.00% HD Endo=5.81mm HD Epi=6.69mm
		Sunnybrook	45 Subjects				
		MICCAI 2017	150 Subjects				
		MICCAI 2019	56 Subjects				
		LVSC 2011	200 Subjects				
[210]	LV and RV	Clinical	63 Subjects	DA	U-Net	Keras, TensorFlow	Acc=97.00%
		MICCAI 2017	100 Subjects				
[211]	LV Blood-Pool, MYO and RV Blood-Pool	MICCAI 2017	100 Subjects	DA	SegAN and 2D U-Net	NA	Different Results
[212]	MYO Infarction	Infarction Segmentation Challenge	15 Subjects	Different Methods	Chained U-Net	NA	DM=32.00%
[213]	MYO	Clinical	355 Subjects	--	U-Net	TensorFlow Keras	DM MYO=94.34% Acc MYO=99.873%
[214]	LV	Clinical	42 Female Breast Cancer Datasets	SFP, Zero-Crossing Edge Detection	DeepLabV3+ DCNN	NA	Acc=97.00% Dice=89.00%
[215]	MYO	HVSMR 2016	20 MR Images	--	3D FCNN	Keras	DM MYO=76.20%
[216]	LV, RV, and MYO	Clinical	150 Subjects	ROIs Extraction, DA	U-Net	TensorFlow	DM=92.00% HD=12.18mm Acc=92.00%
[217]	LV	Clinical	150 Subjects	ROIs Extraction, DA	2D FCN	MATLAB	DM= 93.00% Sen=98.00% Spec=94.00%
[218]	LV,RV	UK Biobank	1000 Subjects	--	CNN	NA	--
[219]	LV, RV, and MYO	MICCAI 2017	150 Patients	U-Net For ROIs Extraction	FCN, U-Net	Keras TensorFlow	DM LV=96.30%
[220]	LV, RV	MICCAI 2017	100 Subjects	--	U-Net	NA	Acc=90.00%
[221]	LV	MICCAI 2009	45 Subjects	--	LsU-Net	TensorFlow	DM LV Endo=92.15% DM LV Epi=95.42%
		2012 RV Segmentation Challenges	16 Subjects				
		Clinical	17 Subjects				
[222]	LV Myocardium	Clinical	56 Subjects	Contrast Enhancement	2D-Residual Neural Network	PyTorch	DM=85.43%
[223]	Four Cardiac Chambers	Clinical	150 Subjects	DA	U-Net CNN	MATLAB	DM=89.00%
[224]	LV, RV-LV	Clinical	108 Subjects	DA	U-Nets	TensorFlow	DM=87.00% HD=5.9mm
[225]	Blood Pool And Myocardium	HVSMR	10 Subjects	NA	GCEFG-R^{2}Net	PyTorch	DM Blood Pool=95.80% DM MYO=83.60%
[226]	LV and MYO	Kaggle	1140 Subjects	DA	U-Net (ResNet34 Backbone)	PyTorch, FastAI	DM LV=90.00% DM MYO=79.10%
		Clinical	22 Subjects				
[227]	LV, RV, and MYO	imATFIB	20 Cases	ROIs Extraction, DA	U-Net, DeepLabV3+	NA	DM=92.90%
[228]	LV	Sunnybrook	805 Images of 45 Cine-CMR	--	ROR-Unet	Keras	Different Results
[229]	FCEA Tissue	Clinical	100 Subjects	DA	U-Net	TensorFlow	DM=77.00%
[230]	Pathology	MICCAI 2020	45 Subjects	DA	TAU-Net	PyTorch	DM=63.60%
[231]	RVC,LVC,LVM	MICCAI 2017	150 Subjects	ROIs Extraction	U-Net	TensorFlow	Acc=92.00% Acc=91.00%
[232]	LV	Clinical	NA	ROIs Extraction	U-Net	NA	DM Epi= 94.07% DM MYO=88.27% DM Endo=91.77%

[233]	LV, RV	DBI	Different Subjects	ROIs Extraction, DA	U-Net	TensorFlow	DM LV=96.1%
[234]	LV	MICCAI 2017	100 Subjects	Data Enhancement	MMNet	PyTorch	DM=95.10% HD=7.00mm
[235]	RV	Clinical	45 Subjects	DA	FCDL	TensorFlow	DM=87.00% HD=7.55mm
[236]	Different Segmentation	2019 MSCMRSeg	45 Subjects	DA	Proposed Method	NA	Different Results
[237]	LV,RV, and MYO	MICCAI 2017	150 Subjects	DA	Proposed Method	PyTorch	ED: DM LV=89.67% DM RV=81.46% DM MYO=72.60%
							ES DM LV=81.33% DM RV=70.80% DM MYO=76.56%
[238]	MYO And Scar/Fibrosis	MICCAI Cardiac MR LV Segmentation Challenge	Different Subjects	--	ACSNet	Keras TensorFlow	DM LVM=79.00% HD LVM=6.70mm
[239]	RV	RVSC	48 Subjects	DA	TSU-net	Keras TensorFlow	DM Endo=86.00% DM Epi=90.00%
		MMWHS	80 Subjects				
[240]	CMR	MM-WHS Challenge 2017	60 CMR,60 CT Images	GAN	GBCUDA	NA	DM=59.20%
[241]	LV	Clinical	33 Subjects	ROIs Extraction	GAN, U-Net	PyTorch	DM=96.97%
[242]	LV	LVSC	200 Subjects	--	Attention U-Net	Keras TensorFlow	Sen=87.00% Spec=92.00%
[243]	CMR	Clinical	3333 Frames	--	MIFNet	PyTorch	DM=97.23% Sen=93.55%
[244]	LV	MICCAI 2017	150 Subjects	DA	FCN-MSPN and Co-Discriminators	Keras TensorFlow	Different Results
[245]	MYO	MyoPS 2020	45 Subjects	DA	AWSnet	PyTorch	DM=72.00%
[246]	LV, RV, and MYO	York University MICCAI 2009 MICCAI 2017	Different Subjects	Gamma Transformation	BLU-Net	PyTorch	Different Results
[247]	CMR Images	MICCAI 2018	145 Subjects	ROIs Extraction	U-Net, MC-Seg	PyTorch	DM=88.60% HD=4.21mm
[248]	CMR Images	MICCAI 2009	45 Subjects	--	U-Net Backbone	Keras, TensorFlow	DM LV=93.41% DM RV=89.74% DM MYO=89.74%
		MICCAI 2017	100 Subjects				
[249]	LV, RV, and MYO	MICCAI 2017	100 Subjects	DA	U-Net	NA	DM LV=72.00% DM RV=53.00% DM MYO=69.00%
[250]	LV, Scar	Clinical	34 Subjects	DA	CTAEM-Net	Keras a TensorFlow	Acc LV=86.43% Acc Scar=90.18%
[251]	LA	LASC	20 Subjects	--	3D SR-Net	NA	DM=93.29% F1-S=82.37%
[252]	LV	MICCAI 2009	45 Subjects	DA	FCDA-Net	PyTorch	DM ED= 93.59% DM EP=94.81% HD ED= 4.95% HD EP=3.18%
[253]	MYO	Clinical	60 Subjects	--	U-Net, Dense Nets, Attention Nets	Keras, TensorFlow	Different Results

4.5. Applications of DL for classification of CMR images

In this section, CVDs diagnosis papers using DL classification models are presented. A primary objective of these papers is to diagnose CVDs from HC. A summary of papers about CMR-based CVD diagnosis using DL classification models is presented in Table (5). Additionally, the number of DL classification models used to diagnose CVDs is depicted in Figure (14). As shown in Figure (14) and Table (5), CNN models are most exploited in classifying CMR images to diagnose CVDs. CNN models have performed extremely well in various medical applications to diagnose CVDs.
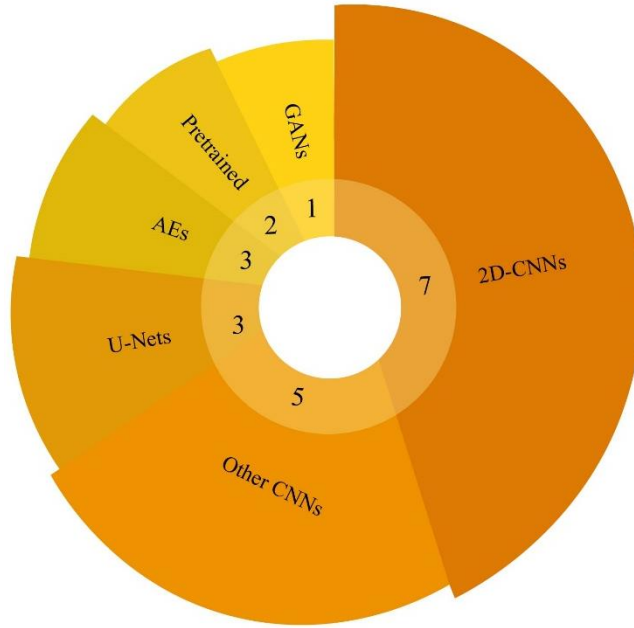
Fig. 14. Deep learning methods in classification of CMR images for Diagnosis of CVDs

Table 5. Research in classification of CMR imagers for in diagnosis of CVDs using DL methods

Ref	Application	Dataset	Number of cases	Preprocessing	DNN	Classifier	Toolbox	Performance
[254]	LV	ADSB	937 Subjects	Gabor Filter	2D-CNN	FC	Keras	Different Results
[255]	End-Diastole and End-Systole Frames	Clinical	420 Subjects	DA	TempReg-Net	FC layer	Caffe	ADF ED=0.38 ADF ES=0.44
[256]	LV	DSBCCD	1140 Subjects	ROIs Extraction, DA	2D-CNN	FC Layer	Keras	--
[257]	Classification	ILSVRC 2012	215 Subjects	DA	CaffeNet, CardioViewNet	Different	Caffe	F1-S=97.66% Recall=97.62%
[258]	MYO Ischemia	MICCAI 2009	21 Subjects	ROIs Extraction	CNN	NA	NA	Acc=86.39% Sen=90.00%
[259]	End-Diastole and End-Systole Frames	Free-Breathing CMR Data	10 Subjects	DA	2D-CNN	NA	Caffe	Acc=76.50%
		STACOM2011	200 Subjects					
[260]	Heart and right ventricle	Clinical	65 Subjects	DA	NF-RCNN	Softmax	--	AUC=98.00% Recall=96.00%
		York University	33 Subjects					
[261]	LV	DSBCCD	1140 Subjects	ROI Extraction	CNN	FC layer	Keras	EDV R^2=97.40 ESV R^2=97.60 EF R^2=82.80
[262]	LV	Sunnybrook, Kaggle	1140 Subjects	LBP Cascade Detector, DA	HFCN	Softmax	--	RMSE=13.20 ESV RMSE=9.31
[263]	Dense Thickness Estimation	MICCAI 2017	100 Subjects	--	U-Net-k	NA	NA	MSE=14.30 MAE=28.50
		Synthetic	Different Subjects					
		MICCAI 2019						
		MS-CMRSeg						
[264]	Detection	Clinical	363 Subjects	BBoxes, Visualization	2D-CNN	NA	NA	AUC=89.10%
[265]	Detection	Clinical	350 Subjects	ROIs Extraction	2D-CNN	Softmax	Keras	Acc=94.84% Sen=92.73% Spec=94.27%
[266]	Classification	MICCAI 2017	150 Subjects	Feature Extraction	Modified 2D and 3D U-Nets	Ensemble Learning	--	Acc=92.00%
[267]	Classification of MYO	Clinical	200 Subjects	--	Pretrained Models	Softmax	--	Acc=82.10%
[268]		Clinical		--	DeeplabV3		Keras	Different Results

	Classification and Prediction		198 HCM Subjects		InceptionResnet V2	LSTM Model		
[269]	Cardiac view	Clinical	Different Subjects	--	AE	Softmax	--	Acc=96.70%
[270]	Multitype cardiac indices estimation	Clinical	145 Subjects	ROIs Extraction	DCAE	?????	Caffe	NA
[271]	LV	Clinical	26 Subjects	ROIs Extraction	AE	--	--	Acc=97.50% Sens=84.20% Spec=98.60%
[272]	MYO	Clinical	566 Subjects	--	CNNEC	FC layer	--	Acc=95.30%
[273]	Cardiac Contraction	UK Biobank	12000 Subjects	--	CGAN	Softmax	--	DM=89.00%

4.6. Applications of DL for CMR images (other approaches)

This section discusses other applications of DL on CMR images. Table (6) presents DL applications using CMR data. Some of the most important applications of DL on CMR images comprises reconstruction [294], automatically computing cardiac views, generating CMR slices, and motion artifact correction. The number of DL models used for this are displayed in Figure (15). As can be seen, CNN models have gained great popularity in medical imaging.
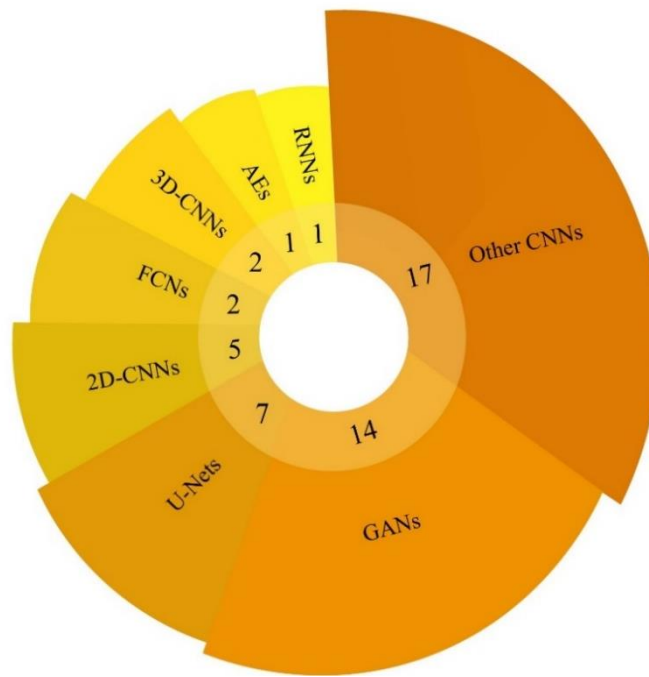
Fig. 15. Deep learning methods used for different approaches in CMR images.

Table 6. Deep leering models used in CMR images for different approaches.

Ref	Application	Dataset	Number of cases	Preprocessing	DNN	Classifier	Toolbox	Performance
[274]	Identifying the Missing Apical and Basal Slices	UK Biobank	100 Subjects	Global mask	2D-CNN	Softmax	NA	Pec=81.61% Pec=88.73%
[275]	Incomplete LV Coverage	UK Biobank	3400 Subjects	--	SCGANs	SVM	TensorFlow	Ac=92.50% Prec=87.60% Rec=90.50%
[276]	MRCA	Clinical	10 Subjects	ROIs Extraction	DLR	--	NA	DLR-HR-MRCA:11.3
[277]	Left Ventricle	York University	33 Subjects	Pyramid of Scales	2D-CNN	Softmax	NA	Acc=98.66% Sen=83.91% Spec=99.07%

Ref	Task	Dataset	Subjects	Preprocessing	Model	Activation	Framework	Results
[278]	LV and RV on short-axis CMR Images, LA, and RA	UK Biobank	4875 Subjects	DA	2D-CNN	Softmax	TensorFlow	Different Results
[279]	LV classification	SCD / CAP	140 Subjects	DA	2D-CNN	Softmax	Keras	DM=90.00%
[280]	Identifying	Clinical	Different Subjects	DA, ROIs Extraction	U-Net	--	NA	DM=76.00%
[281]	LV	STACOM18 LVQuan	145 Subjects	DA	U-Net	--	PyTorch	Different Results
[282]	Cardiac Cavity Segmentation Task	MICCAI 2017	200 CMR Images	DA	XCAT-GAN	--	NA	Different Results
		York University	33 CMR Images					
		XCAT Simulated	66 CMR Images					
		SCD	45 CMR Images					
		Clinical CMR	156 CMR Images					
[283]	Accurate Ventricular Volume Measurements	UK Biobank	4848 Subjects	--	I2-GAN	--	NA	CC LV=99.91
[284]	Accelerated Multi-Channel CMR	Publicly available abdominal	28 Subjects	Undersampling	PIC-GAN	Softmax	TensorFlow	Different Results
		Knee	20 Subjects					
[285]	NA	2019 MS-CMRSeg	45 Subjects	--	STN	--	NA	Different Results
[286]	Reconstruction	Clinical	58 Subjects		FCN	--	PyTorch	R^2=95.00%
[287]	Reconstruction	Clinical	35 Subjects	--	U-Net	--	NA	ESV=0.1 ml EDV=−0.9 ml
[288]	Reduce Motion Artifacts	MICCAI 2017 Cedars	159 Subjects	2D FFT	RNN	--	PyTorch	SSIM=88.40 PSNR=28.51
[289]	Enhance Spatial Detail	Clinical	367 Subjects	--	2D-CNN	--	Keras TensorFlow	LV EF=64
[290]	Reduce Scan Time	Clinical	108 Subjects	NUFFT, IFFT	MD-CNN	--	PyTorch	SSIM=87 MSE=11 DM LV=98%
[291]	Reconstruction	3D LGE CMR	219 Subjects	3D IFFT	CNN	--	PyTorch	SSIM=87.6 MSE=7.7
[292]	Spatial Resolution of CMR	Clinical / MICCAI 2012	Different Subjects	DA, IFFT	4DFlowNet	Sigmoid	TensorFlow	Flow Rate= 10.7
[293]	Reconstruction	Clinical	22 Subjects	DA	DL-ESPIRiT	--	TensorFlow	--
[294]	Reconstruction	MICCAI 2013	Different Datasets with Subjects	Using IFT and UFT Transform	NISTAD	--	NA	SSIM=98
[295]	Automatically Compute Cardiac Views	Clinical	391 Subjects	--	3D Extension of the 2D ENet	--	NA	Different Results
[296]	Reconstruction	Clinical	10 Subjects	??	Deep Cascade of CNNs	--	NA	--
[297]	Reconstruction	Clinical	Different Subjects	??	MoDL-STORM	--	TensorFlow	--
[298]	Produce CMR Images	MICCAI 2017	2980 Slices	DA	Proposed Model	--	NA	Different Results
		Sunnybrook	714 Slices					
[299]	Artefact Detection	UK Biobank	3465 CMR Images	ROIs Extraction, DA	3D Spatio-Temporal CNNs	Softmax	Keras TensorFlow	Acc= 98.20% Prec= 80.90%
[300]	Super Resolution CMR	Clinical	64 Subjects	DA	LSRGAN	--	NA	--
[301]	Motion Correction in CMR	Clinical	192 Subjects	???	Adversarial Autoencoder Network	--	TensorFlow	--
[302]	Analysis of MYO Native T1 Mapping Images	Clinical	665 Subjects	ROIs Extraction, DA	FCN	Softmax	TensorFlow	DM=85.00%

Ref	Task	Dataset	Subjects	Pre-processing	Model	Classifier	Framework	Results
[303]	Undersampling Artefact Reduction	Clinical	19 Subjects	--	Modified U-Net	--	NA	--
[304]	LV volumes and function	Clinical	50 Subjects	--	Inspired by U-Net	--	NA	LV ESV=73.1 LV SV=78.8 LV EF=52.2
[305]	Reconstruction	Clinical	4 Subjects	--	MoDL-SToRM	--	TensorFlow	--
[306]	Reconstruction	Clinical	178 Subjects	--	Cascaded CNN Models	--	NA	Different Results
[307]	LV segmentation	Sunnybrook	15 Subjects	--	P-GAN, U-Net	--	TensorFlow	--
[308]	Cardiovascular MR Scans	Clinical	159 LGE CMR Scans	DA	ScarGAN U-Net	--	NA	DM: LV End=89.90% LV Epi=90.60%
[309]	Reconstruction	MICCAI 2013	Different Subjects	--	DA-FWGAN	--	Python and TensorFlow	Different Results
[310]	4D Semantic CMR Synthesis	MICCAI 2017	100 Subjects	--	SPADE GAN	--	NA	--
[311]	generating CMR Slices	UK Biobank	402 Subjects	--	SPSGAN	--	NA	--
[312]	Medical synthetic images	Clinical	292 Subjects	ROIs Extraction	E-GAN and SimGAN	ResNet-50 and Xception	TensorFlow Keras	Acc=88.00%
[313]	Congenital heart disease	Clinical	345 Subjects	DA	PG-GAN	Softmax	TensorFlow	DM LV: 97.80%
[314]	Simulation for cardiac fiber structure	Clinical	246 Subjects	??	DCGAN	--	NA	--
[315]	motion artifact correction	Clinical	60 Subjects	DA	ResNet	Sigmoid + Convolution	PyTorch	PSNR=31.22
[316]	MYO infarction Classification	Clinical	73 Subjects	--	SDAE	SVM	PyTorch	Acc=87.60% Prec=86.20%
[317]	Full LV Coverage	UK Biobank	800000 volumes	DA	Fisher-Discriminative 3D-CNN	Fisher	NA	Prec:91.81%
		Sunnybrook	1120 volumes					
[318]	Cardiac Indices	MICCAI 2019	56 Subjects	--	U-Net and DenseNet	--	NA	DM=93.00%
[319]	Reconstruction	Clinical	45 Subjects	2D IFFT	DeepT1	FC	NA	--
[320]	LV cavity, RV, MYO at ED and ES	MICCAI 2017	100 Subjects	DA	DCNN	--	PyTorch	--
[321]	CMR Orientation and Segmentation	MyoPS	45 Subjects	--	CMRadjustNet	--	NA	Acc=98.70%
		MICCAI 2017	100 Subjects					
[322]	LV Segmentation	Sunnybrook	45 CMR Images	--	Registration Network	--	TensorFlow	DM=93.00%

4.7. Applications of DL for diagnosis of CVDs based on multimodal data

Much research is currently being conducted using multimodality to diagnose various diseases. In clinical research, multimodality has proved successful in diagnosing diseases. To this end, research has been presented in the field of CVDs diagnosis by combining CMR data with other medical imaging methods. In Table (7) and figure (16), the papers on diagnosing CVDs based on multimodalities using DL techniques are reported. As can be seen, to achieve high diagnostic accuracy for various CVDs, researchers have combined the CMR modality with other medical imaging modalities such as CT.
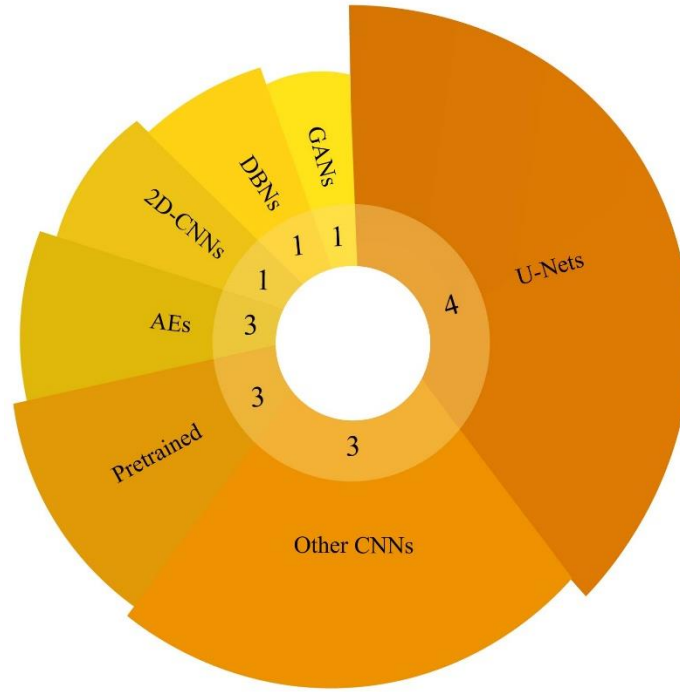
Fig.16. Deep learning conducted for diagnosing CVDs from multimodality data.

Table 7. Summary of deep learning studies conducted for diagnosing CVDs from multimodality data.

Ref	Application	Dataset	Modalities	Number of cases	Preprocessing	DNN	Classifier	Toolbox	Performance
[323]	Multi-task Image Segmentation	OASIS project	CMR and CT	Different Subjects	--	2D-CNN	Softmax	--	--
[324]	LV Segmentation	CETUS Challenge 2014	Echo	45 Subjects	ROIs Extraction	SAE,GVF-Snake	--	--	DM ED=11.20%
									DM ES=16.00%
[325]	Direct LV Estimation	Clinical	3D Echo	150 Subjects	--	CDBN	RF	--	Different Results
[326]	Cardiac substructures segmentation	STACOM 2017	CT and CMR	20 MR and 20 CT Images for Training, 40 Test Images	DA	MO-MP-CNN	Softmax	TensorFlow	Sen=83.10% Spec=99.90% Prec=86.80%
[327]	Whole Heart Segmentation	MMWHS Challenge	CT and CMR	20 Contrast-Enhanced CT Scans and 20 CMR	--	U-Net	--	Keras, Theano	Different Results
[328]	Segmentation	MICCAI 2017	CT and CMR	20 CMR and 20 CT	DA	PnP-AdaNet	Softmax	--	DM=63.90%
[329]	Estimating Multitype Cardiac Indices	NA	CT and CMR	2360 CT and 2900 CMR					
[330]	Anatomically Plausible Segmentation	JSRT, Sunnybrook	X-ray and CMR	247 X-ray and 45 CMR	DA	Post-DAE	RF	Keras	DM=47.00%
[331]	Cardiac Segmentation	MICCAI 2017	CMR and Ultrasound	150 Subjects	--	cVAE	--	--	--
		CAMUS		500 Subjects					
[332]	Segmentation	MM-WHS 2017	CT, CMR	20 CMR and 20 CT	--	GANSA	--	NA	DM=80.10%

5. Challenges

This section discusses the challenges faced during the CVDs diagnosis from using CMR data and DL techniques. Researchers constantly confront multiple challenges when presenting new approaches for

diagnosing CVDs using DL models, including datasets, DL models, rehabilitation tools, and hardware resources.

5.1. Datasets

Datasets are an essential part of DL-based CADS for detecting CVDs. Previously publicly available datasets of CMR data were introduced in Section 4.1. The available datasets of CMR images suffer from a scarcity of subjects, which hinders researchers using state-of-the-art DL models in CVDs diagnosis. Available datasets with CMR image segmentation applications contain confined subjects. In these datasets, there are limited ground truth images for each class. As a result, researchers face challenges when deploying advanced DL models to precisely segment CMR images. There are many types of heart disease for which early diagnosis is of pivotal significance. However, there are no available datasets of CMR modalities for different types of CVDs, which is another challenge.

5.2. Multimodality Dataset

CMR imaging is one of the most important screening methods to diagnose CVDs. In clinical applications, it is challenging for physicians to diagnose some CVDs from CMR images. To this end, physicians take advantage of multimodality imaging to diagnose CVDs. In this procedure, medical specialists exploit CMR images and other imaging techniques such as echo to diagnose CVDs. In [333-334], researchers have indicated that the utilization of multimodality imaging methods to obtain a more accurate diagnosis of CVDs.

In [326-332], to the diagnosis of CVDs, researchers have exploited multimodality datasets. It may be noted that there are multimodal datasets available for the diagnosis of CVDs. However, these datasets have limited subjects and few CVDs. Therefore, restricted access to multimodal datasets with various diseases and a large number of subjects is another associated challenge in the dataset section.

Due to these challenges in this field, until now, researchers have not been able to incorporate advanced DL methods using multimodality imaging to diagnose CVDs. Therefore, providing multimodality imaging datasets based on CMR images with a large number of subjects could facilitate valuable research in the field of CVDs diagnosis. Additionally, the availability of multimodality imaging datasets with a large number of subjects allows researchers to develop state-of-the-art DL methods to aid specialist physicians in diagnosing various types of CVDs.

5.3. Limitation CMR Data for Training of DL Models

Researchers have advanced in developing DL models, but there are still many challenges in achieving a real tool for diagnosing CVDs using these approaches. As discussed in the previous sections, many studies have been presented to diagnose CVDs from CMR images using DL techniques. However, achieving real diagnosis software requires the development of DL models based on CMR images. The lack of access to huge CMR datasets for researchers is an important challenge. Some papers have used pre-trained [98-100] or DA [71-73] models to overcome these challenges. Although pre-trained and DA techniques have an array of advantages, there are also challenges associated with them. For example, pre-trained models are trained on ImageNet data [98-100]. Researchers have employed these architectures in many works on medical images such as CMR and have achieved satisfactory results [268]. To enhance the effectiveness of pre-trained models, it is better to train them first on grayscale medical images and then use them to diagnose CVDs. In addition, DA methods play an important role in the generation of synthetic medical data for training DL models [71-73]. GAN models are very popular in synthetic data generation, such as CMR data [307]. Although these models have been largely successful in training the model and preventing overfitting of DL models, they need further development for real-world applications in diagnosing CVDs.

5.4. DL Models

This paper reviewed researches on the diagnosis of CVDs from CMR images using DL techniques. This section introduces the challenges associated with DL models in CVDs diagnosis research. Standard CNN models are often utilized in papers on CVD diagnosis based on CMR images. CNN models include segmentation and classification architectures in two dimensions [96-97]. Meanwhile, some papers have exploited 3D-CNN models which need a lot of input data for training and have more complex training compared to 2D-CNN models [96-97]. Besides, 3D-CNNs models require strong hardware resources for training [96-97]. Considering these cases, researchers face various challenges in developing 3D-CNN models to diagnose CVDs from CMR images. The lack of trust by physicians in the results of DL models about CVDs is another challenge. DL models normally yield high evaluation parameters (such as accuracy) in diagnosing CVDs from CMR images. The use of uncertainty techniques and explainable approaches can increase the trust of physicians in DL models to diagnose CVDs.

5.5. Explainable AI Models

To date, researchers have applied various DL models to diagnose CVDs. As previously discussed, various segmentation and classification techniques based on DL are employed to diagnose CVDs from CMR images. DL-based segmentation techniques are used to extract CVD-related areas from CMR images. DL-based classification models are also used to diagnose CVDs based on CMR images. One of the challenges of DL models in diagnosing CVDs is the failure to identify areas suspected of CVDs in the early stages and indicate them to physicians. Meanwhile, physicians require AI techniques that can diagnose CVDs in the early stages from CMR images. For this purpose, explainable AI methods have been presented by some researchers, which show disease diagnosis in the early stages using medical images [335-336]. For instance, explainable AI has been presented in research to display the early stages of brain tumors from CMR images [337-338]. Providing explainable AI techniques in conjunction with DL models can help specialists to more accurately diagnose CVDs using CMR images.

5.6. Hardware Resources

In this section, hardware resources for the implementation of DL models are presented as another challenge. As discussed above, implementing DL methods requires suitable hardware resources. Although a variety of high-performance hardware is offered for various applications, including the implementation of DL models, their high cost has made it impossible for all researchers to use them in research. For example, detecting CVDs from 3D data requires high hardware resources. Due to the lack of access to appropriate hardware resources, researchers convert 3D data to 2D. Additionally, they employ 2D models to detect different types of CVDs. Because implementing 3D DL models has several challenges, including memory shortage, increasing computational load, hardware cost, etc. [96-97]. Although Google and Amazon provide researchers with computing servers to implement advanced DL models [339-340], these tools are not suitable in real-time applications for detecting CVDs from CMR images.

6. Discussion

This study accomplished a comprehensive review of CVDs diagnosis research through CMR images using DL methods. CVDs diagnosis using CMR images based on DL techniques is summarized in Tables (4) to (7). A description of each paper is provided in Tables (4) to (7), including the application, dataset, number of samples, preprocessing methods, DL model, implementation tool, and evaluation parameters. A complete comparison is made between all studies in this field in terms of applications, datasets, DL models, and implementation tools.

6.1. Comparison of our work with other review papers

Review papers on diagnosing CVDs using ML and DL is summarized in Table (2). It can be noted from Table (2) that, some researchers have analyzed ML, DL, and ML-DL papers for the segmentation of different parts of the heart. Further, few researchers have proposed review papers on diagnosing CVDs through ECG signals using DL techniques. In this work, papers on the diagnosis of cardiac diseases from CMR images using DL schemes are reviewed. In our paper, all free and publicly available CMR datasets were first reported and then summarized in Table (2). The papers on segmentation, classification and other applications from CMR images using DL models were reviewed. In similar review papers, CMR papers for different applications have not been reviewed so far. Meanwhile, we have reviewed all the research in this field. Additionally, in our review paper, the challenges of diagnosing CVDs from CMR data using various DL methods are discussed in detail. Furthermore, the main future directions in our study are explained in detail, but they are not fully discussed in other reviews. In figure (17), our work is compared with other review papers in the diagnosis of CVDs using AI methods.
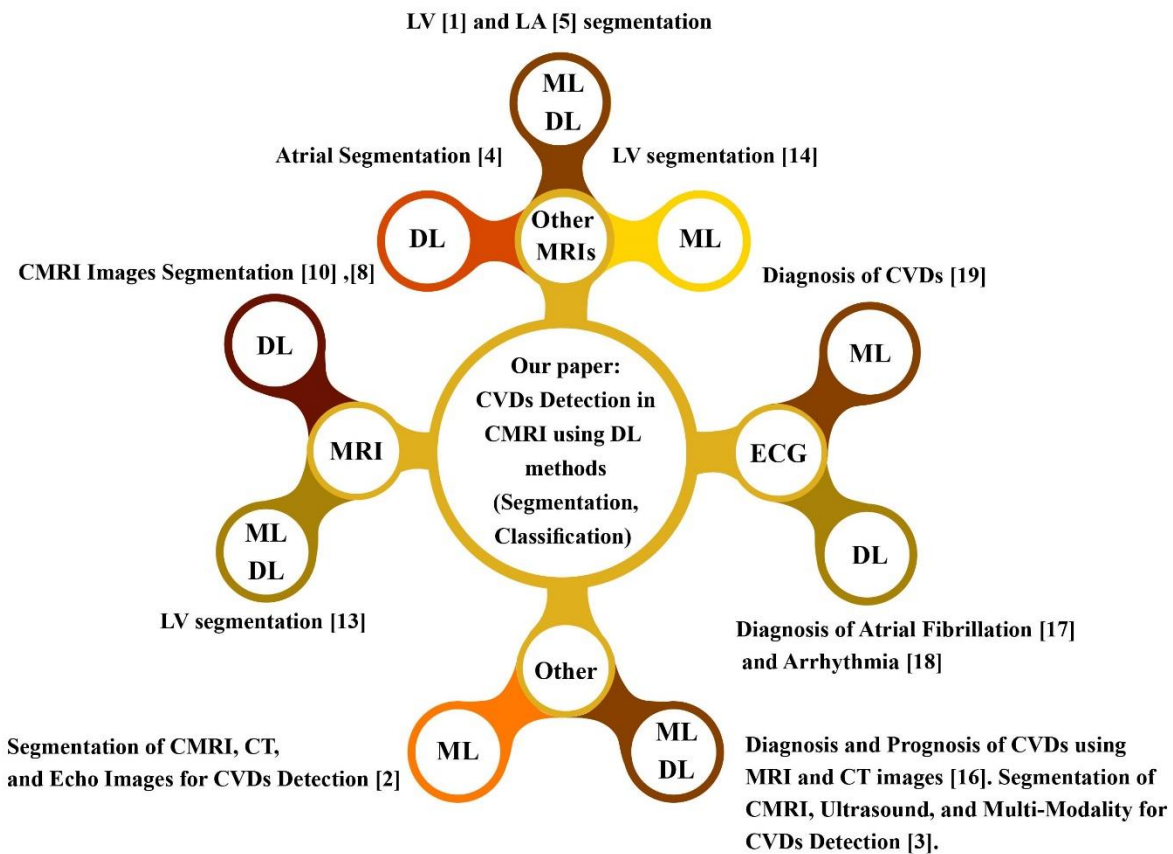
Fig. 17. Comparison of our study with other review papers published on CVDs detection using DL techniques.

6.2. Applications

In this section, various applications of DL on CMR data are introduced. The most important section of this paper deals with the presentation of segmentation and classification models based on DL for diagnosing CVDs from CMR images. In Tables (4) and (5), research on CVDs diagnosis using DL-based segmentation and classification techniques were presented, respectively. Other applications of DL models on CMR images are summarized in Table (6). Table (6) indicates few most important applications of DL on CMR images, including reconstruction [296], automatically computing cardiac views [295], and motion artifact

correction [301]. Besides, CVDs diagnosis research on the multimodal dataset using DL techniques is also reported in Table (7). The types of DL applications on CMR images are shown in Figure (18). As shown in Figure (18), it can be perceived that the DL-based segmentation methods are the most widely exploited in CVDs diagnosis using CMR images.
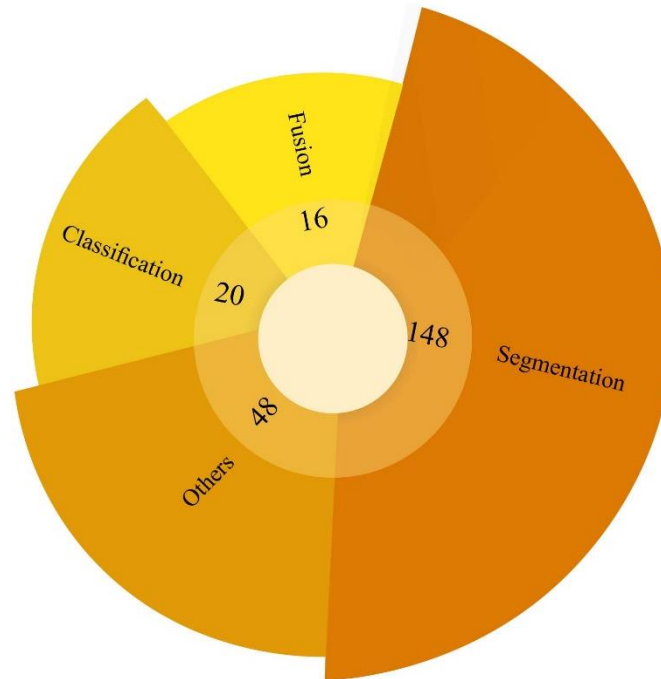
Fig. 18. Deep learning methods used in different applications with CMR images.

6.3. Datasets

In section 4.1, a variety of free and publicly available datasets of CMR images were described. It was observed that multiple CMR images datasets have been provided for segmentation and classification applications for diagnosing CVDs. The datasets used in the CVDs research are presented inthe part of the Tables (4) to (7). Accordingly, the datasets used for research in this field are shown in Figure (19). Figure (19) illustrates that the researchers focused most on the MICCAI 2017 dataset.

6.4. Deep learning models

DL-based applications for CMR images are discussed in this section. An overview of the famous DL models, such as CNN's, RNNs, AEs, GANs, U-Nets, and FCNs, are presented in this review paper. In the following, the types of DL models in CVDs detection research are summarized in Tables (4) to (7). Figure (20) displays the types of DL models used in this field. According to Figure (20), CNNs models are the most commonly used in this field of research. CNN models perform well on medical gray-scale images. As a result, researchers take advantage of CNNs models on CMR images due to their benefits. Additionally, Figure (20) shows that CNN-based segmentation models are highly popular for diagnosing CVDs in CMR images.
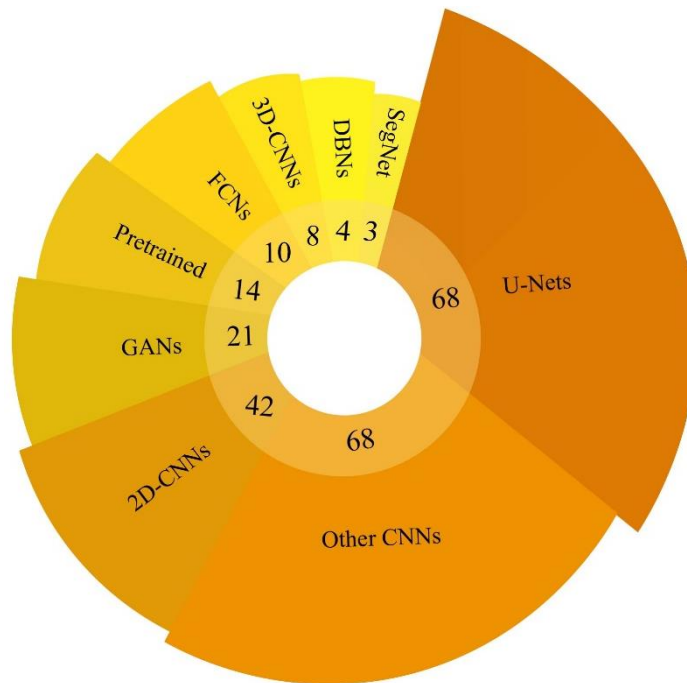
Fig. 19. CMR dataset used in diagnosis of CVDs using DL methods.
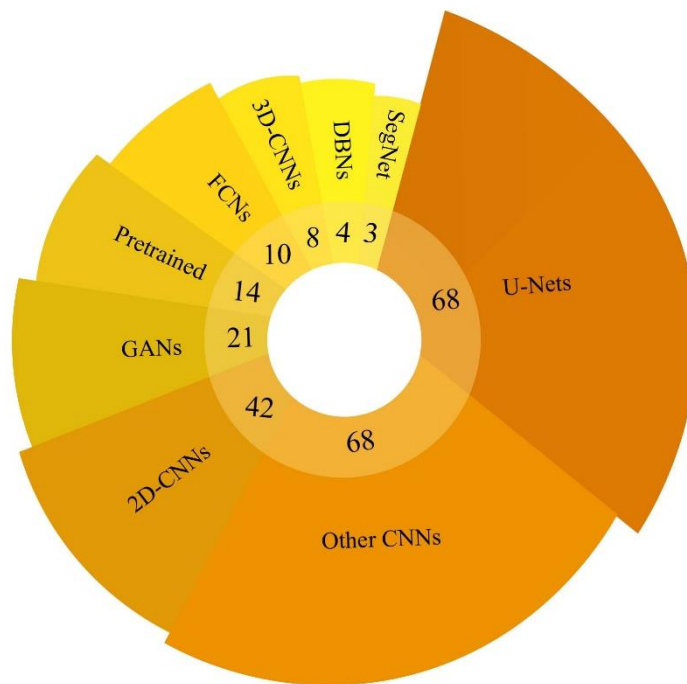
Fig. 20. Deep learning models used for diagnosis of CVDs from CMR images.

6.5. Toolboxes

To date, various toolboxes have been developed for implementing DL models. The toolboxes exploited to implement DL models are listed in Tables (4) to (7). TensorFlow, Keras, PyTorch, Theano, and Caffe are the most important toolboxes in DL applications for CMR images. In Figure (21), the types of DL toolboxes are displayed. According to Figure (21), the TensorFlow toolbox has been applied in most researches to

implement DL models. Due to its efficiency and simplicity, many researchers employed the Keras Toolbox to implement DL models in CMR research.
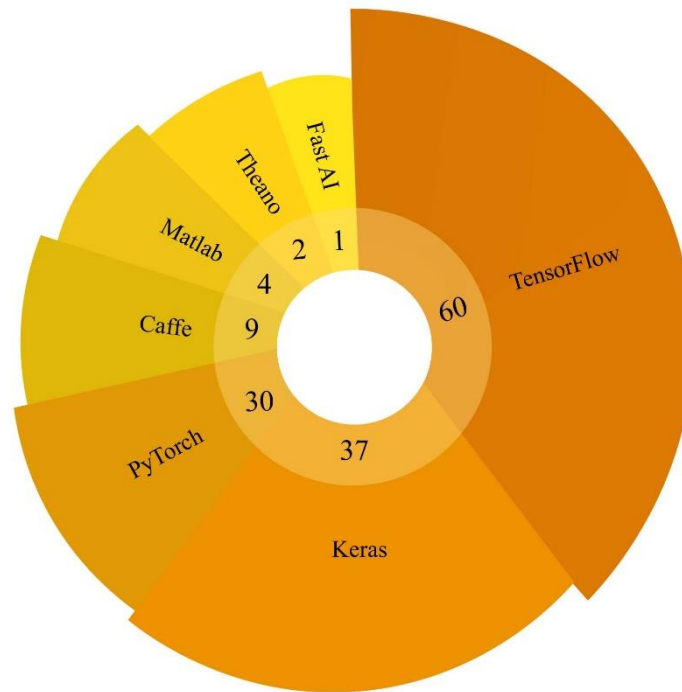
Fig. 21. Deep learning toolboxes used in the diagnosis of CVDs using CMR images.

7. Future work

This section outlines potential directions for future research on CVDs diagnosis from CMR images using DL techniques. The challenges related to CVDs detection using CMR data were discussed in the previous section. In this section, suggestions are made to overcome the challenges faced in diagnosing CVDs using DL techniques. Future work in this area includes dataset, DL models, and hardware resources. Addressing any challenges in the CVDs diagnosis field can lead to providing real software to assist specialists in the future.

7.1. Future works in datasets

This section is dedicated to future work on CVDs datasets containing CMR images. As mentioned earlier, researchers lack access to free datasets with large number of subjects of CMR images for diagnosis of CVDs. As a future work, providing available datasets with many cases from CMR images will bring about important research in CVDs. Additionally, for future work, providing available datasets of CAD, Arrhythmia, cardiomyopathy, CHD, mitral regurgitation, and angina can lead to more applied research.

By providing CMR datasets belonging to large number of subjects, can help to diagnose CVDs using state-of-the-art DL techniques. Also, datasets of CMR images with many subjects have not been made available to researchers to predict various types of CVDs, and this issue can be considered another future work. A discussion of the available datasets for the segmentation of CMR images is presented in Section 4.1. These datasets are provided to diagnose few CVDs. On the other hand, these datasets have limited number of subjects with few CVDs. As another future insight, researchers' access to CMR segmentation datasets with a large number of subjects could yield invaluable research in diagnosing CVDs.

7.2. Future Works in Multimodality Datasets

As previously discussed, the diagnosis of diseases by multimodality medical imaging techniques is of particular significance for specialist doctors. A medical imaging method often does not provide all the information necessary to diagnose a disease in full detail. Therefore, multimodality imaging techniques minimize doctors' errors when diagnosing CVDs. In references [333-334] few researchers have taken advantage of multimodality cardiac imaging methods for diagnosing CVDs and obtained promising results. For multimodality imaging research, various datasets available for detecting CVDs are not provided. For future work, researchers' access to datasets of multimodality cardiac imaging methods with many subjects can bring about worthy research to diagnose CVDs using DL techniques. For example, CMR-CT, CMR X-ray, and CMR-Ultrasound datasets have not yet been provided to the diagnosis of myocarditis disease. As a result, the provision of these datasets can yield valuable research in diagnosingdiagnosis of myocarditis disease with DL architectures.

7.3. DL Models

This section presents future works for DL methods in diagnosing CVDs using CMR images. As shown in Tables (4) to (7), the researchers used standard DL techniques for CVDs detection. In these studies, researchers have often applied the CNNs, RNNs, AEs, U-Nets, and FCNs models and improved models. Some state-of-the-art DL models include attention mechanism [341-343], transformers [344-345], GANs [74-76], graph CNNs [346-347], and deep reinforcement learning (RL) [348-349]. In the following, details of the state-of-the-art DL methods are discussed.

7.4. Deep Attention Mechanism

The attention mechanism is one of the newest areas of DL and has received attention from researchers in diagnosing various diseases [350-351]. These procedures use important input information to predict outputs [341-342]. Attention models are widely diverse, some of the most important of which comprise Attention CNNs [352], attention AEs [353], graph attention [354], and attention RNNs [355]. Researchers can utilize attention mechanism models in CVDs diagnosis using CMR images for future work.

7.4.1. Transformers

Recently, researchers introduced a novel class of DL models called transformers and exploited them in various applications. According to the reference [344], transformer techniques consist of two parts: decoder, and encoder, and use the self-attention architecture [344-345]. ViT is the most significant transformer architecture and has been employed in research for various disease diagnosis using medical data [356-357]. Graph transformers [358], polar transformers [359], and Vit transformers [360] are among the most important models.

7.4.2. Generative Adversarial Networks (GAN)

Another direction that can be investigated in the future is the applications of novel models of GANs in the diagnosis of CVDs. Recent variations of GANs can be used in various possible ways, for example, disentangled representation learning GAN (DR-GAN) and information maximizing GAN (InFoGAN) for representation learning [74-76]. Alternatively, researchers can use GANs for style transfer and unpaired image-to-image translation with Gated-GAN and CycleGAN [74-76]. Moreover, networks such as super-resolution GAN (SRGAN) have introduced methods for improving the quality of data [74-76], which can be used in CADS to help clinicians in their diagnosis.

7.4.3. Graph CNNs

Graph is one of the most popular fields of AI that is of great interest to researchers in ML and DL applications [346-347]. Until a few years ago, graph-based techniques were widely used in ML. However, DL-based graph approaches have recently been introduced, and satisfactory results have been achieved in various aspects [346-347]. DL-based graphs enjoy considerable diversity, some of the most important of which include graph CNNs [346-347], graph RNN [361], etc. In the future, Graph models can be used to diagnose CVDs.

7.4.4. Deep Reinforcement Learning (RL)

This field combines RL and DL and is used to address various problems such as medicine [362-363]. Deep RL models show impressive performance when dealing with large input data and can make optimal problem-solving decisions. Deep Q network (DQN) [364], deep deterministic policy gradient (DDPG) [365], and double DQN (DDQN) [366] are some of the most popular deep RL architectures.

7.4.5. Explainable AI

As mentioned in the previous section, DL models exploit segmentation or classification methods for diagnosing CVDs. However, physicians tend to distrust DL methods to diagnose CVDs using CMR images in the early stages. Because DL models are not efficient at detecting CVDs in the early stages from CMR images. To address this issue, explainable AI methods have been presented, which can be used as a post-processing step in DL-based CADS to the diagnosis of diseases. In future, explainable AI techniques [335-336] can be used to visualize the decisions made by AI by visualizing the abnormality. Hence, it helps to provide confidence to the clinicians in the automatic diagnosis of CVDs from CMR images using DL techniques.

7.4.6. Hardware Resources

In the previous section, lack of access to hardware resources was presented as an important challenge. To deal with this issue, researchers have proposed several techniques for the efficient implementation of DL models. The utilization of quantization and compression techniques for DL networks can be introduced as future work in this field [367-368]. Quantization and compression techniques greatly reduce the demanded computations in DL models [367-368]. This leads to deploying the proposed DL model on a computer, requiring fewer hardware resources. Recently, deep compact-size CNNs techniques have been introduced that do not require more powerful hardware resources to be implemented [369]. The most important models of deep compact-size CNNs are TinyNet [370] and MobileNets models [371].

8. Conclusion and findings

CVDs cause an adverse impact on the structure and function of the heart muscle, endangering human health worldwide. CAD, arrhythmia, heart failure, myocarditis, and HCD are the most critical CVDs [1-6]. CVDs are conditions affecting the heart or blood vessels and are usually due to the accumulation of fatty deposits inside the arteries and an increased risk of blood clots [9-11]. Uncontrolled high blood pressure can lead to hardening and thickening of the arteries and narrowing the vessels through which blood flows [14]. According to the Centers for Disease Control and Prevention (CDC), CVDs are the leading cause of death in the United States [15-17].

To date, various screening approaches for CVDs diagnosis have been introduced by specialists. ECG [19], Echo [27], exercise stress test [cite], carotid ultrasound [28], CT-Scan [32], and CMR images [35-36] are among the most significant methods for diagnosis of CVDs. On account of its merits, in recent years, CMR

imaging has been recognized as one of the best diagnostic techniques used for CVDs by specialist physicians [35-36].

To examine the structure of the heart, physicians use CMR images in CVDs diagnosis. The advantages of CMR data involve the absence of ionizing radiation, superior soft tissue contrast resolution, and high resolution [35-36]. However, despite the advantages mentioned above, CMR images are affected by different artifacts [36]. Additionally, analyzing CMR data is highly time-consuming and labor-intensive for specialist physicians due to the large number of slides recorded. To alleviate these challenges, extensive research is being conducted on the detection of CVDs on CMR images using DL models. This literature investigated the detection of CVDs from CMR images using DL models.

In the introduction section, a comprehensive discussion of CVDs, diagnostic methods in conjunction with advantages and disadvantages, the importance of DL techniques in CVDs diagnosis, and, ultimately, the structure of the review paper are discussed. This section discusses the merits and demerits of using medical imaging techniques such as CMR data to diagnose CVDs.

In the search strategy section, according to the PRISMA guidelines three levels of analysis were performed to select the papers. Additionally, the inclusion and exclusion criteria for selecting papers on the diagnosis of CVDs were summarized in Table (1).

In section 3, review papers published on detecting CVDs from CMR images were investigated using AI methods. First, each review paper was briefly described, and then their details were summarized in Table (2). At the end of this section, the novelty of our review paper is compared with other published works.

Section 4 introduced DL-based CADS to diagnose CVDs using CMR images. First, CADS steps were presented, including datasets, preprocessing techniques, and DL methods. In the following, the research on the diagnosis of CVDs from CMR data are summarized in four Tables: 1) segmentation, 2) classification, 3) other research, and 4) fusion research. According to this section, it was observed that researchers have carried out the most research in the field of CMR image segmentation to the diagnosis of CVDs.

The most important challenges for the diagnosis of CVDs from CMR images were reported in Section 5. This section discusses the challenges of datasets, multi-modality, DL models, and lack of hardware resources accessibility in diagnosing CVDs. Addressing existing challenges allows researchers to access applications to detect CVDs from CMR images.

The discussion section contains several subsections and important information on CVDs detection research is reported based on Tables (4) to (7). This section includes datasets, types of CVDs, applications, DL models, DL implementation tools, and classification techniques.

Section 7 is dedicated to future work on the detection of CVDs from CMR images using DL methods. Future directions are outlined for dataset, DL models, and hardware resources. A complete explanation is introduced for each of the future tasks, along with few novel approaches. This section allows researchers to exploit new ideas for datasets, DL models, and hardware resources in future research.

In recent years, invaluable research has been conducted to detect CVDs from CMR images using various AI techniques. Research shows that it will be possible to achieve real CVDs detection tools based on DL algorithms in the near future. We feel that, state-of-the-art technologies such as telemedicine [372] and IoMT [373] need to be applied with DL models to diagnose CVDs accurately.

Appendix A: Performance metrics

Accuracy is the ratio of correctly predicted observations to the total number of observations.

$$Acc = \frac{TP + TN}{FP + FN + TP + TN}$$

Sensitivity, or recall, is the ratio of the number of correctly predicted positive observations to the total number of cases with the condition of interest.

$$Sen = \frac{TP}{FN + TP}$$

Specificity is the number of correctly predicted negative observations to the total number of negative observations.

$$Spec = \frac{TN}{FN + TN}$$

Precision, or positive predictive value, is the number of correctly predicted positive observations to the total number of positive observations.

$$Prec = \frac{TP}{TP + FP}$$

F-score is the harmonic mean of precision and recall. F-core is preferred for datasets with imbalanced numbers of cases with and without the condition of interest.

$$F - Score = \frac{2\,TP}{2\,TP + FP + FN}$$

The dice coefficient, or Sørensen–Dice index, measures the similarity between two datasets.

$$Dice = \frac{2\,TP}{2\,TP + FP + FN}$$

Hausdorff distance, or Pompeiu–Hausdorff distance, measures how far two subsets of a metric space are from each other.

$$HD(A_s, B_s) = max\left\{\max_{a \in A_s}\min_{b \in B_s} d(a, b), \max_{b \in B_s}\min_{a \in A_s} d(b, a)\right\}$$

The Jaccard index, or the Jaccard similarity coefficient, measures the similarity and diversity of sample sets.

$$JAC(R, G) = \frac{|R \cap G|}{|R \cup G|}$$

References
[1] Ammari, A., Mahmoudi, R., Hmida, B., Saouli, R., & Bedoui, M. H. (2021). A review of approaches investigated for right ventricular segmentation using short-axis cardiac MRI. *IET Image Processing*.

[2] Chen, C., Qin, C., Qiu, H., Tarroni, G., Duan, J., Bai, W., & Rueckert, D. (2020). Deep learning for cardiac image segmentation: a review. *Frontiers in Cardiovascular Medicine*, 25.

[3] Savaashe, A. K., & Dharwadkar, N. V. (2019, March). A review on cardiac image segmentation. In *2019 3rd International Conference on Computing Methodologies and Communication (ICCMC)* (pp. 545-550). IEEE.

[4] Jamart, K., Xiong, Z., Maso Talou, G. D., Stiles, M. K., & Zhao, J. (2020). Mini review: deep learning for atrial segmentation from late gadolinium-enhanced MRIs. *Frontiers in Cardiovascular Medicine*, 7, 86.

[5] Li, L., Zimmer, V. A., Schnabel, J. A., & Zhuang, X. (2022). Medical image analysis on left atrial LGE MRI for atrial fibrillation studies: A review. *Medical Image Analysis*, 102360.

[6] Kwan, A. C., Salto, G., Cheng, S., & Ouyang, D. (2021). Artificial Intelligence in Computer Vision: Cardiac MRI and Multimodality Imaging Segmentation. *Current Cardiovascular Risk Reports*, 15(9), 1-8.

[7] Friedrich, S., Groß, S., König, I. R., Engelhardt, S., Bahls, M., Heinz, J., ... & Friede, T. (2021). Applications of artificial intelligence/machine learning approaches in cardiovascular medicine: A systematic review with recommendations. *European Heart Journal-Digital Health*, 2(3), 424-436.

[8] Wu, Y., Tang, Z., Li, B., Firmin, D., & Yang, G. (2021). Recent Advances in Fibrosis and Scar Segmentation From Cardiac MRI: A State-of-the-Art Review and Future Perspectives. *Frontiers in Physiology*, 12.

[9] Litjens, G., Ciompi, F., Wolterink, J. M., de Vos, B. D., Leiner, T., Teuwen, J., & Išgum, I. (2019). State-of-the-art deep learning in cardiovascular image analysis. *JACC: Cardiovascular imaging*, 12(8 Part 1), 1549-1565.

[10] Bala, S. A., & Kant, S. (2020). Deep learning-based model architectures for cardiac MRI segmentation: A Survey. *International Journal of Innovative Science, Engineering & Technology*, 129-135.

[11] Leiner, T., Rueckert, D., Suinesiaputra, A., Baeßler, B., Nezafat, R., Išgum, I., & Young, A. A. (2019). Machine learning in cardiovascular magnetic resonance: basic concepts and applications. *Journal of Cardiovascular Magnetic Resonance*, 21(1), 1-14.

[12] Krittanawong, C., Virk, H. U. H., Bangalore, S., Wang, Z., Johnson, K. W., Pinotti, R., ... & Tang, W. H. (2020). Machine learning prediction in cardiovascular diseases: a meta-analysis. *Scientific Reports*, 10(1), 1-11.

[13] Ribeiro, M. A., & Nunes, F. L. (2022). Left ventricle segmentation in cardiac MR: a systematic mapping of the last decade. *ACM Computing Surveys (CSUR)*.

[14] Irshad, M., Sharif, M., Yasmin, M., & Khan, A. (2018). A survey on left ventricle segmentation techniques in cardiac short axis MRI. *Current Medical Imaging*, 14(2), 223-237.

[15] Somani, S., Russak, A. J., Richter, F., Zhao, S., Vaid, A., Chaudhry, F., ... & Glicksberg, B. S. (2021). Deep learning and the electrocardiogram: review of the current state-of-the-art. *EP Europace*, 23(8), 1179-1191.

[16] Jiang, B., Guo, N., Ge, Y., Zhang, L., Oudkerk, M., & Xie, X. (2020). Development and application of artificial intelligence in cardiac imaging. *The British Journal of Radiology*, 93(1113), 20190812.

[17] Murat, F., Sadak, F., Yildirim, O., Talo, M., Murat, E., Karabatak, M., ... & Acharya, U. R. (2021). Review of deep learning-based atrial fibrillation detection studies. *International journal of environmental research and public health*, 18(21), 11302.

[18] Ebrahimi, Z., Loni, M., Daneshtalab, M., & Gharehbaghi, A. (2020). A review on deep learning methods for ECG arrhythmia classification. *Expert Systems with Applications: X*, 7, 100033.

[19] Chen, S. W., Wang, S. L., Qi, X. Z., Samuri, S. M., & Yang, C. (2022). Review of ECG detection and classification based on deep learning: Coherent taxonomy, motivation, open challenges and recommendations. *Biomedical Signal Processing and Control*, 74, 103493.

[20] Cassar, A., Holmes Jr, D. R., Rihal, C. S., & Gersh, B. J. (2009, December). Chronic coronary artery disease: diagnosis and management. In *Mayo Clinic Proceedings* (Vol. 84, No. 12, pp. 1130-1146). Elsevier.

[21] Alizadehsani, R., Abdar, M., Roshanzamir, M., Khosravi, A., Kebria, P. M., Khozeimeh, F., ... & Acharya, U. R. (2019). Machine learning-based coronary artery disease diagnosis: A comprehensive review. *Computers in biology and medicine*, 111, 103346.

[22] Otaki, Y., Singh, A., Kavanagh, P., Miller, R. J., Parekh, T., Tamarappoo, B. K., ... & Slomka, P. J. (2022). Clinical deployment of explainable artificial intelligence of SPECT for diagnosis of coronary artery disease. *Cardiovascular Imaging*, 15(6), 1091-1102.

[23] Yadav, S. S., & Jadhav, S. M. (2021). Detection of common risk factors for diagnosis of cardiac arrhythmia using machine learning algorithm. *Expert systems with applications*, *163*, 113807.

[24] Houssein, E. H., Hassaballah, M., Ibrahim, I. E., AbdElminaam, D. S., & Wazery, Y. M. (2022). An automatic arrhythmia classification model based on improved marine predators algorithm and convolutions neural networks. *Expert Systems with Applications*, *187*, 115936.

[25] Rodriguez Lozano, P. F., Rrapo Kaso, E., Bourque, J. M., Morsy, M., Taylor, A. M., Villines, T. C., ... & Salerno, M. (2022). Cardiovascular imaging for ischemic heart disease in women: time for a paradigm shift. *Cardiovascular Imaging*, *15*(8), 1488-1501.

[26] Li, J., Ke, L., Du, Q., Chen, X., & Ding, X. (2022). Multi-modal cardiac function signals classification algorithm based on improved DS evidence theory. *Biomedical Signal Processing and Control*, *71*, 103078.

[27] Alsharqi, M., Woodward, W. J., Mumith, J. A., Markham, D. C., Upton, R., & Leeson, P. (2018). Artificial intelligence and echocardiography. *Echo research and practice*, *5*(4), R115-R125.

[28] Narula, S., Shameer, K., Salem Omar, A. M., Dudley, J. T., & Sengupta, P. P. (2016). Machine-learning algorithms to automate morphological and functional assessments in 2D echocardiography. *Journal of the American College of Cardiology*, *68*(21), 2287-2295.

[29] Gottdiener, J. S. (2001). Overview of stress echocardiography: uses, advantages, and limitations. *Progress in cardiovascular diseases*, *43*(4), 315-334.

[30] van Velzen, S. G., Lessmann, N., Velthuis, B. K., Bank, I. E., van den Bongard, D. H., Leiner, T., ... & Išgum, I. (2020). Deep learning for automatic calcium scoring in CT: validation using multiple cardiac CT and chest CT protocols. *Radiology*, *295*(1), 66.

[31] Singh, G., Al'Aref, S. J., Van Assen, M., Kim, T. S., van Rosendael, A., Kolli, K. K., ... & Min, J. K. (2018). Machine learning in cardiac CT: basic concepts and contemporary data. *Journal of Cardiovascular Computed Tomography*, *12*(3), 192-201.

[32] Kirişli, H. A., Schaap, M., Metz, C. T., Dharampal, A. S., Meijboom, W. B., Papadopoulou, S. L., ... & van Walsum, T. (2013). Standardized evaluation framework for evaluating coronary artery stenosis detection, stenosis quantification and lumen segmentation algorithms in computed tomography angiography. *Medical image analysis*, *17*(8), 859-876.

[33] Lin, A., Kolossváry, M., Motwani, M., Išgum, I., Maurovich-Horvat, P., Slomka, P. J., & Dey, D. (2021). Artificial intelligence in cardiovascular CT: Current status and future implications. *Journal of cardiovascular computed tomography*, *15*(6), 462-469.

[34] van Assen, M., Martin, S. S., Varga-Szemes, A., Rapaka, S., Cimen, S., Sharma, P., ... & Schoepf, U. J. (2021). Automatic coronary calcium scoring in chest CT using a deep neural network in direct comparison with non-contrast cardiac CT: A validation study. *European journal of radiology*, *134*, 109428.

[35] Cau, R., Solinas, C., De Silva, P., Lambertini, M., Agostinetto, E., Scartozzi, M., ... & Saba, L. (2022). Role of cardiac MRI in the diagnosis of immune checkpoint inhibitor-associated myocarditis. *International Journal of Cancer*.

[36] Rahman, H., Scannell, C. M., Demir, O. M., Ryan, M., McConkey, H., Ellis, H., ... & Chiribiri, A. (2021). High-resolution cardiac magnetic resonance imaging techniques for the identification of coronary microvascular dysfunction. *Cardiovascular Imaging*, *14*(5), 978-986.

[37] Avard, E., Shiri, I., Hajianfar, G., Abdollahi, H., Kalantari, K. R., Houshmand, G., ... & Zaidi, H. (2022). Non-contrast Cine Cardiac Magnetic Resonance image radiomics features and machine learning algorithms for myocardial infarction detection. *Computers in biology and medicine*, *141*, 105145.

[38] Muscogiuri, G., Martini, C., Gatti, M., Dell'Aversana, S., Ricci, F., Guglielmo, M., ... & Pontone, G. (2021). Feasibility of late gadolinium enhancement (LGE) in ischemic cardiomyopathy using 2D-multisegment LGE combined with artificial intelligence reconstruction deep learning noise reduction algorithm. *International Journal of Cardiology*, *343*, 164-170.

[39] Leiner, T., Rueckert, D., Suinesiaputra, A., Baeßler, B., Nezafat, R., Išgum, I., & Young, A. A. (2019). Machine learning in cardiovascular magnetic resonance: basic concepts and applications. *Journal of Cardiovascular Magnetic Resonance*, *21*(1), 1-14.

[40] Shoeibi, A., Ghassemi, N., Heras, J., Rezaei, M., & Gorriz, J. M. (2022). Automatic Diagnosis of Myocarditis in Cardiac Magnetic Images Using CycleGAN and Deep PreTrained Models. In *International Work-Conference on the Interplay Between Natural and Artificial Computation* (pp. 145-155). Springer, Cham.

[41] Arafati, A., Hu, P., Finn, J. P., Rickers, C., Cheng, A. L., Jafarkhani, H., & Kheradvar, A. (2019). Artificial intelligence in pediatric and adult congenital cardiac MRI: an unmet clinical need. *Cardiovascular diagnosis and therapy*, *9*(Suppl 2), S310.

[42] Sander, J., de Vos, B. D., Wolterink, J. M., & Išgum, I. (2019, March). Towards increased trustworthiness of deep learning segmentation methods on cardiac MRI. In *Medical imaging 2019: image Processing* (Vol. 10949, pp. 324-330). SPIE.

[43] Delmondes, P. H., & Nunes, F. L. (2022). A systematic review of multi-slice and multi-frame descriptors in cardiac MRI exams. *Computer Methods and Programs in Biomedicine*, 106889.

[44] Chauhan, D., Anyanwu, E., Goes, J., Besser, S. A., Anand, S., Madduri, R., ... & Patel, A. R. (2022). Comparison of machine learning and deep learning for view identification from cardiac magnetic resonance images. *Clinical Imaging*, *82*, 121-126.

[45] Moridian, P., Ghassemi, N., Jafari, M., Salloum-Asfar, S., Sadeghi, D., Khodatars, M., ... & Acharya, U. R. (2022). Automatic Autism Spectrum Disorder Detection Using Artificial Intelligence Methods with MRI Neuroimaging: A Review. *arXiv preprint arXiv:2206.11233*.

[46] Shoeibi, A., Ghassemi, N., Khodatars, M., Moridian, P., Khosravi, A., Zare, A., ... & Acharya, U. R. (2022). Automatic Diagnosis of Schizophrenia and Attention Deficit Hyperactivity Disorder in rs-fMRI Modality using Convolutional Autoencoder Model and Interval Type-2 Fuzzy Regression. *arXiv preprint arXiv:2205.15858*.

[47] Shoeibi, A., Rezaei, M., Ghassemi, N., Namadchian, Z., Zare, A., & Gorriz, J. M. (2022). Automatic Diagnosis of Schizophrenia in EEG Signals Using Functional Connectivity Features and CNN-LSTM Model. In *International Work-Conference on the Interplay Between Natural and Artificial Computation* (pp. 63-73). Springer, Cham.

[48] Sadeghi, D., Shoeibi, A., Ghassemi, N., Moridian, P., Khadem, A., Alizadehsani, R., ... & Acharya, U. R. (2022). An overview of artificial intelligence techniques for diagnosis of Schizophrenia based on magnetic resonance imaging modalities: Methods, challenges, and future works. *Computers in Biology and Medicine*, 105554.

[49] Radau, P., Lu, Y., Connelly, K., Paul, G., Dick, A. J. W. G., & Wright, G. (2009). Evaluation framework for algorithms segmenting short axis cardiac MRI. *The MIDAS Journal-Cardiac MR Left Ventricle Segmentation Challenge*, *49*.

[50] Bernard, O., Lalande, A., Zotti, C., Cervenansky, F., Yang, X., Heng, P. A., ... & Jodoin, P. M. (2018). Deep learning techniques for automatic MRI cardiac multi-structures segmentation and diagnosis: is the problem solved?. *IEEE transactions on medical imaging*, *37*(11), 2514-2525.

[51] https://www.kaggle.com/c/second-annual-data-science-bowl

[52] Kadish, A. H., Bello, D., Finn, J. P., Bonow, R. O., Schaechter, A., Subacius, H., ... & Goldberger, J. J. (2009). Rationale and design for the defibrillators to reduce risk by magnetic resonance imaging evaluation (DETERMINE) trial. *Journal of cardiovascular electrophysiology*, *20*(9), 982-987.

[53] Petitjean, C., Zuluaga, M. A., Bai, W., Dacher, J. N., Grosgeorge, D., Caudron, J., ... & Yuan, J. (2015). Right ventricle segmentation from cardiac MRI: a collation study. *Medical image analysis*, *19*(1), 187-202.

[54] Andreopoulos, A., & Tsotsos, J. K. (2008). Efficient and generalizable statistical models of shape and appearance for analysis of cardiac MRI. *Medical image analysis*, *12*(3), 335-357.

[55] Pop, M., Sermesant, M., Zhao, J., Li, S., McLeod, K., Young, A., ... & Mansi, T. (Eds.). (2019). *Statistical Atlases and Computational Models of the Heart. Atrial Segmentation and LV Quantification Challenges: 9th International Workshop, STACOM 2018, Held in Conjunction with MICCAI 2018, Granada, Spain, September 16, 2018, Revised Selected Papers* (Vol. 11395). Springer.

[56] Yang, G., Hua, T., Xue, W., & Shuo, L. (2020). Left ventricle full quantification challenge MICCAI 2019.

[57] Mortazi, A., Karim, R., Rhode, K., Burt, J., & Bagci, U. (2017, September). CardiacNET: Segmentation of left atrium and proximal pulmonary veins from MRI using multi-view CNN. In *International Conference on Medical Image Computing and Computer-Assisted Intervention* (pp. 377-385). Springer, Cham.

[58] Mortazi, A., Burt, J., & Bagci, U. (2017, September). Multi-planar deep segmentation networks for cardiac substructures from MRI and CT. In *International Workshop on Statistical Atlases and Computational Models of the Heart* (pp. 199-206). Springer, Cham.

[59] Oakes, R. S., Badger, T. J., Kholmovski, E. G., Akoum, N., Burgon, N. S., Fish, E. N., ... & Marrouche, N. F. (2009). Detection and quantification of left atrial structural remodeling with delayed-enhancement magnetic resonance imaging in patients with atrial fibrillation. *Circulation*, *119*(13), 1758-1767.

[60] Zhuang, X., Li, L., Payer, C., Štern, D., Urschler, M., Heinrich, M. P., ... & Yang, G. (2019). Evaluation of algorithms for multi-modality whole heart segmentation: an open-access grand challenge. *Medical image analysis*, *58*, 101537.

[61] Littlejohns, T. J., Holliday, J., Gibson, L. M., Garratt, S., Oesingmann, N., Alfaro-Almagro, F., ... & Allen, N. E. (2020). The UK Biobank imaging enhancement of 100,000 participants: rationale, data collection, management and future directions. *Nature communications*, *11*(1), 1-12.

[62] Davis, C. A., Li, J., & Denney, T. J. (2006, April). Analysis of spectral changes and filter design in tagged cardiac MRI. In *3rd IEEE International Symposium on Biomedical Imaging: Nano to Macro, 2006.* (pp. 137-140). IEEE.

[63] Khozeimeh, F., Sharifrazi, D., Izadi, N. H., Joloudari, J. H., Shoeibi, A., Alizadehsani, R., ... & Islam, S. M. S. (2022). RF-CNN-F: random forest with convolutional neural network features for coronary artery disease diagnosis based on cardiac magnetic resonance. *Scientific Reports*, *12*(1), 1-12.

[64] Moravvej, S. V., Alizadehsani, R., Khanam, S., Sobhaninia, Z., Shoeibi, A., Khozeimeh, F., ... & Acharya, U. R. (2022). RLMD-PA: A Reinforcement Learning-Based Myocarditis Diagnosis Combined with a Population-Based Algorithm for Pretraining Weights. *Contrast Media & Molecular Imaging*, *2022*.

[65] Sharifrazi, D., Alizadehsani, R., Joloudari, J. H., Shamshirband, S., Hussain, S., Sani, Z. A., ... & Alinejad-Rokny, H. (2020). CNN-KCL: Automatic myocarditis diagnosis using convolutional neural network combined with k-means clustering.

[66] Khader, F., Schock, J., Truhn, D., Morsbach, F., & Haarburger, C. (2020, October). Adaptive preprocessing for generalization in cardiac MR image segmentation. In *International Workshop on Statistical Atlases and Computational Models of the Heart* (pp. 269-276). Springer, Cham.

[67] Chang, S., Han, K., Suh, Y. J., & Choi, B. W. (2022). Quality of science and reporting for radiomics in cardiac magnetic resonance imaging studies: a systematic review. *European Radiology*, 1-13.

[68] Gering, D. T. (2003, November). Automatic segmentation of cardiac MRI. In *International Conference on Medical Image Computing and Computer-Assisted Intervention* (pp. 524-532). Springer, Berlin, Heidelberg.

[69] Yang, F., Zuo, W. M., Wang, K. Q., & Zhang, H. (2008, September). 3D cardiac MRI data visualization based on volume data preprocessing and transfer function design. In *2008 Computers in Cardiology* (pp. 717-720). IEEE.

[70] Haarburger, C. (2021, January). Adaptive Preprocessing for Generalization in Cardiac MR Image Segmentation. In *Statistical Atlases and Computational Models of the Heart. M&Ms and EMIDEC Challenges: 11th International Workshop, STACOM 2020, Held in Conjunction with MICCAI 2020, Lima, Peru, October 4, 2020, Revised Selected Papers* (Vol. 12592, p. 269). Springer Nature.

[71] Wei, J., & Zou, K. (2019). Eda: Easy data augmentation techniques for boosting performance on text classification tasks. *arXiv preprint arXiv:1901.11196*.

[72] Perez, L., & Wang, J. (2017). The effectiveness of data augmentation in image classification using deep learning. *arXiv preprint arXiv:1712.04621*.

[73] Zhong, Z., Zheng, L., Kang, G., Li, S., & Yang, Y. (2020, April). Random erasing data augmentation. In *Proceedings of the AAAI conference on artificial intelligence* (Vol. 34, No. 07, pp. 13001-13008).

[74] Yi, X., Walia, E., & Babyn, P. (2019). Generative adversarial network in medical imaging: A review. *Medical image analysis*, *58*, 101552.

[75] Creswell, A., White, T., Dumoulin, V., Arulkumaran, K., Sengupta, B., & Bharath, A. A. (2018). Generative adversarial networks: An overview. *IEEE signal processing magazine*, *35*(1), 53-65.

[76] Goodfellow, I., Pouget-Abadie, J., Mirza, M., Xu, B., Warde-Farley, D., Ozair, S., ... & Bengio, Y. (2020). Generative adversarial networks. *Communications of the ACM*, *63*(11), 139-144.

[77] Goodfellow, I., Bengio, Y., & Courville, A. (2016). *Deep learning*. MIT press.

[78] Tajbakhsh, N., Jeyaseelan, L., Li, Q., Chiang, J. N., Wu, Z., & Ding, X. (2020). Embracing imperfect datasets: A review of deep learning solutions for medical image segmentation. *Medical Image Analysis*, *63*, 101693.

[79] Litjens, G., Kooi, T., Bejnordi, B. E., Setio, A. A. A., Ciompi, F., Ghafoorian, M., ... & Sánchez, C. I. (2017). A survey on deep learning in medical image analysis. *Medical image analysis*, *42*, 60-88.

[80] Cai, L., Gao, J., & Zhao, D. (2020). A review of the application of deep learning in medical image classification and segmentation. *Annals of translational medicine*, *8*(11).

[81] Bank, D., Koenigstein, N., & Giryes, R. (2020). Autoencoders. *arXiv preprint arXiv:2003.05991*.

[82] Pinaya, W. H. L., Vieira, S., Garcia-Dias, R., & Mechelli, A. (2020). Autoencoders. In *Machine learning* (pp. 193-208). Academic Press.

[83] Zaremba, W., Sutskever, I., & Vinyals, O. (2014). Recurrent neural network regularization. *arXiv preprint arXiv:1409.2329*.

[84] Medsker, L. R., & Jain, L. C. (2001). Recurrent neural networks. *Design and Applications*, *5*, 64-67.

[85] Shoeibi, A., Ghassemi, N., Khodatars, M., Moridian, P., Alizadehsani, R., Zare, A., ... & Gorriz, J. M. (2022). Detection of epileptic seizures on EEG signals using ANFIS classifier, autoencoders and fuzzy entropies. *Biomedical Signal Processing and Control*, *73*, 103417.

[86] Shoeibi, A., Sadeghi, D., Moridian, P., Ghassemi, N., Heras, J., Alizadehsani, R., ... & Gorriz, J. M. (2021). Automatic diagnosis of schizophrenia in EEG signals using CNN-LSTM models. *Frontiers in Neuroinformatics*, *15*.

[87] Shoeibi, A., Khodatars, M., Jafari, M., Moridian, P., Rezaei, M., Alizadehsani, R., ... & Acharya, U. R. (2021). Applications of deep learning techniques for automated multiple sclerosis detection using magnetic resonance imaging: A review. *Computers in Biology and Medicine*, *136*, 104697.

[88] Shoeibi, A., Ghassemi, N., Khodatars, M., Jafari, M., Moridian, P., Alizadehsani, R., ... & Nahavandi, S. (2021). Applications of epileptic seizures detection in neuroimaging modalities using deep learning techniques: methods, challenges, and future works. *arXiv preprint arXiv:2105.14278*.

[89] Ghassemi, N., Shoeibi, A., Khodatars, M., Heras, J., Rahimi, A., Zare, A., ... & Gorriz, J. M. (2021). Automatic diagnosis of covid-19 from ct images using cyclegan and transfer learning. *arXiv preprint arXiv:2104.11949*.

[90] Shoeibi, A., Khodatars, M., Ghassemi, N., Jafari, M., Moridian, P., Alizadehsani, R., ... & Acharya, U. R. (2021). Epileptic seizures detection using deep learning techniques: a review. *International Journal of Environmental Research and Public Health*, *18*(11), 5780.

[91] Shoeibi, A., Khodatars, M., Alizadehsani, R., Ghassemi, N., Jafari, M., Moridian, P., ... & Shi, P. (2020). Automated detection and forecasting of covid-19 using deep learning techniques: A review. *arXiv preprint arXiv:2007.10785*.

[92] Ghassemi, N., Shoeibi, A., & Rouhani, M. (2020). Deep neural network with generative adversarial networks pre-training for brain tumor classification based on MR images. *Biomedical Signal Processing and Control*, *57*, 101678.

[93] Boveiri, H. R., Khayami, R., Javidan, R., & Mehdizadeh, A. (2020). Medical image registration using deep neural networks: a comprehensive review. *Computers & Electrical Engineering*, *87*, 106767.

[94] Fritscher, K., Raudaschl, P., Zaffino, P., Spadea, M. F., Sharp, G. C., & Schubert, R. (2016, October). Deep neural networks for fast segmentation of 3D medical images. In *International Conference on Medical Image Computing and Computer-Assisted Intervention* (pp. 158-165). Springer, Cham.

[95] Niyas, S., Pawan, S. J., Kumar, M. A., & Rajan, J. (2021). Medical image segmentation using 3d convolutional neural networks: A review. *arXiv preprint arXiv:2108.08467*.

[96] Niyas, S., Pawan, S. J., Kumar, M. A., & Rajan, J. (2022). Medical image segmentation with 3D convolutional neural networks: A survey. *Neurocomputing*, *493*, 397-413.

[97] Dou, Q., Chen, H., Yu, L., Zhao, L., Qin, J., Wang, D., ... & Heng, P. A. (2016). Automatic detection of cerebral microbleeds from MR images via 3D convolutional neural networks. *IEEE transactions on medical imaging*, *35*(5), 1182-1195.

[98] Malik, H., Farooq, M. S., Khelifi, A., Abid, A., Qureshi, J. N., & Hussain, M. (2020). A comparison of transfer learning performance versus health experts in disease diagnosis from medical imaging. *IEEE Access*, *8*, 139367-139386.

[99] Kim, M., Yun, J., Cho, Y., Shin, K., Jang, R., Bae, H. J., & Kim, N. (2019). Deep learning in medical imaging. *Neurospine*, *16*(4), 657.

[100] Kim, D. H., & MacKinnon, T. (2018). Artificial intelligence in fracture detection: transfer learning from deep convolutional neural networks. *Clinical radiology*, *73*(5), 439-445.

[101] Chao, J., Badawi, A. A., Unnikrishnan, B., Lin, J., Mun, C. F., Brown, J. M., ... & Aung, K. M. M. (2019). CaRENets: Compact and resource-efficient CNN for homomorphic inference on encrypted medical images. *arXiv preprint arXiv:1901.10074*.

[102] Li, Y., Lin, S., Liu, J., Ye, Q., Wang, M., Chao, F., ... & Ji, R. (2021). Towards compact cnns via collaborative compression. In *Proceedings of the IEEE/CVF Conference on Computer Vision and Pattern Recognition* (pp. 6438-6447).

[103] Shamshad, F., Khan, S., Zamir, S. W., Khan, M. H., Hayat, M., Khan, F. S., & Fu, H. (2022). Transformers in medical imaging: A survey. *arXiv preprint arXiv:2201.09873*.

[104] Dalmaz, O., Yurt, M., & Çukur, T. (2021). ResViT: Residual vision transformers for multi-modal medical image synthesis. *arXiv preprint arXiv:2106.16031*.

[105] Anwar, S. M., Majid, M., Qayyum, A., Awais, M., Alnowami, M., & Khan, M. K. (2018). Medical image analysis using convolutional neural networks: a review. *Journal of medical systems*, *42*(11), 1-13.

[106] Shoeibi, A., Ghassemi, N., Alizadehsani, R., Rouhani, M., Hosseini-Nejad, H., Khosravi, A., ... & Nahavandi, S. (2021). A comprehensive comparison of handcrafted features and convolutional autoencoders for epileptic seizures detection in EEG signals. *Expert Systems with Applications*, *163*, 113788.

[107] Seyfioğlu, M. S., Özbayoğlu, A. M., & Gürbüz, S. Z. (2018). Deep convolutional autoencoder for radar-based classification of similar aided and unaided human activities. *IEEE Transactions on Aerospace and Electronic Systems*, *54*(4), 1709-1723.

[108] Tan, Q., Ye, M., Ma, A. J., Yang, B., Yip, T. C. F., Wong, G. L. H., & Yuen, P. C. (2020). Explainable uncertainty-aware convolutional recurrent neural network for irregular medical time series. *IEEE Transactions on Neural Networks and Learning Systems*, *32*(10), 4665-4679.

[109] Avendi, M. R., Kheradvar, A., & Jafarkhani, H. (2016). A combined deep-learning and deformable-model approach to fully automatic segmentation of the left ventricle in cardiac MRI. Medical image analysis, 30, 108-119.

[110] Avendi, M. R., Kheradvar, A., & Jafarkhani, H. (2016). Fully automatic segmentation of heart chambers in cardiac MRI using deep learning. Journal of Cardiovascular Magnetic Resonance, 18(1), 1-3.

[111] Luo, G., An, R., Wang, K., Dong, S., & Zhang, H. (2016, September). A deep learning network for right ventricle segmentation in short-axis MRI. In 2016 Computing in Cardiology Conference (CinC) (pp. 485-488). IEEE.

[112] Tran, P. V. (2016). A fully convolutional neural network for cardiac segmentation in short-axis MRI. arXiv preprint arXiv:1604.00494.

[113] Poudel, R. P., Lamata, P., & Montana, G. (2016). Recurrent fully convolutional neural networks for multi-slice MRI cardiac segmentation. In Reconstruction, segmentation, and analysis of medical images (pp. 83-94). Springer, Cham.

[114] Yang, X., Gobeawan, L., Yeo, S. Y., Tang, W. T., Wu, Z. Z., & Su, Y. (2016, September). Automatic segmentation of left ventricular myocardium by deep convolutional and de-convolutional neural networks. In 2016 Computing in Cardiology Conference (CinC) (pp. 81-84). IEEE.

[115] Yu, L., Yang, X., Qin, J., & Heng, P. A. (2016). 3D FractalNet: dense volumetric segmentation for cardiovascular MRI volumes. In Reconstruction, segmentation, and analysis of medical images (pp. 103-110). Springer, Cham.

[116] Wolterink, J. M., Leiner, T., Viergever, M. A., & Išgum, I. (2016). Dilated convolutional neural networks for cardiovascular MR segmentation in congenital heart disease. In Reconstruction, segmentation, and analysis of medical images (pp. 95-102). Springer, Cham.

[117] Avendi, M. R., Kheradvar, A., & Jafarkhani, H. (2017). Automatic segmentation of the right ventricle from cardiac MRI using a learning-based approach. Magnetic resonance in medicine, 78(6), 2439-2448.

[118] Curiale, A. H., Colavecchia, F. D., Kaluza, P., Isoardi, R. A., & Mato, G. (2017, September). Automatic myocardial segmentation by using a deep learning network in cardiac MRI. In 2017 XLIII Latin American Computer Conference (CLEI) (pp. 1-6). IEEE.

[119] Mortazi, A., Karim, R., Rhode, K., Burt, J., & Bagci, U. (2017, September). CardiacNET: Segmentation of left atrium and proximal pulmonary veins from MRI using multi-view CNN. In International Conference on Medical Image Computing and Computer-Assisted Intervention (pp. 377-385). Springer, Cham.

[120] Romaguera, L. V., Costa, M. G. F., Romero, F. P., & Costa Filho, C. F. F. (2017, March). Left ventricle segmentation in cardiac MRI images using fully convolutional neural networks. In Medical Imaging 2017: Computer-Aided Diagnosis (Vol. 10134, p. 101342Z). International Society for Optics and Photonics.

[121] Baumgartner, C. F., Koch, L. M., Pollefeys, M., & Konukoglu, E. (2017, September). An exploration of 2D and 3D deep learning techniques for cardiac MR image segmentation. In International Workshop on Statistical Atlases and Computational Models of the Heart (pp. 111-119). Springer, Cham.

[122] Winther, H. B., Hundt, C., Schmidt, B., Czerner, C., Bauersachs, J., Wacker, F., & Vogel-Claussen, J. (2017). ν-net: Deep Learning for Generalized Biventricular Cardiac Mass and Function Parameters. arXiv preprint arXiv:1706.04397.

[123] Ngo, T. A., Lu, Z., & Carneiro, G. (2017). Combining deep learning and level set for the automated segmentation of the left ventricle of the heart from cardiac cine magnetic resonance. Medical image analysis, 35, 159-171.

[124] Xiong, Z., Fedorov, V. V., Fu, X., Cheng, E., Macleod, R., & Zhao, J. (2018). Fully automatic left atrium segmentation from late gadolinium enhanced magnetic resonance imaging using a dual fully convolutional neural network. IEEE transactions on medical imaging, 38(2), 515-524.

[125] Duan, J., Bello, G., Schlemper, J., Bai, W., Dawes, T. J., Biffi, C., ... & Rueckert, D. (2019). Automatic 3D bi-ventricular segmentation of cardiac images by a shape-refined multi-task deep learning approach. IEEE transactions on medical imaging, 38(9), 2151-2164.

[126] Du, X., Yin, S., Tang, R., Zhang, Y., & Li, S. (2019). Cardiac-DeepIED: Automatic pixel-level deep segmentation for cardiac bi-ventricle using improved end-to-end encoder-decoder network. IEEE journal of translational engineering in health and medicine, 7, 1-10.

[127] Lan, Y., & Jin, R. (2019). Automatic Segmentation of the Left Ventricle from Cardiac MRI Using Deep Learning and Double Snake Model. IEEE Access, 7, 128641-128650.

[128] Zheng, Q., Delingette, H., Duchateau, N., & Ayache, N. (2018). 3-D consistent and robust segmentation of cardiac images by deep learning with spatial propagation. IEEE transactions on medical imaging, 37(9), 2137-2148.

[129] Bernard, O., Lalande, A., Zotti, C., Cervenansky, F., Yang, X., Heng, P. A., ... & Jodoin, P. M. (2018). Deep learning techniques for automatic MRI cardiac multi-structures segmentation and diagnosis: is the problem solved? IEEE transactions on medical imaging, 37(11), 2514-2525.

[130] Zhang, H., Cao, X., Xu, L., & Qi, L. (2019, August). Conditional Convolution Generative Adversarial Network for Bi-ventricle Segmentation in Cardiac MR Images. In Proceedings of the Third International Symposium on Image Computing and Digital Medicine (pp. 118-122).

[131] Nasr-Esfahani, M., Mohrekesh, M., Akbari, M., Soroushmehr, S. R., Nasr-Esfahani, E., Karimi, N., ... & Najarian, K. (2018, July). Left ventricle segmentation in cardiac MR images using fully convolutional network. In 2018 40th Annual International Conference of the IEEE Engineering in Medicine and Biology Society (EMBC) (pp. 1275-1278). IEEE.

[132] Moccia, S., Banali, R., Martini, C., Muscogiuri, G., Pontone, G., Pepi, M., & Caiani, E. G. (2019). Development and testing of a deep learning-based strategy for scar segmentation on CMR-LGE images. Magnetic Resonance Materials in Physics, Biology and Medicine, 32(2), 187-195.

[133] Leng, S., Yang, X., Zhao, X., Zeng, Z., Su, Y., Koh, A. S., ... & Zhong, L. (2018, July). Computational platform based on deep learning for segmenting ventricular endocardium in long-axis cardiac MR imaging. In 2018 40th Annual International Conference of the IEEE Engineering in Medicine and Biology Society (EMBC) (pp. 4500-4503). IEEE.

[134] Dong, J., Liu, C., Yang, C., Lin, N., & Cao, Y. (2018, October). Robust Segmentation of the Left Ventricle from Cardiac MRI via Capsule Neural Network. In Proceedings of the 2nd International Symposium on Image Computing and Digital Medicine (pp. 88-91).

[135] Hu, H., Pan, N., Wang, J., Yin, T., & Ye, R. (2019). Automatic segmentation of left ventricle from cardiac MRI via deep learning and region constrained dynamic programming. Neurocomputing, 347, 139-148.

[136] Ngo, T. A., & Carneiro, G. (2013, September). Left ventricle segmentation from cardiac MRI combining level set methods with deep belief networks. In 2013 IEEE International Conference on Image Processing (pp. 695-699). IEEE.

[137] Yang, F., Zhang, Y., Lei, P., Wang, L., Miao, Y., Xie, H., & Zeng, Z. (2019). A deep learning segmentation approach in free-breathing real-time cardiac magnetic resonance imaging. BioMed research international, 2019.

[138] Khened, M., Kollerathu, V. A., & Krishnamurthi, G. (2019). Fully convolutional multi-scale residual DenseNets for cardiac segmentation and automated cardiac diagnosis using ensemble of classifiers. Medical image analysis, 51, 21-45.

[139] Zotti, C., Luo, Z., Lalande, A., & Jodoin, P. M. (2018). Convolutional neural network with shape prior applied to cardiac MRI segmentation. IEEE journal of biomedical and health informatics, 23(3), 1119-1128.

[140] Qi, L., Zhang, H., Tan, W., Qi, S., Xu, L., Yao, Y., & Qian, W. (2019). Cascaded Conditional Generative Adversarial Networks With Multi-Scale Attention Fusion for Automated Bi-Ventricle Segmentation in Cardiac MRI. IEEE Access, 7, 172305-172320.

[141] Abdelmaguid, E., Huang, J., Kenchareddy, S., Singla, D., Wilke, L., Nguyen, M. H., & Altintas, I. (2018). Left ventricle segmentation and volume estimation on cardiac mri using deep learning. arXiv preprint arXiv:1809.06247.

[142] Seo, B., Mariano, D., Beckfield, J., Madenur, V., Hu, Y., Reina, T., ... & Altintas, I. (2019). Cardiac MRI Image Segmentation for Left Ventricle and Right Ventricle using Deep Learning. arXiv preprint arXiv:1909.08028.

[143] Li, Z., Lou, Y., Yan, Z., Al'Aref, S., Min, J. K., Axel, L., & Metaxas, D. N. (2019, April). Fully Automatic Segmentation Of Short-Axis Cardiac MRI Using Modified Deep Layer Aggregation. In 2019 IEEE 16th International Symposium on Biomedical Imaging (ISBI 2019) (pp. 793-797). IEEE.

[144] Abdeltawab, H., Khalifa, F., Taher, F., Beache, G., Mohamed, T., Elmaghraby, A., ... & El-Baz, A. (2019, December). Automatic Segmentation and Functional Assessment of the Left Ventricle using U-net Fully Convolutional Network. In 2019 IEEE International Conference on Imaging Systems and Techniques (IST) (pp. 1-6). IEEE.

[145] Yang, X., Tjio, G., Yang, F., Ding, J., Kumar, S., Leng, S., ... & Su, Y. (2019, July). A Multi-channel Deep Learning Approach for Segmentation of the Left Ventricular Endocardium from Cardiac Images. In 2019 41st Annual International Conference of the IEEE Engineering in Medicine and Biology Society (EMBC) (pp. 4016-4019). IEEE.

[146] Tan, L. K., Liew, Y. M., Lim, E., & McLaughlin, R. A. (2016, December). Cardiac left ventricle segmentation using convolutional neural network regression. In 2016 IEEE EMBS Conference on Biomedical Engineering and Sciences (IECBES) (pp. 490-493). IEEE.

[147] Chen, M., Fang, L., & Liu, H. (2019, April). FR-NET: Focal loss constrained deep residual networks for segmentation of cardiac MRI. In 2019 IEEE 16th International Symposium on Biomedical Imaging (ISBI 2019) (pp. 764-767). IEEE.

[148] Abdeltawab, H., Khalifa, F., Taher, F., Alghamdi, N. S., Ghazal, M., Beache, G., ... & El-Baz, A. (2020). A deep learning-based approach for automatic segmentation and quantification of the left ventricle from cardiac cine MR images. Computerized Medical Imaging and Graphics, 101717.

[149] Ye, M., Huang, Q., Yang, D., Wu, P., Yi, J., Axel, L., & Metaxas, D. (2020). PC-U Net: Learning to Jointly Reconstruct and Segment the Cardiac Walls in 3D from CT Data. arXiv preprint arXiv:2008.08194.

[150] Decourt, C., & Duong, L. (2020). Semi-supervised generative adversarial networks for the segmentation of the left ventricle in pediatric MRI. Computers in Biology and Medicine, 123, 103884.

[151] Yang, X., Zhang, Y., Lo, B., Wu, D., Liao, H., & Zhang, Y. (2020). DBAN: Adversarial Network with Multi-Scale Features for Cardiac MRI Segmentation. IEEE Journal of Biomedical and Health Informatics.

[152] Abramson, H. G., Popescu, D. M., Yu, R., Lai, C., Shade, J. K., Wu, K. C., ... & Trayanova, N. A. (2020). Anatomically-Informed Deep Learning on Contrast-Enhanced Cardiac MRI for Scar Segmentation and Clinical Feature Extraction. arXiv preprint arXiv:2010.11081.

[153] Zhang, Y. (2020). Cascaded Convolutional Neural Network for Automatic Myocardial Infarction Segmentation from Delayed-Enhancement Cardiac MRI. arXiv preprint arXiv:2012.14128.

[154] Yang, W., & Li, S. (2020, April). A Lightweight Fully Convolutional Network for Cardiac MRI Segmentation. In 2020 International Conference on Computer Information and Big Data Applications (CIBDA) (pp. 168-171). IEEE.

[155] Li, W., Wang, L., & Qin, S. (2020, October). CMS-UNet: Cardiac Multi-task Segmentation in MRI with a U-Shaped Network. In Myocardial Pathology Segmentation Combining Multi-Sequence CMR Challenge (pp. 92-101). Springer, Cham.

[156] Scannell, C. M., Veta, M., Villa, A. D., Sammut, E. C., Lee, J., Breeuwer, M., & Chiribiri, A. (2020). Deep-learning-based preprocessing for quantitative myocardial perfusion MRI. Journal of Magnetic Resonance Imaging, 51(6), 1689-1696.

[157] Ma, J. (2020). Cascaded Framework for Automatic Evaluation of Myocardial Infarction from Delayed-Enhancement Cardiac MRI. arXiv preprint arXiv:2012.14556.

[158] Full, P. M., Isensee, F., Jäger, P. F., & Maier-Hein, K. (2020). Studying Robustness of Semantic Segmentation under Domain Shift in cardiac MRI. arXiv preprint arXiv:2011.07592.

[159] Morris, E. D., Ghanem, A. I., Dong, M., Pantelic, M. V., Walker, E. M., & Glide-Hurst, C. K. (2020). Cardiac substructure segmentation with deep learning for improved cardiac sparing. Medical physics, 47(2), 576-586.

[160] Retson, T. A., Masutani, E. M., Golden, D., & Hsiao, A. (2020). Clinical performance and role of expert supervision of deep learning for cardiac ventricular volumetry: a validation study. Radiology: Artificial Intelligence, e190064.

[161] Vesal, S., Maier, A., & Ravikumar, N. (2020). Fully Automated 3D Cardiac MRI Localisation and Segmentation Using Deep Neural Networks. Journal of Imaging, 6(7), 65.

[162] Guo, F., Ng, M., Goubran, M., Petersen, S. E., Piechnik, S. K., Neubauer, S., & Wright, G. (2020). Improving cardiac MRI convolutional neural network segmentation on small training datasets and dataset shift: A continuous kernel cut approach. Medical image analysis, 61, 101636.

[163] Simantiris, G., & Tziritas, G. (2020). Cardiac MRI Segmentation with a Dilated CNN Incorporating Domain-Specific Constraints. IEEE Journal of Selected Topics in Signal Processing, 14(6), 1235-1243.

[164] Bai, W., Oktay, O., Sinclair, M., Suzuki, H., Rajchl, M., Tarroni, G., … & Rueckert, D. (2017, September). Semi-supervised learning for network-based cardiac MR image segmentation. In International Conference on Medical Image Computing and Computer-Assisted Intervention (pp. 253-260). Springer, Cham.

[165] Patravali, J., Jain, S., & Chilamkurthy, S. (2017, September). 2D-3D fully convolutional neural networks for cardiac MR segmentation. In International Workshop on Statistical Atlases and Computational Models of the Heart (pp. 130-139). Springer, Cham.

[166] Narayan, T. (2017). Automated Left Ventricle Segmentation in Cardiac MRIs using Convolutional Neural Networks. ArXiv preprint arXiv, 1705, 13-20.

[167] Yang, G., Zhuang, X., Khan, H., Haldar, S., Nyktari, E., Ye, X., … & Firmin, D. (2017, April). A fully automatic deep learning method for atrial scarring segmentation from late gadolinium-enhanced MRI images. In 2017 IEEE 14th International Symposium on Biomedical Imaging (ISBI 2017) (pp. 844-848). IEEE.

[168] Chen, A., Zhou, T., Icke, I., Parimal, S., Dogdas, B., Forbes, J., … & Chin, C. L. (2017, September). Transfer learning for the fully automatic segmentation of left ventricle myocardium in porcine cardiac cine MR images. In International Workshop on Statistical Atlases and Computational Models of the Heart (pp. 21-31). Springer, Cham.

[169] Tan, L. K., Liew, Y. M., Lim, E., & McLaughlin, R. A. (2017). Convolutional neural network regression for short-axis left ventricle segmentation in cardiac cine MR sequences. Medical image analysis, 39, 78-86.

[170] Yang, X., Zeng, Z., & Yi, S. (2017). Deep convolutional neural networks for automatic segmentation of left ventricle cavity from cardiac magnetic resonance images. IET Computer Vision, 11(8), 643-649.

[171] Yang, X., Bian, C., Yu, L., Ni, D., & Heng, P. A. (2017, September). Class-balanced deep neural network for automatic ventricular structure segmentation. In International workshop on statistical atlases and computational models of the heart (pp. 152-160). Springer, Cham.

[172] Yang, G., Zhuang, X., Khan, H., Haldar, S., Nyktari, E., Ye, X., … & Firmin, D. (2017, July). Segmenting atrial fibrosis from late gadolinium-enhanced cardiac MRI by deep-learned features with stacked sparse auto-encoders. In Annual Conference on Medical Image Understanding and Analysis (pp. 195-206). Springer, Cham.

[173] Zotti, C., Luo, Z., Humbert, O., Lalande, A., & Jodoin, P. M. (2017, September). GridNet with automatic shape prior registration for automatic MRI cardiac segmentation. In International Workshop on Statistical Atlases and Computational Models of the Heart (pp. 73-81). Springer, Cham.

[174] Zhou, T., Icke, I., Dogdas, B., Parimal, S., Sampath, S., Forbes, J., … & Chen, A. (2017, February). Automatic segmentation of left ventricle in cardiac cine MRI images based on deep learning. In Medical Imaging 2017: Image Processing (Vol. 10133, p. 101331W). International Society for Optics and Photonics.

[175] Lieman-Sifry, J., Le, M., Lau, F., Sall, S., & Golden, D. (2017, June). FastVentricle: cardiac segmentation with Enet. In International Conference on Functional Imaging and Modeling of the Heart (pp. 127-138). Springer, Cham.

[176] Yang, G., Yu, S., Dong, H., Slabaugh, G., Dragotti, P. L., Ye, X., … & Firmin, D. (2017). DAGAN: Deep de-aliasing generative adversarial networks for fast compressed sensing MRI reconstruction. IEEE transactions on medical imaging, 37(6), 1310-1321.

[177] Biffi, C., Cerrolaza, J. J., Tarroni, G., de Marvao, A., Cook, S. A., O'Regan, D. P., & Rueckert, D. (2019, April). 3D high-resolution cardiac segmentation reconstruction from 2D views using conditional variational autoencoders. In 2019 IEEE 16th International Symposium on Biomedical Imaging (ISBI 2019) (pp. 1643-1646). IEEE.

[178] Giannakidis, A., Kamnitsas, K., Spadotto, V., Keegan, J., Smith, G., Glocker, B., … & Firmin, D. N. (2016, January). Fast fully automatic segmentation of the severely abnormal human right ventricle from cardiovascular magnetic resonance images using a multi-scale 3D convolutional neural network. In 2016 12th International Conference on Signal-Image Technology & Internet-Based Systems (SITIS) (pp. 42-46). IEEE.

[179] Zhang, L., Karanikolas, G. V., Akçakaya, M., & Giannakis, G. B. (2018, April). Fully automatic segmentation of the right ventricle via multi-task deep neural networks. In 2018 IEEE International Conference on Acoustics, Speech and Signal Processing (ICASSP) (pp. 6677-6681). IEEE.

[180] Abdeltawab, H., Khalifa, F., Taher, F., Beache, G., Mohamed, T., Elmaghraby, A., … & El-Baz, A. (2019, October). A novel deep learning approach for left ventricle automatic segmentation in cardiac cine mr. In 2019 Fifth International Conference on Advances in Biomedical Engineering (ICABME) (pp. 1-4). IEEE.

[181] Qayyum, A., Lalande, A., Decourselle, T., Pommier, T., Cochet, A., & Meriaudeau, F. (2020). Segmentation of the Myocardium on Late-Gadolinium Enhanced MRI based on 2.5 D Residual Squeeze and Excitation Deep Learning Model. ArXiv preprint arXiv:2005.13643.

[182] Yang, G., Chen, J., Gao, Z., Zhang, H., Ni, H., Angelini, E., … & Firmin, D. (2018, July). Multiview sequential learning and dilated residual learning for a fully automatic delineation of the left atrium and pulmonary veins from late gadolinium-enhanced cardiac MRI images. In 2018 40th Annual International Conference of the IEEE Engineering in Medicine and Biology Society (EMBC) (pp. 1123-1127). IEEE.

[183] Qin, C., Bai, W., Schlemper, J., Petersen, S. E., Piechnik, S. K., Neubauer, S., & Rueckert, D. (2018, September). Joint learning of motion estimation and segmentation for cardiac MR image sequences. In International Conference on Medical Image Computing and Computer-Assisted Intervention (pp. 472-480). Springer, Cham.

[184] Moccia, S., Banali, R., Martini, C., Moscogiuri, G., Pontone, G., Pepi, M., & Caiani, E. G. (2018, September). Automated Scar Segmentation From CMR-LGE Images Using a Deep Learning Approach. In 2018 Computing in Cardiology Conference (CinC) (Vol. 45, pp. 1-4). IEEE.

[185] Savioli, N., Vieira, M. S., Lamata, P., & Montana, G. (2018, October). Automated segmentation on the entire cardiac cycle using a deep learning work-flow. In 2018 Fifth International Conference on Social Networks Analysis, Management and Security (SNAMS) (pp. 153-158). IEEE.

[186] Schlemper, J., Oktay, O., Bai, W., Castro, D. C., Duan, J., Qin, C., … & Rueckert, D. (2018, September). Cardiac MR segmentation from undersampled k-space using deep latent representation learning. In International Conference on Medical Image Computing and Computer-Assisted Intervention (pp. 259-267). Springer, Cham.

[187] Zhao, M., Wei, Y., Lu, Y., & Wong, K. K. (2020). A novel U-Net approach to segment the cardiac chamber in magnetic resonance images with ghost artifacts. Computer Methods and Programs in Biomedicine, 196, 105623.

[188] Tilborghs, S., Dresselaers, T., Claus, P., Bogaert, J., & Maes, F. (2020). Shape Constrained CNN for Cardiac MR Segmentation with Simultaneous Prediction of Shape and Pose Parameters. ArXiv preprint arXiv:2010.08952.

[189] Wu, B., Fang, Y., & Lai, X. (2020). Left Ventricle Automatic Segmentation in Cardiac MRI Using a Combined CNN and U-net Approach. Computerized Medical Imaging and Graphics, 101719.

[190] Rostami, A., Amirani, M. C., & Yousef-Banaem, H. (2020). Segmentation of the left ventricle in cardiac MRI based on convolutional neural network and level set function. Health and Technology, 10(5), 1155-1162.

[191] Du, X., Zhang, W., Zhang, H., Chen, J., Zhang, Y., Warrington, J. C., ... & Li, S. (2018). Deep regression segmentation for cardiac bi-ventricle MR images. IEEE Access, 6, 3828-3838.

[192] Yan, W., Wang, Y., van der Geest, R. J., & Tao, Q. (2019). Cine MRI analysis by deep learning of optical flow: Adding the temporal dimension. Computers in biology and medicine, 111, 103356.

[193] Dong, Z., Du, X., & Liu, Y. (2020). Automatic segmentation of left ventricle using parallel end–end deep convolutional neural networks framework. Knowledge-Based Systems, 204, 106210.

[194] Zotti, C., Luo, Z., Lalande, A., Humbert, O., & Jodoin, P. M. (2017). Novel deep convolution neural network applied to MRI cardiac segmentation. arXiv preprint arXiv:1705.08943.

[195] Upendra, R. R., Dangi, S., & Linte, C. A. (2019, June). An adversarial network architecture using 2d U-Net models for segmentation of left ventricle from cine cardiac MRI. In International Conference on Functional Imaging and Modeling of the Heart (pp. 415-424). Springer, Cham.

[196] Yue, Q., Luo, X., Ye, Q., Xu, L., & Zhuang, X. (2019, October). Cardiac segmentation from LGE MRI using deep neural network incorporating shape and spatial priors. In International Conference on Medical Image Computing and Computer-Assisted Intervention (pp. 559-567). Springer, Cham.

[197] Chen, J., Li, H., Zhang, J., & Menze, B. (2019, October). Adversarial convolutional networks with weak domain-transfer for multi-sequence cardiac MR images segmentation. In International Workshop on Statistical Atlases and Computational Models of the Heart (pp. 317-325). Springer, Cham.

[198] Rezaei, M., Yang, H., & Meinel, C. (2018, December). Generative adversarial framework for learning multiple clinical tasks. In 2018 Digital Image Computing: Techniques and Applications (DICTA) (pp. 1-8). IEEE.

[199] Ghosh, S., Ray, N., Boulanger, P., Punithakumar, K., & Noga, M. (2020, April). Automated Left Atrial Segmentation from Magnetic Resonance Image Sequences Using Deep Convolutional Neural Network with Autoencoder. In 2020 IEEE 17th International Symposium on Biomedical Imaging (ISBI) (pp. 1756-1760). IEEE.

[200] Irmawati, D., Wahyunggoro, O., & Soesanti, I. (2020, October). Recent Trends of Left and Right Ventricle Segmentation in Cardiac MRI Using Deep Learning. In 2020 12th International Conference on Information Technology and Electrical Engineering (ICITEE) (pp. 380-383). IEEE.

[201] Liu, T., Tian, Y., Zhao, S., Huang, X., & Wang, Q. (2020). Residual convolutional neural network for cardiac image segmentation and heart disease diagnosis. IEEE Access, 8, 82153-82161.

[202] Chen, Z., Lalande, A., Salomon, M., Decourselle, T., Pommier, T., Perrot, G., & Couturier, R. (2020, July). Myocardial Infarction Segmentation From Late Gadolinium Enhancement MRI By Neural Networks and Prior Information. In 2020 International Joint Conference on Neural Networks (IJCNN) (pp. 1-8). IEEE.

[203] Hasan, S. K., & Linte, C. A. (2020, July). L-CO-Net: Learned Condensation-Optimization Network for Segmentation and Clinical Parameter Estimation from Cardiac Cine MRI. In 2020 42nd Annual International Conference of the IEEE Engineering in Medicine & Biology Society (EMBC) (pp. 1217-1220). IEEE.

[204] Penso, M., Moccia, S., Scafuri, S., Muscogiuri, G., Pontone, G., Pepi, M., & Caiani, E. G. (2020, September). Automated Left and Right Chamber Segmentation in Cardiac MRI Using Dense Fully Convolutional Neural Network. In 2020 Computing in Cardiology (pp. 1-4). IEEE.

[205] Chang, Q., Yan, Z., Lou, Y., Axel, L., & Metaxas, D. N. (2020, April). Soft-Label Guided Semi-Supervised Learning for Bi-Ventricle Segmentation in Cardiac Cine MRI. In 2020 IEEE 17th International Symposium on Biomedical Imaging (ISBI) (pp. 1752-1755). IEEE.

[206] Cigánek, J., & Képešiová, Z. Processing and Visualization of Medical Images Using Machine Learning and Virtual Reality. In 2020 Cybernetics & Informatics (K&I) (pp. 1-6). IEEE.

[207] Lu, Y., Fu, X., Li, X., & Qi, Y. (2020, July). Cardiac chamber segmentation using deep learning on magnetic resonance images from patients before and after atrial septal occlusion surgery. In 2020 42nd Annual International Conference of the IEEE Engineering in Medicine & Biology Society (EMBC) (pp. 1211-1216). IEEE.

[208] Regehr, M., Volk, A., Noga, M., & Punithakumar, K. (2020, April). Machine Learning and Graph Based Approach to Automatic Right Atrial Segmentation from Magnetic Resonance Imaging. In 2020 IEEE 17th International Symposium on Biomedical Imaging (ISBI) (pp. 826-829). IEEE.

[209] Graves, C. V., Moreno, R. A., Rebelo, M. S., Nomura, C. H., & Gutierrez, M. A. (2020, July). Improving the generalization of deep learning methods to segment the left ventricle in short axis MR images. In 2020 42nd Annual International Conference of the IEEE Engineering in Medicine & Biology Society (EMBC) (pp. 1203-1206). IEEE.

[210] Vigneault, D. M., Xie, W., Bluemke, D. A., & Noble, J. A. (2017, June). Feature tracking cardiac magnetic resonance via deep learning and spline optimization. In International Conference on Functional Imaging and Modeling of the Heart (pp. 183-194). Springer, Cham.

[211] Upendra, R. R., Dangi, S., & Linte, C. A. (2020, March). Automated segmentation of cardiac chambers from cine cardiac MRI using an adversarial network architecture. In Medical Imaging 2020: Image-Guided Procedures, Robotic Interventions, and Modeling (Vol. 11315, p. 113152Y). International Society for Optics and Photonics.

[212] Sharma, R., Eick, C. F., & Tsekos, N. V. (2020, October). Myocardial Infarction Segmentation in Late Gadolinium Enhanced MRI Images using Data Augmentation and Chaining Multiple U-Net. In 2020 IEEE 20th International Conference on Bioinformatics and Bioengineering (BIBE) (pp. 975-980). IEEE.

[213] Brahim, K., Qayyum, A., Lalande, A., Boucher, A., Sakly, A., & Meriaudeau, F. (2021, January). A deep learning approach for the segmentation of myocardial diseases. In 2020 25th International Conference on Pattern Recognition (ICPR) (pp. 4544-4551). IEEE.

[214] Kar, J., Cohen, M. V., McQuiston, S. P., & Malozzi, C. M. (2021). A deep-learning semantic segmentation approach to fully automated MRI-based left-ventricular deformation analysis in cardiotoxicity. Magnetic Resonance Imaging, 78, 127-139.

[215] Wang, T., Wang, J., Zhao, J., & Zhang, Y. (2021). A Myocardial Segmentation Method Based on Adversarial Learning. BioMed Research International, 2021.

[216] Ammar, A., Bouattane, O., & Youssfi, M. (2021). Automatic cardiac cine MRI segmentation and heart disease classification. Computerized Medical Imaging and Graphics, 88, 101864.

[217] Shaaf, Z. F., Jamil, M. M. A., Ambar, R., Alattab, A. A., Yahya, A. A., & Asiri, Y. (2022). Automatic Left Ventricle Segmentation from Short-Axis Cardiac MRI Images Based on Fully Convolutional Neural Network. *Diagnostics*, *12*(2), 414.

[218] Hu, H., Pan, N., Liu, H., Liu, L., Yin, T., Tu, Z., & Frangi, A. F. (2021). Automatic segmentation of left and right ventricles in cardiac MRI using 3D-ASM and deep learning. *Signal Processing: Image Communication*, *96*, 116303.

[219] da Silva, I. F. S., Silva, A. C., de Paiva, A. C., & Gattass, M. (2022). A cascade approach for automatic segmentation of cardiac structures in short-axis cine-MR images using deep neural networks. *Expert Systems with Applications*, *197*, 116704.

[220] Niharika Das, Sujoy Das. Cardiac MRI Segmentation Using Deep Learning, 31 January 2022, PREPRINT (Version 1) available at Research Square [https://doi.org/10.21203/rs.3.rs-1271768/v1]

[221] Wang, Y., Zhang, Y., Wen, Z., Tian, B., Kao, E., Liu, X., ... & Liu, J. (2021). Deep learning based fully automatic segmentation of the left ventricular endocardium and epicardium from cardiac cine MRI. *Quantitative Imaging in Medicine and Surgery*, *11*(4), 1600.

[222] Ahmad, I., Qayyum, A., Gupta, B. B., Alassafi, M. O., & AlGhamdi, R. A. (2022). Ensemble of 2D Residual Neural Networks Integrated with Atrous Spatial Pyramid Pooling Module for Myocardium Segmentation of Left Ventricle Cardiac MRI. *Mathematics*, *10*(4), 627.

[223] Arai, H., Kawakubo, M., Sanui, K., Iwamoto, R., Nishimura, H., & Kadokami, T. (2022). Assessment of Bi-Ventricular and Bi-Atrial Areas Using Four-Chamber Cine Cardiovascular Magnetic Resonance Imaging: Fully Automated Segmentation with a U-Net Convolutional Neural Network. *International Journal of Environmental Research and Public Health*, *19*(3), 1401.

[224] Ghadimi, S., Auger, D. A., Feng, X., Sun, C., Meyer, C. H., Bilchick, K. C., ... & Epstein, F. H. (2021). Fully-automated global and segmental strain analysis of DENSE cardiovascular magnetic resonance using deep learning for segmentation and phase unwrapping. *Journal of Cardiovascular Magnetic Resonance*, *23*(1), 1-13.

[225] Liu, J., Wei, A., Guo, Z., & Tang, C. (2021). Global Context and Enhanced Feature Guided Residual Refinement Network for 3D Cardiovascular Image Segmentation. *IEEE Access*, *9*, 155861-155870.

[226] Ankenbrand, M. J., Lohr, D., Schlötelburg, W., Reiter, T., Wech, T., & Schreiber, L. M. (2021). Deep learning-based cardiac cine segmentation: Transfer learning application to 7T ultrahigh-field MRI. *Magnetic Resonance in Medicine*, *86*(4), 2179-2191.

[227] Galea, R. R., Diosan, L., Andreica, A., Popa, L., Manole, S., & Bálint, Z. (2021). Region-of-Interest-Based Cardiac Image Segmentation with Deep Learning. *Applied Sciences*, *11*(4), 1965.

[228] Zarvani, M., Saberi, S., Azmi, R., & Shojaedini, S. V. (2021). Residual learning: A new paradigm to improve deep learning-based segmentation of the left ventricle in magnetic resonance imaging cardiac images. *Journal of Medical Signals and Sensors*, *11*(3), 159.

[229] Daudé, P., Ancel, P., Confort Gouny, S., Jacquier, A., Kober, F., Dutour, A., ... & Rapacchi, S. (2022). Deep-Learning Segmentation of Epicardial Adipose Tissue Using Four-Chamber Cardiac Magnetic Resonance Imaging. *Diagnostics*, *12*(1), 126.

[230] Li, D., Peng, Y., Guo, Y., & Sun, J. (2022). TAUNet: a triple-attention-based multi-modality MRI fusion U-Net for cardiac pathology segmentation. *Complex & Intelligent Systems*, 1-17.

[231] Sandooghdar, A., & Yaghmaee, F. (2022). Deep Learning Approach for Cardiac MRI Images. *Journal of Information Systems and Telecommunication (JIST)*, *1*(37), 61.

[232]. Zou, X., Wang, Q., & Luo, T. (2021). A novel approach for left ventricle segmentation in tagged MRI. *Computers & Electrical Engineering*, *95*, 107416.

[233] Penso, M., Moccia, S., Scafuri, S., Muscogiuri, G., Pontone, G., Pepi, M., & Caiani, E. G. (2021). Automated left and right ventricular chamber segmentation in cardiac magnetic resonance images using dense fully convolutional neural network. *Computer Methods and Programs in Biomedicine*, *204*, 106059.

[234] Wang, Z., Peng, Y., Li, D., Guo, Y., & Zhang, B. (2022). MMNet: A multi-scale deep learning network for the left ventricular segmentation of cardiac MRI images. *Applied Intelligence*, *52*(5), 5225-5240.

[235] Luo, Y., Xu, L., & Qi, L. (2021). A cascaded FC-DenseNet and level set method (FCDL) for fully automatic segmentation of the right ventricle in cardiac MRI. *Medical & Biological Engineering & Computing*, *59*(3), 561-574.

[236] Upendra, R. R., Simon, R., & Linte, C. A. (2021, February). Joint deep learning framework for image registration and segmentation of late gadolinium enhanced MRI and cine cardiac MRI. In *Medical Imaging 2021: Image-Guided Procedures, Robotic Interventions, and Modeling* (Vol. 11598, p. 115980F). International Society for Optics and Photonics.

[237] Chen, Y., Xie, W., Zhang, J., Qiu, H., Zeng, D., Shi, Y., ... & Xu, X. (2022). Myocardial Segmentation of Cardiac MRI Sequences with Temporal Consistency for Coronary Artery Disease Diagnosis. *Frontiers in Cardiovascular Medicine*, *9*.

[238] Huisi Wu, Xuheng Lu, Baiying Lei, Zhenkun Wen,Automated left ventricular segmentation from cardiac magnetic resonance images via adversarial learning with multi-stage pose estimation network and co-discriminator,Medical Image Analysis,Volume 68,2021,101891,ISSN 1361-8415,

[239] Du, X., Xu, X., Liu, H., & Li, S. (2021). TSU-net: Two-stage multi-scale cascade and multi-field fusion U-net for right ventricular segmentation. *Computerized Medical Imaging and Graphics*, *93*, 101971.

[240] Cui, H., Yuwen, C., Jiang, L., Xia, Y., & Zhang, Y. (2021). Bidirectional cross-modality unsupervised domain adaptation using generative adversarial networks for cardiac image segmentation. *Computers in Biology and Medicine*, *136*, 104726.

[241] Zhang, Y., Feng, J., Guo, X., & Ren, Y. (2022). Comparative analysis of U-Net and TLMDB GAN for the cardiovascular segmentation of the ventricles in the heart. *Computer Methods and Programs in Biomedicine*, 106614.

[242] Cui, H., Yuwen, C., Jiang, L., Xia, Y., & Zhang, Y. (2021). Multiscale attention guided U-Net architecture for cardiac segmentation in short-axis MRI images. *Computer Methods and Programs in Biomedicine*, *206*, 106142.

[243] Shi, J., Ye, Y., Zhu, D., Su, L., Huang, Y., & Huang, J. (2021). Automatic segmentation of cardiac magnetic resonance images based on multi-input fusion network. *Computer Methods and Programs in Biomedicine*, *209*, 106323. Shi, J., Ye, Y., Zhu, D., Su, L., Huang, Y., & Huang, J. (2021). Automatic segmentation of cardiac magnetic resonance images based on multi-input fusion network. *Computer Methods and Programs in Biomedicine*, *209*, 106323.

[244] Wu, H., Lu, X., Lei, B., & Wen, Z. (2021). Automated left ventricular segmentation from cardiac magnetic resonance images via adversarial learning with multi-stage pose estimation network and co-discriminator. *Medical Image Analysis*, *68*, 101891.

[245] Wang, K. N., Yang, X., Miao, J., Li, L., Yao, J., Zhou, P., ... & Ni, D. (2022). AWSnet: An Auto-weighted Supervision Attention Network for Myocardial Scar and Edema Segmentation in Multi-sequence Cardiac Magnetic Resonance Images. *Medical Image Analysis*, 102362.

[246] Zhang, H., Zhang, W., Shen, W., Li, N., Chen, Y., Li, S., ... & Wang, Y. (2021). Automatic segmentation of the cardiac MR images based on nested fully convolutional dense network with dilated convolution. *Biomedical signal processing and control*, *68*, 102684. Hassan, M. R., Huda, S., Hassan, M. M., Abawajy, J., Alsanad, A., & Fortino, G. (2022).

[247] Liu, Z., Li, P., Li, J., Xie, Q., & Wang, X. (2021, March). Left ventricular full segmentation from cardiac Magnetic Resonance Imaging via multi-task learning. In *2021 IEEE 2nd International Conference on Big Data, Artificial Intelligence and Internet of Things Engineering (ICBAIE)* (pp. 71-75). IEEE.

[248] Tripathi, S., Sharan, T. S., Sharma, S., & Sharma, N. (2021). An augmented deep learning network with noise suppression feature for efficient segmentation of magnetic resonance images. *IETE Technical Review*, 1-14.

[249] Janik, A., Dodd, J., Ifrim, G., Sankaran, K., & Curran, K. (2021, February). Interpretability of a deep learning model in the application of cardiac MRI segmentation with an ACDC challenge dataset. In *Medical Imaging 2021: Image Processing* (Vol. 11596, p. 1159636). International Society for Optics and Photonics.

[250] Cascaded triplanar autoencoder M-Net for fully automatic segmentation of left ventricle myocardial scar from three-dimensional late gadolinium-enhanced MR images

[251] Kausar, A., Razzak, I., Shapiai, M. I., & Beheshti, A. (2021). 3d shallow deep neural network for fast and precise segmentation of left atrium. *Multimedia Systems*, 1-11.

[252] Lu, C., Guo, Z., Yuan, J., Xia, K., & Yu, H. (2022). Fine-grained calibrated double-attention convolutional network for left ventricular segmentation. *Physics in Medicine & Biology*, *67*(5), 055013.

[253] Farrag, N. A., Lochbihler, A., White, J. A., & Ukwatta, E. (2021). Evaluation of fully automated myocardial segmentation techniques in native and contrast-enhanced T1-mapping cardiovascular magnetic resonance images using fully convolutional neural networks. *Medical Physics*, *48*(1), 215-226.

[254] Luo, G., Sun, G., Wang, K., Dong, S., & Zhang, H. (2016, September). A novel left ventricular volumes prediction method based on deep learning network in cardiac MRI. In 2016 Computing in Cardiology Conference (CinC) (pp. 89-92). IEEE.

[255] Kong, B., Zhan, Y., Shin, M., Denny, T., & Zhang, S. (2016, October). Recognizing end-diastole and end-systole frames via deep temporal regression network. In International conference on medical image computing and computer-assisted intervention (pp. 264-272). Springer, Cham.

[256] Luo, G., Dong, S., Wang, K., & Zhang, H. (2016, December). Cardiac left ventricular volumes prediction method based on atlas location and deep learning. In 2016 IEEE International Conference on Bioinformatics and Biomedicine (BIBM) (pp. 1604-1610). IEEE.

[257] Margeta, J., Criminisi, A., Cabrera Lozoya, R., Lee, D. C., & Ayache, N. (2017). Fine-tuned convolutional neural nets for cardiac MRI acquisition plane recognition. Computer Methods in Biomechanics and Biomedical Engineering: Imaging & Visualization, 5(5), 339-349.

[258] Muthulakshmi, M., & Kavitha, G. (2019, July). Deep CNN with LM learning based myocardial ischemia detection in cardiac magnetic resonance images. In 2019 41st Annual International Conference of the IEEE Engineering in Medicine and Biology Society (EMBC) (pp. 824-827). IEEE.

[259] Yang, F., He, Y., Hussain, M., Xie, H., & Lei, P. (2017). Convolutional neural network for the detection of end-diastole and end-systole frames in free-breathing cardiac magnetic resonance imaging. Computational and mathematical methods in medicine, 2017.

[260] Kermani, S., Oghli, M. G., Mohammadzadeh, A., & Kafieh, R. (2020). NF-RCNN: Heart localization and right ventricle wall motion abnormality detection in cardiac MRI. Physica Medica, 70, 65-74.

[261] Luo, G., Dong, S., Wang, K., Zuo, W., Cao, S., & Zhang, H. (2017). Multi-views fusion CNN for left ventricular volumes estimation on cardiac MR images. IEEE Transactions on Biomedical Engineering, 65(9), 1924-1934.

[262] Liao, F., Chen, X., Hu, X., & Song, S. (2017). Estimation of the volume of the left ventricle from MRI images using deep neural networks. IEEE transactions on cybernetics, 49(2), 495-504.

[263] Huang, Q., Chen, E. Z., Yu, H., Guo, Y., Chen, T., Metaxas, D., & Sun, S. (2020). Measure Anatomical Thickness from Cardiac MRI with Deep Neural Networks. arXiv preprint arXiv:2008.11109.

[264] Komatsu, M., Sakai, A., Komatsu, R., Matsuoka, R., Yasutomi, S., Shozu, K., ... & Hamamoto, R. (2021). Detection of Cardiac Structural Abnormalities in Fetal Ultrasound Videos Using Deep Learning. Applied Sciences, 11(1), 371.

[265] Pu, B., Zhu, N., Li, K., & Li, S. (2021). Fetal cardiac cycle detection in multi-resource echocardiograms using hybrid classification framework. Future Generation Computer Systems, 115, 825-836.

[266] Isensee, F., Jaeger, P. F., Full, P. M., Wolf, I., Engelhardt, S., & Maier-Hein, K. H. (2017, September). Automatic cardiac disease assessment on cine-MRI via time-series segmentation and domain specific features. In International workshop on statistical atlases and computational models of the heart (pp. 120-129). Springer, Cham.

[267] Ohta, Y., Yunaga, H., Kitao, S., Fukuda, T., & Ogawa, T. (2019). Detection and classification of myocardial delayed enhancement patterns on mr images with deep neural networks: a feasibility study. Radiology: Artificial Intelligence, 1(3), e180061.

[268] Zhou, H., Li, L., Liu, Z., Zhao, K., Chen, X., Lu, M., … & Tian, J. (2020). Deep learning algorithm to improve hypertrophic cardiomyopathy mutation prediction using cardiac cine images. European Radiology, 1-10.

[269] Shaker, M. S., Wael, M., Yassine, I. A., & Fahmy, A. S. (2014, December). Cardiac MRI view classification using autoencoder. In 2014 Cairo International Biomedical Engineering Conference (CIBEC) (pp. 125-128). IEEE.

[270] Xue, W., Islam, A., Bhaduri, M., & Li, S. (2017). Direct multitype cardiac indices estimation via joint representation and regression learning. IEEE transactions on medical imaging, 36(10), 2057-2067.

[271] Dekhil, O., Taher, F., Khalifa, F., Beache, G., Elmaghraby, A., & El-Baz, A. (2018, December). A Novel Fully Automated CAD System for Left Ventricle Volume Estimation. In 2018 IEEE International Symposium on Signal Processing and Information Technology (ISSPIT) (pp. 602-606). IEEE.

[272] Wang, S. H., McCann, G., & Tyukin, I. (2020, July). Myocardial Infarction Detection and Quantification Based on a Convolution Neural Network with Online Error Correction Capabilities. In 2020 International Joint Conference on Neural Networks (IJCNN) (pp. 1-8). IEEE.

[273] Ossenberg-Engels, J., & Grau, V. (2019, October). Conditional Generative Adversarial Networks for the Prediction of Cardiac Contraction from Individual Frames. In International Workshop on Statistical Atlases and Computational Models of the Heart (pp. 109-118). Springer, Cham.

[274] Zhang, L., Gooya, A., Dong, B., Hua, R., Petersen, S. E., Medrano-Gracia, P., & Frangi, A. F. (2016, October). Automated quality assessment of cardiac MR images using convolutional neural networks. In International Workshop on Simulation and Synthesis in Medical Imaging (pp. 138-145). Springer, Cham.

[275] Zhang, L., Gooya, A., & Frangi, A. F. (2017, September). Semi-supervised assessment of incomplete LV coverage in cardiac MRI using generative adversarial nets. In International Workshop on Simulation and Synthesis in Medical Imaging (pp. 61-68). Springer, Cham.

[276] Yokota, Y., Takeda, C., Kidoh, M., Oda, S., Aoki, R., Ito, K., ... & Utsunomiya, D. (2020). Effects of Deep Learning Reconstruction Technique in High-Resolution Non-contrast Magnetic Resonance Coronary Angiography at a 3-Tesla Machine. Canadian Association of Radiologists Journal, 0846537119900469.

[277] Emad, O., Yassine, I. A., & Fahmy, A. S. (2015, August). Automatic localization of the left ventricle in cardiac MRI images using deep learning. In 2015 37th Annual International Conference of the IEEE Engineering in Medicine and Biology Society (EMBC) (pp. 683-686). IEEE.

[278] Bai, W., Sinclair, M., Tarroni, G., Oktay, O., Rajchl, M., Vaillant, G., ... & Rueckert, D. (2018). Automated cardiovascular magnetic resonance image analysis with fully convolutional networks. Journal of Cardiovascular Magnetic Resonance, 20(1), 65.

[279] Curiale, A. H., Colavecchia, F. D., & Mato, G. (2019). Automatic quantification of the LV function and mass: a deep learning approach for cardiovascular MRI. Computer methods and programs in biomedicine, 169, 37-50.

[280] Goldfarb, J. W., Craft, J., & Cao, J. J. (2019). Water–fat separation and parameter mapping in cardiac MRI via deep learning with a convolutional neural network. Journal of Magnetic Resonance Imaging, 50(2), 655-665.

[281] Kerfoot, E., Clough, J., Oksuz, I., Lee, J., King, A. P., & Schnabel, J. A. (2018, September). Left-ventricle quantification using residual U-Net. In International Workshop on Statistical Atlases and Computational Models of the Heart (pp. 371-380). Springer, Cham.

[282] Amirrajab, S., Abbasi-Sureshjani, S., Al Khalil, Y., Lorenz, C., Weese, J., Pluim, J., & Breeuwer, M. (2020, October). XCAT-GAN for Synthesizing 3D Consistent Labeled Cardiac MR Images on Anatomically Variable XCAT Phantoms. In International Conference on Medical Image Computing and Computer-Assisted Intervention (pp. 128-137). Springer, Cham.

[283] Xia, Y., Zhang, L., Ravikumar, N., Attar, R., Piechnik, S. K., Neubauer, S., ... & Frangi, A. F. (2020). Recovering from missing data in population imaging–Cardiac MR image imputation via conditional generative adversarial nets. Medical Image Analysis, 67, 101812.

[284] Lv, J., Wang, C., & Yang, G. (2021). PIC-GAN: A Parallel Imaging Coupled Generative Adversarial Network for Accelerated Multi-Channel MRI Reconstruction. Diagnostics, 11(1), 61.

[285] Upendra, R. R., Simon, R., & Linte, C. A. (2020, July). A Supervised Image Registration Approach for Late Gadolinium Enhanced MRI and Cine Cardiac MRI Using Convolutional Neural Networks. In Annual Conference on Medical Image Understanding and Analysis (pp. 208-220). Springer, Cham.

[286] Hamilton, J. I., Currey, D., Rajagopalan, S., & Seiberlich, N. (2021). Deep learning reconstruction for cardiac magnetic resonance fingerprinting T1 and T2 mapping. Magnetic Resonance in Medicine.

[287] Küstner, T., Fuin, N., Hammernik, K., Bustin, A., Qi, H., Hajhosseiny, R., ... & Prieto, C. (2020). CINENet: deep learning-based 3D cardiac CINE MRI reconstruction with multi-coil complex-valued 4D spatio-temporal convolutions. Scientific reports, 10(1), 1-13.

[288] Lyu, Q., Shan, H., Xie, Y., Li, D., & Wang, G. (2020). Cine cardiac MRI motion artifact reduction using a recurrent neural network. arXiv preprint arXiv:2006.12700.

[289] Masutani, E. M., Bahrami, N., & Hsiao, A. (2020). Deep learning single-frame and multiframe super-resolution for cardiac MRI. Radiology, 295(3), 552-561.

[290] El-Rewaidy, H., Fahmy, A. S., Pashakhanloo, F., Cai, X., Kucukseymen, S., Csecs, I., ... & Nezafat, R. (2021). Multi-domain convolutional neural network (MD-CNN) for radial reconstruction of dynamic cardiac MRI. Magnetic Resonance in Medicine, 85(3), 1195-1208.

[291] El-Rewaidy, H., Neisius, U., Mancio, J., Kucukseymen, S., Rodriguez, J., Paskavitz, A., ... & Nezafat, R. (2020). Deep complex convolutional network for fast reconstruction of 3D late gadolinium enhancement cardiac MRI. NMR in Biomedicine, 33(7), e4312.

[292] Ferdian, E., Suinesiaputra, A., Dubowitz, D. J., Zhao, D., Wang, A., Cowan, B., & Young, A. A. (2020). 4DFlowNet: Super-resolution 4D Flow MRI using deep learning and computational fluid dynamics. Frontiers in Physics, 8, 138.

[293] Sandino, C. M., Lai, P., Vasanawala, S. S., & Cheng, J. Y. (2021). Accelerating cardiac cine MRI using a deep learning-based ESPIRiT reconstruction. Magnetic Resonance in Medicine, 85(1), 152-167.

[294] Qiu, W., Li, D., Jin, X., Liu, F., & Sun, B. (2020). Deep neural network inspired by iterative shrinkage-thresholding algorithm with data consistency (NISTAD) for fast Undersampled MRI reconstruction. Magnetic resonance imaging, 70, 134-144.

[295] Le, M., Lieman-Sifry, J., Lau, F., Sall, S., Hsiao, A., & Golden, D. (2017). Computationally efficient cardiac views projection using 3D Convolutional Neural Networks. In Deep Learning in Medical Image Analysis and Multimodal Learning for Clinical Decision Support (pp. 109-116). Springer, Cham.

[296] Schlemper, J., Caballero, J., Hajnal, J. V., Price, A. N., & Rueckert, D. (2017). A deep cascade of convolutional neural networks for dynamic MR image reconstruction. IEEE transactions on Medical Imaging, 37(2), 491-503.

[297] Biswas, S., Aggarwal, H. K., Poddar, S., & Jacob, M. (2018, April). Model-based free-breathing cardiac MRI reconstruction using deep learned & storm priors: MoDL-storm. In 2018 IEEE International Conference on Acoustics, Speech and Signal Processing (ICASSP) (pp. 6533-6537). IEEE.

[298] Skandarani, Y., Painchaud, N., Jodoin, P. M., & Lalande, A. (2020). On the effectiveness of GAN generated cardiac MRIs for segmentation. ArXiv preprint arXiv:2005.09026.

[299] Oksuz, I., Ruijsink, B., Puyol-Antón, E., Bustin, A., Cruz, G., Prieto, C., … & King, A. P. (2018, September). Deep learning using K-space based data augmentation for automated cardiac MR motion artefact detection. In International Conference on Medical Image Computing and Computer-Assisted Intervention (pp. 250-258). Springer, Cham.

[300] Zhao, M., Liu, X., Liu, H., & Wong, K. K. (2020). Super-resolution of cardiac magnetic resonance images using Laplacian Pyramid based on Generative Adversarial Networks. Computerized Medical Imaging and Graphics, 80, 101698.

[301] Ghodrati, V., Bydder, M., Ali, F., Gao, C., Prosper, A., Nguyen, K. L., & Hu, P. (2021). Retrospective respiratory motion correction in cardiac cine MRI reconstruction using adversarial autoencoder and unsupervised learning. NMR in Biomedicine, 34(2), e4433.

[302] Fahmy, A. S., El-Rewaidy, H., Nezafat, M., Nakamori, S., & Nezafat, R. (2019). Automated analysis of cardiovascular magnetic resonance myocardial native T 1 mapping images using fully convolutional neural networks. Journal of Cardiovascular Magnetic Resonance, 21(1), 1-12.

[303] Kofler, A., Dewey, M., Schaeffter, T., Wald, C., & Kolbitsch, C. (2019). Spatio-temporal deep learning-based undersampling artefact reduction for 2D radial cine MRI with limited training data. IEEE transactions on medical imaging, 39(3), 703-717.

[304] Böttcher, B., Beller, E., Busse, A., Cantré, D., Yücel, S., Öner, A., ... & Meinel, F. G. (2020). Fully automated quantification of left ventricular volumes and function in cardiac MRI: clinical evaluation of a deep learning-based algorithm. The international journal of cardiovascular imaging, 36(11), 2239-2247.

[305] Biswas, S., Aggarwal, H. K., & Jacob, M. (2019). Dynamic MRI using model-based deep learning and SToRM priors: MoDL-SToRM. Magnetic resonance in medicine, 82(1), 485-494.

[306] Schlemper, J., Yang, G., Ferreira, P., Scott, A., McGill, L. A., Khalique, Z., ... & Rueckert, D. (2018, September). Stochastic deep compressive sensing for the reconstruction of diffusion tensor cardiac MRI. In International conference on medical image computing and computer-assisted intervention (pp. 295-303). Springer, Cham.

[307] Mahapatra, D., Bozorgtabar, B., & Garnavi, R. (2019). Image super-resolution using progressive generative adversarial networks for medical image analysis. Computerized Medical Imaging and Graphics, 71, 30-39.

[308] Lau, F., Hendriks, T., Lieman-Sifry, J., Sall, S., & Golden, D. (2018). Scargan: chained generative adversarial networks to simulate pathological tissue on cardiovascular mr scans. In Deep learning in medical image analysis and multimodal learning for clinical decision support (pp. 343-350). Springer, Cham.

[309] Jiang, M., Yuan, Z., Yang, X., Zhang, J., Gong, Y., Xia, L., & Li, T. (2019). Accelerating CS-MRI reconstruction with fine-tuning Wasserstein generative adversarial network. IEEE Access, 7, 152347-152357.

[310] Abbasi-Sureshjani, S., Amirrajab, S., Lorenz, C., Weese, J., Pluim, J., & Breeuwer, M. (2020, September). 4D semantic cardiac magnetic resonance image synthesis on XCAT anatomical model. In Medical Imaging with Deep Learning (pp. 6-18). PMLR.

[311] Zhang, L., Pereañez, M., Bowles, C., Piechnik, S. K., Neubauer, S., Petersen, S. E., & Frangi, A. F. (2019, October). Unsupervised Standard Plane Synthesis in Population Cine MRI via Cycle-Consistent Adversarial Networks. In International Conference on Medical Image Computing and Computer-Assisted Intervention (pp. 660-668). Springer, Cham.

[312] Fu, Y., Gong, M., Yang, G., Hu, J., Wei, H., & Zhou, J. Optimization of Cardiac Magnetic Resonance Synthetic Image Based on Simulated Generative Adversarial Network. Mathematical Problems in Engineering, 2021.

[313] Diller, G. P., Vahle, J., Radke, R., Vidal, M. L. B., Fischer, A. J., Bauer, U. M., ... & Orwat, S. (2020). Utility of deep learning networks for the generation of artificial cardiac magnetic resonance images in congenital heart disease. BMC Medical Imaging, 20(1), 1-8.

[314] Liu, B., Wang, L., Zhang, J., Cheng, X., Yang, F., Huang, J., & Zhu, Y. (2018, August). Cardiac diffusion tensor imaging simulation based on deep convolutional generative adversarial network. In 2018 14th IEEE International Conference on Signal Processing (ICSP) (pp. 1189-1193). IEEE.

[315] Zhang, Y., Zhang, W., Zhang, Q., Yang, J., Chen, X., & Zhao, S. (2019). CMR motion artifact correction using generative adversarial nets. arXiv preprint arXiv:1902.11121.

[316] Chen, M., Fang, L., Zhuang, Q., & Liu, H. (2019). Deep learning assessment of myocardial infarction from MR image sequences. Ieee Access, 7, 5438-5446.

[317] Zhang, L., Gooya, A., Pereanez, M., Dong, B., Piechnik, S. K., Neubauer, S., ... & Frangi, A. F. (2018). Automatic assessment of full left ventricular coverage in cardiac cine magnetic resonance imaging with fisher-discriminative 3-D CNN. IEEE Transactions on Biomedical Engineering, 66(7), 1975-1986.

[318] Pereira, R. F., Rebelo, M. S., Moreno, R. A., Marco, A. G., Lima, D. M., Arruda, M. A., ... & Gutierrez, M. A. (2020, July). Fully Automated Quantification of Cardiac Indices from Cine MRI Using a Combination of Convolution Neural Networks. In 2020 42nd Annual International Conference of the IEEE Engineering in Medicine & Biology Society (EMBC) (pp. 1221-1224). IEEE.

[319] Jeelani, H., Yang, Y., Zhou, R., Kramer, C. M., Salerno, M., & Weller, D. S. (2020, April). A Myocardial T1-Mapping Framework with Recurrent and U-Net Convolutional Neural Networks. In 2020 IEEE 17th International Symposium on Biomedical Imaging (ISBI) (pp. 1941-1944). IEEE.

[320] Sander, J., de Vos, B. D., Wolterink, J. M., & Išgum, I. (2019, March). Towards increased trustworthiness of deep learning segmentation methods on cardiac MRI. In Medical Imaging 2019: Image Processing (Vol. 10949, p. 1094919). International Society for Optics and Photonics.

[321] Zhang, K., & Zhuang, X. (2020, October). Recognition and standardization of cardiac MRI orientation via multi-tasking learning and deep neural networks. In Myocardial Pathology Segmentation Combining Multi-Sequence CMR Challenge (pp. 167-176). Springer, Cham.

[322] Sang, Y., & Ruan, D. (2020, October). Deformable Image Registration with a Scale-adaptive Convolutional Neural Network. In 2020 IEEE 20th International Conference on Bioinformatics and Bioengineering (BIBE) (pp. 556-562). IEEE.

[323] Moeskops, P., Wolterink, J. M., van der Velden, B. H., Gilhuijs, K. G., Leiner, T., Viergever, M. A., & Išgum, I. (2016, October). Deep learning for multi-task medical image segmentation in multiple modalities. In International Conference on Medical Image Computing and Computer-Assisted Intervention (pp. 478-486). Springer, Cham.

[324] Dong, S., Luo, G., Sun, G., Wang, K., & Zhang, H. (2016, September). A left ventricular segmentation method on 3D echocardiography using deep learning and snake. In 2016 Computing in Cardiology Conference (CinC) (pp. 473-476). IEEE.

[325] Dong, S., Luo, G., Sun, G., Wang, K., & Zhang, H. (2016, September). A combined multi-scale deep learning and random forests approach for direct left ventricular volumes estimation in 3D echocardiography. In 2016 Computing In Cardiology Conference (Cinc) (pp. 889-892). IEEE.

[326] Mortazi, A., Burt, J., & Bagci, U. (2017, September). Multi-planar deep segmentation networks for cardiac substructures from MRI and CT. In International Workshop on Statistical Atlases and Computational Models of the Heart (pp. 199-206). Springer, Cham.

[327] Wang, C., & Smedby, Ö. (2017, September). Automatic whole heart segmentation using deep learning and shape context. In International Workshop on Statistical Atlases and Computational Models of the Heart (pp. 242-249). Springer, Cham.

[328] Dou, Q., Ouyang, C., Chen, C., Chen, H., Glocker, B., Zhuang, X., & Heng, P. A. (2019). PnP-AdaNet: Plug-and-play adversarial domain adaptation network at unpaired cross-modality cardiac segmentation. IEEE Access, 7, 99065-99076.

[329] Yu, C., Gao, Z., Zhang, W., Yang, G., Zhao, S., Zhang, H., ... & Li, S. (2020). Multitask learning for estimating multitype cardiac indices in MRI and CT based on adversarial reverse mapping. IEEE transactions on neural networks and learning systems.

[330] Larrazabal, A. J., Martínez, C., Glocker, B., & Ferrante, E. (2020). Post-dae: Anatomically plausible segmentation via post-processing with denoising autoencoders. IEEE Transactions on Medical Imaging, 39(12), 3813-3820.

[331] Painchaud, N., Skandarani, Y., Judge, T., Bernard, O., Lalande, A., & Jodoin, P. M. (2020). Cardiac segmentation with strong anatomical guarantees. IEEE Transactions on Medical Imaging, 39(11), 3703-3713.

[332] Yuwen, C., Jiang, L., & Cui, H. (2022, February). Multiple GANs guided by self-attention mechanism for automatic cardiac image segmentation. In *Thirteenth International Conference on Graphics and Image Processing (ICGIP 2021)* (Vol. 12083, pp. 509-515). SPIE.

[333] Mortensen, K. H., Gopalan, D., Nørgaard, B. L., Andersen, N. H., & Gravholt, C. H. (2016). Multimodality cardiac imaging in Turner syndrome. *Cardiology in the Young*, 26(5), 831-841.

[334] Biersmith, M. A., Tong, M. S., Guha, A., Simonetti, O. P., & Addison, D. (2020). Multimodality cardiac imaging in the era of emerging cancer therapies. *Journal of the American Heart Association*, 9(2), e013755.

[335] Xu, F., Uszkoreit, H., Du, Y., Fan, W., Zhao, D., & Zhu, J. (2019, October). Explainable AI: A brief survey on history, research areas, approaches and challenges. In *CCF international conference on natural language processing and Chinese computing* (pp. 563-574). Springer, Cham.

[336] Adadi, A., & Berrada, M. (2018). Peeking inside the black-box: a survey on explainable artificial intelligence (XAI). *IEEE access*, 6, 52138-52160.

[337] Esmaeili, M., Vettukattil, R., Banitalebi, H., Krogh, N. R., & Geitung, J. T. (2021). Explainable artificial intelligence for human-machine interaction in brain tumor localization. *Journal of Personalized Medicine*, 11(11), 1213.

[338] Marmolejo-Saucedo, J. A., & Kose, U. (2022). Numerical Grad-Cam Based Explainable Convolutional Neural Network for Brain Tumor Diagnosis. *Mobile Networks and Applications*, 1-10.

[339] Zeng, A., Yu, K. T., Song, S., Suo, D., Walker, E., Rodriguez, A., & Xiao, J. (2017, May). Multi-view self-supervised deep learning for 6d pose estimation in the amazon picking challenge. In *2017 IEEE international conference on robotics and automation (ICRA)* (pp. 1386-1383). IEEE.

[340] Carneiro, T., Da Nóbrega, R. V. M., Nepomuceno, T., Bian, G. B., De Albuquerque, V. H. C., & Reboucas Filho, P. P. (2018). Performance analysis of google colaboratory as a tool for accelerating deep learning applications. *IEEE Access*, 6, 61677-61685.

[341] Niu, Z., Zhong, G., & Yu, H. (2021). A review on the attention mechanism of deep learning. *Neurocomputing*, 452, 48-62.

[342] Lieskovská, E., Jakubec, M., Jarina, R., & Chmulík, M. (2021). A review on speech emotion recognition using deep learning and attention mechanism. *Electronics*, 10(10), 1163.

[343] Liu, X., & Milanova, M. (2018). Visual attention in deep learning: a review. *Int Rob Auto J*, 4(3), 154-155.

[344] Lin, T., Wang, Y., Liu, X., & Qiu, X. (2021). A survey of transformers. *arXiv preprint arXiv:2106.04554*.

[345] Tay, Y., Dehghani, M., Bahri, D., & Metzler, D. (2020). Efficient transformers: A survey. *ACM Computing Surveys (CSUR)*.

[346] Georgousis, S., Kenning, M. P., & Xie, X. (2021). Graph deep learning: State of the art and challenges. *IEEE Access*, 9, 22106-22140.

[347] Zhang, S., Tong, H., Xu, J., & Maciejewski, R. (2019). Graph convolutional networks: a comprehensive review. *Computational Social Networks*, 6(1), 1-23.

[348] Mousavi, S. S., Schukat, M., & Howley, E. (2016, September). Deep reinforcement learning: an overview. In *Proceedings of SAI Intelligent Systems Conference* (pp. 426-440). Springer, Cham.

[349] Li, Y. (2017). Deep reinforcement learning: An overview. *arXiv preprint arXiv:1701.07274*.

[350] Djenouri, Y., Belhadi, A., Yazidi, A., Srivastava, G., & Lin, J. C. W. (2022). Artificial intelligence of medical things for disease detection using ensemble deep learning and attention mechanism. *Expert Systems*, e13093.

[351] Ranjbarzadeh, R., Bagherian Kasgari, A., Jafarzadeh Ghoushchi, S., Anari, S., Naseri, M., & Bendechache, M. (2021). Brain tumor segmentation based on deep learning and an attention mechanism using MRI multi-modalities brain images. *Scientific Reports*, 11(1), 1-17.

[352] Zhu, Q., Zhou, X., Song, Z., Tan, J., & Guo, L. (2019, July). Dan: Deep attention neural network for news recommendation. In *Proceedings of the AAAI Conference on Artificial Intelligence* (Vol. 33, No. 01, pp. 5973-5980).

[353] Ghorbani, M., Prasad, S., Brooks, B. R., & Klauda, J. B. (2022). Deep attention based variational autoencoder for antimicrobial peptide discovery. *bioRxiv*.

[354] Bai, J., Ding, B., Xiao, Z., Jiao, L., Chen, H., & Regan, A. C. (2021). Hyperspectral image classification based on deep attention graph convolutional network. *IEEE Transactions on Geoscience and Remote Sensing*, *60*, 1-16.

[355] Chen, T., Li, X., Yin, H., & Zhang, J. (2018, June). Call attention to rumors: Deep attention based recurrent neural networks for early rumor detection. In *Pacific-Asia conference on knowledge discovery and data mining* (pp. 40-52). Springer, Cham.

[356] Chen, J., He, Y., Frey, E. C., Li, Y., & Du, Y. (2021). Vit-v-net: Vision transformer for unsupervised volumetric medical image registration. *arXiv preprint arXiv:2104.06468*.

[357] Chen, J., Lu, Y., Yu, Q., Luo, X., Adeli, E., Wang, Y., ... & Zhou, Y. (2021). Transunet: Transformers make strong encoders for medical image segmentation. *arXiv preprint arXiv:2102.04306*.

[358] Yun, S., Jeong, M., Kim, R., Kang, J., & Kim, H. J. (2019). Graph transformer networks. *Advances in neural information processing systems*, *32*.

[359] Esteves, C., Allen-Blanchette, C., Zhou, X., & Daniilidis, K. (2017). Polar transformer networks. *arXiv preprint arXiv:1709.01889*.

[360] Yin, H., Vahdat, A., Alvarez, J. M., Mallya, A., Kautz, J., & Molchanov, P. (2022). A-ViT: Adaptive Tokens for Efficient Vision Transformer. In *Proceedings of the IEEE/CVF Conference on Computer Vision and Pattern Recognition* (pp. 10809-10818).

[361] Ruiz, L., Gama, F., & Ribeiro, A. (2020). Gated graph recurrent neural networks. *IEEE Transactions on Signal Processing*, *68*, 6303-6318.

[362] Zhou, S. K., Le, H. N., Luu, K., Nguyen, H. V., & Ayache, N. (2021). Deep reinforcement learning in medical imaging: A literature review. *Medical image analysis*, *73*, 102193.

[363] Coronato, A., Naeem, M., De Pietro, G., & Paragliola, G. (2020). Reinforcement learning for intelligent healthcare applications: A survey. *Artificial Intelligence in Medicine*, *109*, 101964.

[364] Duan, J., Shi, D., Diao, R., Li, H., Wang, Z., Zhang, B., ... & Yi, Z. (2019). Deep-reinforcement-learning-based autonomous voltage control for power grid operations. *IEEE Transactions on Power Systems*, *35*(1), 814-817.

[365] Vecerik, M., Hester, T., Scholz, J., Wang, F., Pietquin, O., Piot, B., ... & Riedmiller, M. (2017). Leveraging demonstrations for deep reinforcement learning on robotics problems with sparse rewards. *arXiv preprint arXiv:1707.08817*.

[366] Van Hasselt, H., Guez, A., & Silver, D. (2016, March). Deep reinforcement learning with double q-learning. In *Proceedings of the AAAI conference on artificial intelligence* (Vol. 30, No. 1).

[367] Guo, Y. (2018). A survey on methods and theories of quantized neural networks. arXiv preprint arXiv:1808.04752.

[368] Liang, T., Glossner, J., Wang, L., Shi, S., & Zhang, X. (2021). Pruning and quantization for deep neural network acceleration: A survey. *Neurocomputing*, *461*, 370-403.

[369] Chen, L., Fu, J., Wu, Y., Li, H., & Zheng, B. (2020). Hand gesture recognition using compact CNN via surface electromyography signals. *Sensors*, *20*(3), 672.

[370] Chen, G., Wang, Y., Li, H., & Dong, W. (2019, August). TinyNET: a lightweight, modular, and unified network architecture for the internet of things. In *Proceedings of the ACM SIGCOMM 2019 conference posters and demos* (pp. 9-11).

[371] Phan, H., Liu, Z., Huynh, D., Savvides, M., Cheng, K. T., & Shen, Z. (2020). Binarizing mobilenet via evolution-based searching. In *Proceedings of the IEEE/CVF Conference on Computer Vision and Pattern Recognition* (pp. 13420-13429).

[372] Ekeland, A. G., Bowes, A., & Flottorp, S. (2010). Effectiveness of telemedicine: a systematic review of reviews. *International journal of medical informatics*, *79*(11), 736-771.

[373] Al-Turjman, F., Nawaz, M. H., & Ulusar, U. D. (2020). Intelligence in the Internet of Medical Things era: A systematic review of current and future trends. *Computer Communications*, *150*, 644-660.

[374] Fuchs, A., Kühl, J. T., Lønborg, J., Engstrøm, T., Vejlstrup, N., Køber, L., & Kofoed, K. F. (2012). Automated assessment of heart chamber volumes and function in patients with previous myocardial infarction using multidetector computed tomography. *Journal of Cardiovascular Computed Tomography*, *6*(5), 325-334.

[375] Eitel, I., de Waha, S., Wöhrle, J., Fuernau, G., Lurz, P., Pauschinger, M., ... & Thiele, H. (2014). Comprehensive prognosis assessment by CMR imaging after ST-segment elevation myocardial infarction. *Journal of the American College of Cardiology*, *64*(12), 1217-1226.

[376] Wess, G., Mäurer, J., Simak, J., & Hartmann, K. (2010). Use of Simpson's method of disc to detect early echocardiographic changes in Doberman Pinschers with dilated cardiomyopathy. *Journal of veterinary internal medicine*, *24*(5), 1069-1076.

[377] Queirós, S., Barbosa, D., Heyde, B., Morais, P., Vilaça, J. L., Friboulet, D., ... & D'hooge, J. (2014). Fast automatic myocardial segmentation in 4D cine CMR datasets. *Medical image analysis*, *18*(7), 1115-1131.

[378] Green, J. J., Berger, J. S., Kramer, C. M., & Salerno, M. (2012). Prognostic value of late gadolinium enhancement in clinical outcomes for hypertrophic cardiomyopathy. *JACC: Cardiovascular Imaging*, *5*(4), 370-377.

[379] White, H. D., & Chew, D. P. (2008). Acute myocardial infarction. *The Lancet*, *372*(9638), 570-584.

[380] Bekkers, S. C., Yazdani, S. K., Virmani, R., & Waltenberger, J. (2010). Microvascular obstruction: underlying pathophysiology and clinical diagnosis. *Journal of the American College of Cardiology*, *55*(16), 1649-1660.

[381] Bing, R., & Dweck, M. R. (2019). Myocardial fibrosis: why image, how to image and clinical implications. *Heart*, *105*(23), 1832-1840.